

THE INFLUENCE OF STRESS ON THE DETECTABILITY
OF FATIGUE CRACKS USING ULTRASONICS

Sobhi Ismail Ibrahim

Doctor of Philosophy

The University of Aston in Birmingham

October 1981

TITLE: THE INFLUENCE OF STRESS ON THE DETECTABILITY
OF FATIGUE CRACKS USING ULTRASONICS

NAME: Sobhi Ismail Ibrahim

DEGREE: Doctor of Philosophy

YEAR: 1981

SUMMARY

Under favourable conditions fatigue cracks can be readily detected by a variety of ultrasonic techniques. There are indications, however, that compressive stresses can render the detection of these cracks very difficult, if not impossible. The factors which influence the detection of both stressed and unstressed cracks such as, probe angle and frequency, crack size and type, scanning position and material have been investigated. Compressive bending stresses were found to have a considerable influence on the ease of crack detection in steel and aluminium alloy. "Complete closure" of certain crack configurations was found to occur under elastic compressive stresses when using certain ultrasonic techniques.

Detailed work has been carried out to examine the interaction of ultrasound with fatigue cracks in the weld metal of QT35-steel, mainly to study the influence of elastic compressive stresses and related factors. These results indicate that fatigue cracks can best be located using 45° probes. Heat treatment prior to fatigue cracking allows fatigue cracks to be grown which are more readily detected and which are less prone to crack closure under compressive stresses. These findings and others are interpreted in terms of the topography of the fatigue cracks.

This work also investigates the effectiveness of shear wave inspection of fatigue cracks in the HAZ of austenitic stainless steel weldments which have always been considered difficult to inspect using ultrasonics. However, there is now some experimental evidence to suggest that shear wave inspection techniques can be applied in certain circumstances. The limitations of these techniques are demonstrated and possible solutions are proposed.

KEY WORDS: COMPRESSIVE STRESSES, FATIGUE CRACKS,
ULTRASONIC INSPECTION

ACKNOWLEDGEMENTS

I would like to thank the University of Mosul for having provided me with adequate financial support and study leave to carry out this research work.

I am greatly indebted to Mr. V.N. Whittaker for his expert guidance and continual encouragement, not only during the research work, but also during the writing up of the thesis.

I wish to express my gratitude to Professor I.L. Dillamore, former Head of Metallurgy and Materials Engineering Department and Professor R.H. Thornley of the Department of Production Technology and Management for the provision of laboratory facilities.

I also wish to thank Dr. D.R. Andrews for the many helpful suggestions and advice.

My thanks are also due to Messrs J. Foden, P. Cox, E. Watson and S. Witherington who have always been helpful and willing to assist me in the laboratories.

I am thankful to Mrs. H. Howell for her immense co-operation and excellent typing.

Last, but not the least, I am grateful to my wife, Bothayna, for her valuable support and understanding throughout the period of research, without which this work would not have been possible.

CONTENTS

	<u>PAGE</u>
Summary	(i)
List of Figures	(ii)
List of Tables	(iii)
1. INTRODUCTION	1
2. LITERATURE REVIEW	4
2.1 Ultrasonics - Pulse/Echo Technique	4
2.1.1 Historical Background	4
2.1.2 General	5
2.2 Ultrasonic Detection of Fatigue Cracks and other Planar Defects	8
2.3 Reflection of Ultrasonic Shear Waves at Air Gap in Steel and Mode Conversion	14
2.4 Limitations of Pulse-Echo Techniques	18
2.5 The Influence of Compressive Stresses on the Ultrasonic Response from Fatigue Cracks	21
2.5.1 Fatigue Cracks Surface Topography	24
2.5.2 Fatigue Crack Closure	26
2.6 Ultrasonic Inspection of Austenitic Weldments	27
3. EXPERIMENTAL TECHNIQUE	33
3.1 Mild Steel and Aluminium Alloy	33
3.1.1 Ultrasonic Testing	33
3.1.2 Preparation of Fatigue Cracks	35
3.1.2 Compression Testing	35
3.2 QT35-Steel	37
3.2.1 Preparation of QT35-Welded Plate	37

		<u>PAGE</u>
3.2.2	Preparation of Fatigue Cracks in QT35- Welds	38
3.3	316 Austenitic Stainless Steel	39
3.3.1	Preparation of the 316 Austenitic Steel Weldment	39
3.3.2	Preparation of Fatigue Cracks in HAZ of 316 Austenitic Weldment	39
4.	RESULTS AND DISCUSSION	48
4.1	Preliminary Tests	48
4.2	Fatigue Cracks in Mild Steel and Aluminium Alloy	55
4.3	Fatigue Cracks in QT35-Welds	72
4.4	The Influence of the Material Factor on the Detection and Sizing of Unstressed Fatigue Cracks	89
4.5	Fatigue Cracks in 316 Austenitic Weldment	92
5.	CONCLUSIONS	102
6.	FUTURE WORK	105
7.	REFERENCES	106
8.	APPENDICES	

LIST OF FIGURES

<u>FIGURE</u>	<u>TITLE</u>	<u>PAGE</u>
1	Reflection of incident shear wave with partial conversion into compression wave at steel/air boundary	15
2	Reflection intensity of shear and compression wave component after reflection of shear wave beam	15
3	Shear waves from 60° probe are incident on a vertical planar defect at 30° and are reflected as a mixture of shear and compression waves, after double reflection	17
4	Vertical beam spread chart of the 45°, 60° and 70° probes at both 2MHz and 5MHz frequencies	49
5	Ultrasonic echo amplitude response of different probes from the 100 mm quadrant of the IIW block	50
6a	Comparison between the ultrasonic responses of fatigue cracks, machined slots and drilled holes of various sizes using different angle probes at 5 MHz	51
6b	Comparison between the ultrasonic responses of fatigue cracks, machined slots and drilled holes of different sizes, using different angle probes at 2MHz	52

<u>FIGURE</u>	<u>TITLE</u>	<u>PAGE</u>
7a	Angle probe scanning at $\frac{1}{2}$ skip (position 1) and full skip (position 2) for maximum echo height from fatigue cracks scanned from both sides on each surface of the test bar under zero load	56
7b	Test piece mounted on three-point bending jig for angle probe scanning of fatigue cracks under compressive loading using the maximum echo technique at both $\frac{1}{2}$ skip (position 1) and full skip (position 2)	56
8	The effect of compressive stresses on the response of fatigue cracks when examined from both sides	57
9	Comparison between the response of fatigue cracks to compressive bending stress using 45° and 60° probes at $\frac{1}{2}$ skip position in mild steel	59
10	Comparison between the response of fatigue cracks to compressive bending stress using 45° and 60° probes at full skip position in mild steel	60
11	Effect of probe angle on the response of 2 mm fatigue crack to compressive bending stress in NP8	62
12	Effect of probe angle on the response of 4 mm fatigue crack to compressive bending stress in NP8	63

<u>FIGURE</u>	<u>TITLE</u>	<u>PAGE</u>
13	Effect of probe angle on the response of 6 mm fatigue crack to compressive bending stress in NP8	64
14	Comparison between the response of fatigue cracks in mild steel and in NP8 to compressive bending stress using 45 ^o probe	66
15	Comparison between the response of fatigue cracks in mild steel and in NP8 to compressive bending stress using 60 ^o probe	67
16	Comparison between fatigue cracks gap opening in mild steel and aluminium alloy (NP8) (x100)	68
17	Fatigue crack side view profile, showing variation in crack facets roughness and orientation in mild steel and aluminium alloy (NP8) (x150)	68
18	Ultrasonic response to fatigue cracks of different depths in NP8 under zero load to different angle probes	69
19a	Comparison between the responses of fatigue cracks in NP8 to compressive stresses using various angle probes at 5MHz frequency and full skip scanning	70

<u>FIGURE</u>	<u>TITLE</u>	<u>PAGE</u>
19b	Comparison between the response of fatigue cracks in NP8 to compressive stresses using various angle probes at 2MHz frequency and full skip scanning	71
20	Signal amplitude responses from fatigue cracks under compression using 2MHz and 5MHz probes at $\frac{1}{2}$ skip position in QT35-weld in the as-welded condition	73
21	Signal amplitude responses from fatigue cracks under compression using 2MHz and 5MHz probes at full skip position in QT35-weld in the as-welded condition	74
22	Optimum ultrasonic techniques for detecting fatigue cracks under both zero load and compressive stress when using 45° , 60° and 70° probes at 5MHz and $\frac{1}{2}$ skip scanning in QT35-weld in the as-welded condition	75
23	Ultrasonic responses to fatigue cracks under compression using 45° probes at different frequencies and scanning position in QT35-weld in the as-welded condition	78
24	Response to fatigue cracks under zero load in QT35-welds in the as-welded, stress-relieved and normalised conditions using 45° , 60° and 70° probes at 5MHz and $\frac{1}{2}$ skip position	81

<u>FIGURE</u>	<u>TITLE</u>	<u>PAGE</u>
25	Signal amplitude responses from fatigue cracks under compression in QT35-welds in as-welded, stress-relieved and normalised conditions, using a 45 ⁰ probe at 5MHz and ½ skip position	84
26	Ultrasonic screen traces of the signals from 2 mm and 6 mm fatigue cracks in QT35-weld in the as-welded condition, using 2MHz and 5MHz 70 ⁰ probes at ½ skip position	85
27	Comparison between the ultrasonic screen traces of 2 mm fatigue cracks in the as-welded and normalised QT35-welds, using 45 ⁰ , 60 ⁰ and 70 ⁰ probes at 2MHz and ½ skip scanning position	86
28	Surface topography of 6 mm fatigue cracks grown in QT35 submerged arc welds in the as-welded, stress-relieved and normalised conditions (x100)	87
29	Signal amplitude responses from fatigue cracks in different materials (NP8, QT35 and mild steel) under zero load using various angle probes at 2MHz and 5MHz and ½ skip scanning position	90
30	Signal amplitude responses from fatigue cracks in different materials (NP8, QT35 and mild steel), under zero load, using 45 ⁰ , 60 ⁰ and 70 ⁰ probes at 2MHz and 5MHz and ½ skip scanning position	91

<u>FIGURE</u>	<u>TITLE</u>	<u>PAGE</u>
31a	Test-piece mounted on bending jig	94
31b	Graphical representation of the geometrical and screen ranges	94
32	Response to fatigue cracks in the HAZ of 316 austenitic weldment under zero load using 45 ^o , 60 ^o and 70 ^o probes, 2MHz and 5MHz at $\frac{1}{2}$ skip scanning position	95
33	Signal amplitude responses from fatigue cracks in the HAZ of 316 austenitic weldment under compression, using 45 ^o , 60 ^o and 70 ^o probes at 5MHz and $\frac{1}{2}$ skip scanning position	96
34	Signal amplitude responses from fatigue cracks in the HAZ of 316 austenitic weldment under compression, using 45 ^o , 60 ^o and 70 ^o probes at 2MHz and $\frac{1}{2}$ skip scanning position	97
35	Comparison between the ultrasonic screen traces of 8 mm fatigue crack in the HAZ of 316 austenitic weldment, with the sound waves travelling through parent metal and/or through weld metal, using 45 ^o , 60 ^o and 70 ^o , 5MHz probes at $\frac{1}{2}$ skip scanning position	98

<u>FIGURE</u>	<u>TITLE</u>	<u>PAGE</u>
36	Comparison between the ultrasonic screen traces of 8 mm fatigue crack in the HAZ of 316 austenitic weldment, with the sound waves travelling through parent metal and/or through weld metal using 45°, 60° and 70°, 2MHz at $\frac{1}{2}$ skip scanning position	99

LIST OF TABLES

<u>TABLE</u>	<u>TITLE</u>	<u>PAGE</u>
1	Probes characteristics in steel	40
2	Analysed composition weight percent of free-cutting mild steel	41
3	Specified composition weight percent of aluminium alloy (NP8)	41
4	Mechanical properties of both mild steel and NP8	41
5	Fatigue cracks initiation and propagation conditions in both mild steel and NP8	42
6	Screen range/geometrical range values obtained from fatigue cracks in NP8, for 5MHz probes at $\frac{1}{2}$ skip scanning position	42
7	Specified composition weight percent of both QT35-steel welded plate and filler wire	43
8	Mechanical properties of QT35-steel parent metal and welds	43
9	Fatigue cracks initiation and propagation conditions in QT35-steel welds	44
10	Details of austenitic stainless steel parent plate material	45

<u>TABLE</u>	<u>TITLE</u>	<u>PAGE</u>
11	Welding condition details for the austenitic stainless steel	45
12	Mechanical properties of both austenitic stainless steel plate and weld metal	45
13	Fatigue crack initiation and propagation conditions in the HAZ of austenitic stainless steel weldment	46
14	Screen range/geometrical range values obtained from an 8 mm fatigue crack in the HAZ of the 316 austenitic stainless steel weldment (double-U)	47

1. INTRODUCTION

Ultrasonic examination of materials has played a major role in NDT for some thirty years, and a wide range of well established techniques for defect location and sizing is now available. These techniques are based on the measurement of the reflected pulse amplitude of ultrasound. In general, they can be used to detect almost any type of defect and can make useful estimate of defect size ⁽¹⁾. However, with the current state of the art, it is still not possible to report the exact size and precise nature of defects detected ultrasonically ⁽²⁾. This is because, in using the pulse amplitude techniques, it is assumed, that the amplitude is proportional to the size of the defect. The inadequacy of this approach is that there are other factors beside the size which have drastic effects on the signal amplitude of the reflected energy, such as; defect orientation, shape, roughness, etc., i.e. the reflective properties of the defect ^(1,3).

It is clear from the voluminous literature published during the last few years on defect sizing, that a universal solution to the problem does not exist, and may be never will, so there is a considerable need for improvement of ultrasonic testing capability for defect sizing and diagnosis ⁽⁴⁾.

The need exists to establish how the ultrasound interacts with real defects. Such data could be particularly useful, since these interactions are at the core of the ultrasonic testing problem ⁽⁵⁾.

The ultrasonic energy reflected from a defect has long been known to contain considerable information about the nature of the defect. It has also been considered that the ultrasonic signals reflected from a crack surface may contain information on crack closure, crack surface topography and residual stresses. Unfortunately this information is difficult to obtain even with sophisticated equipment. It is also difficult to characterise, as it appears to be affected by many parameters (5,6), among these parameters are:

- (a) Those related to the crack itself, including: its size, shape and morphology of the crack surface, i.e. crack characteristics.
- (b) Net stress acting on the crack faces such as: residual and applied stresses.
- (c) Important parameters related to the ultrasonic technique being used, such as: probe angle and frequency, scanning position and size of the beam at the crack, i.e. ultrasonic procedure.

However, the problem is still far from being completely solved.

In this investigation the experimental techniques were designed mainly to study the influence of elastic compressive stresses and related factors on the detection of fatigue cracks in various materials; both as parent metals and as welds. In addition, particular attention has been

given to the important inter-related experimental variables, in order to obtain results of general application.

It is hoped that quantitative estimates of these parameters will both assist in ultrasonic inspection and at the same time increase our understanding of the interaction of ultrasound with real defects. Eventually some of the current uncertainty in ultrasonic testing might be reduced.

2. LITERATURE REVIEW

2.1 Ultrasonics - Pulse/Echo Technique

2.1.1 Historical Background

Ultrasonics as a technology can probably be said to have had its birth during World War I, where the pulse transit-time, commonly, although not quite correctly, called pulse-echo method, has been used for locating objects under water such as icebergs and submarines ⁽⁷⁾. The foundations of the pulse-echo method was laid in the years immediately after 1920, following the work of Professor P. Langevin in France ⁽⁸⁾.

In spite of the various activities which follow Langevin in investigating various aspects of ultrasonics and looking for practical applications in this new technology (e.g. Wood and Loomis in 1927 ^(9,10)), ultrasonics remained primarily a laboratory technique ⁽⁷⁾ until Sokolov ⁽¹¹⁾ in 1929 suggested the use of ultrasonics for the detection of flaws in metals. However, only since World War II has it been extensively applied to non-destructive testing.

Progress was relatively slow, but the picture began to change with the practical development of what has proved to be a superior method of detecting flaws, namely the use of pulse-echo technique. In 1942, D.O. Sproule ⁽¹²⁾ in England, successfully adapted this principle using separate transmitting and receiving transducers. Almost simultaneously F.A. Firestone ^(13,14) in the United States, produced

an apparatus working on similar lines, but using a single transducer for transmission and reception (8).

Although the pulse transit-time method is also used with sound transmission, the reflection method nevertheless has gained considerably greater importance and even has given the entire method its name, i.e. pulse-echo method (15).

Ultrasonic testing by the pulse-echo method with normal probes has been used for more than 30 years for inspection of plates and forgings with good results. Weld examination by ultrasonics has become important with the development of shear wave angle probes, because of this tool, it was possible to detect flaws nearly perpendicular to the surface. This technique has therefore been widely used for the detection of radial cracks in rotor forgings and since 1953 (16) for the examination of rivet holes and butt welded joints.

Ultrasonic examination of materials has occupied an important position in NDT for several years now and a wide range of well established techniques for defect location and sizing is available. Many of these techniques are based on the measurement of ultrasonic pulse-echo amplitudes to estimate defect size and are taught by established schools of NDT (17).

2.1.2 General

Until recently, the traditional method of detecting defects inside metallic components has been by radiography. The major drawback, however, is that a narrow crack, which

might cause a major failure of the component in service, will not be detected unless it is parallel to the radiation beam. Even if a crack is detected, its depth within the component and its dimensions parallel to the path of the radiation are unknown. Ultrasonic testing suffers from none of these limitations and for crack detection and measurement during manufacture and in service is now unchallenged (18). Ultrasonics, because of its convenience and its greater ability to detect and measure cracks has been gradually supplementing radiography, particularly for the NDT of pressurised components (19).

By far the most widely applied ultrasonic inspection is the simple manual A-scan. Only in exceptional circumstances would defects first be detected and located by any other technique. In many applications, manual A-scan is also quite satisfactory for measuring defect size giving results accurate \pm a few millimetres (4).

The data available to the ultrasonic operator in a conventional inspection are: echo amplitude, echo range, pulse shape and the dynamic behaviour of the echo as the probe is scanned and swivelled. From this information, the position of the echo defect can in principle be determined. Through-wall extent, orientation and defect length can also in principle be estimated (1).

The reasons for the importance of ultrasonic examination in NDT are to be found in the high reflectivity of narrow defects such as cracks when "illuminated" by ultrasound

and the comparative ease of applying ultrasound to detect defects deep within materials. Despite this fundamentally favourable position, there is no doubt that the presently available ultrasonic techniques cannot be relied upon with certainty to detect and accurately size crack-like defects⁽¹⁷⁾.

Ultrasonic defect characterisation, which refers to determination of size, shape, orientation, composition, etc., by ultrasonic interaction with a defect is becoming increasingly important in modern non-destructive evaluation. No longer is it sufficient merely to locate defects in materials. A more definite description of defects is required for input into sophisticated design analysis that will give a better assessment of the probability of failure and hence reduce the number of costly component replacements. In traditional ultrasonic testing, primary interest has centred about the correlation between the amplitude of the received signals and the size of the discontinuities giving rise to these signals. In this approach, it is assumed that the amplitude of the flaw-induced echo is proportional to the size of the defect. The inadequacy of this approach is that defect orientation, attenuation, composition, etc., also have drastic effects on signal amplitude. In addition, amplitude information alone is not capable of providing information about defect shape, which may be of paramount importance, since for certain applications the shape of the discontinuity may determine whether or not its presence will compromise the integrity of the components. The ultrasonic determination of defect character relies upon responses returned usually by

reflection, from features of the defect itself containing sufficient information to enable it to be classified un-ambiguously as planar, no-planar, rough or smooth, etc. Thus from these salient features and knowledge of its position and orientation a prediction of defect type may be made. In conventional testing, as normally applied on-site, this process is almost entirely subjective and based on operator experience (4).

In spite of the development of a variety of sophisticated ultrasonic techniques, there is still only a very limited capability for characterising defects of any orientation or composition without the requirement of very specialised calibration standards (20).

2.2 Ultrasonic Detection of Fatigue Cracks and other Planar Defects

Fatigue is one of the most serious practical problems in metal construction. The fatigue strength of a component is affected by a large number of factors. Therefore, the prediction of the actual fatigue life or the detection of fatigue damage before a catastrophic failure is a very important but difficult task (21). It is hardly surprising that 70-90 percent of all industrial failures, including ships, involve fatigue (22,23,24,25). Using fracture mechanics coupled with the knowledge of crack sizes can give the prospect of predicting the life of cracked structure, and if it has already been in service, how much life remains (26).

The increased interest in the importance of quality assurance has pinpointed a need for a better understanding of the

significance of cracks in engineering components. At one time cracks were quite large before they were detected, but with increased sensitivity more and more cracks are detected during initial inspections or early in the life of a component. It has become important to define a critical defect (crack) size, and this means that detection has to be quantitative. A number of National and International Conferences have been held involving particular aspects of this subject (27).

As fatigue cracks are almost always open to the surface of the material, the conventional methods of crack detection such as the penetrant or magnetic methods may be applied when the crack has grown sufficiently and are, in fact, the basis of most methods of intermittent inspection for detecting fatigue damage. The drawbacks are that inspection is intermittent and is sometimes difficult to apply because of the inaccessibility of components likely to suffer fatigue damage. Hence ultrasonic and/or radiographic inspection are applied (28).

When inspecting structural members for fatigue cracks using ultrasonic pulse-echo techniques, one is faced with the problem of selecting suitable standard reference specimens for interpreting defect signals (29). For the surface breaking cracks (fatigue cracks), reference standards often consist of spark eroded slots or saw cuts produced in a position geometrically similar to that for the crack to be measured. However, many difficulties are associated with

the use of artificial reference defects and successive unsatisfactory results have been reported (30,31). These have been related to the many factors which influence the return signal from real cracks, such as; crack shape, crack surface roughness and crack orientation. In addition fatigue cracks are poorer reflectors of acoustic energy than machined flaws of corresponding size and shape (29). The signal also varies with the frequency, wave mode and beam width of the probe and mode conversion upon reflection. Further, much of the ultrasonic intensity can be transmitted across fatigue crack causing the return pulse to depend on the state of stress in the region of the crack. This state of stress is determined by material type, crack growth history, stress relaxation and induced stresses. These effects prevent the intensity of the reflected pulse from always increasing monotonically with depth (30). Furthermore, using artificial flaws for calibration, the shear wave technique badly underestimates the crack depth and overestimates the crack length (32).

The most common use of ultrasonics is the simple pulse-echo technique which detects the return signal scattered by a defect, i.e. size estimates of a defect depend upon the proportion of the ultrasonic beam reflected back to the probe. Thus "reflectivity" is a decisive factor in estimating the size of a defect. The strength of the signal gives some indication of the size of the defect, but quantitative estimation of size requires careful interpretation (30). The reflection characteristics of sound

waves that are incident on a surface obliquely are of considerable importance in ultrasonic defect detection. Although it is possible that some inspection problems involve simple geometries, nicely oriented cracks, and propagation paths that are always normal to interfaces, these are probably the exception. It is much more common to encounter situations where the opposite is true (7). Changes in the angle of incidence will have large effects on the relative amplitudes of pulses due to the different reflection mechanism involved at various angles. The need exists to establish how this ultrasound interacts with defects. Such data would be particularly useful, since these interactions are at the core of ultrasonic testing problems. Unfortunately, this information is difficult to obtain since sophisticated equipment is required. It is also difficult to characterise, since it is affected by many parameters (5).

To reduce the uncertainty of detecting planar defects oriented at an adverse angle to the ultrasonic beam, it has been found to be advantageous to use several beam angles from several directions. Examination from top and bottom surfaces of the plate is another valuable technique (34). "Looking" at a crack from two directions at various angles increases the probability of coping with poor reflectivity due to crack orientation, tightness and smoothness (35).

The angle probe choice is very important, since it is desirable to have the sound beam striking as perpendicular as possible to get the greatest response. Thus to search for cracks in a variety of orientations, it is desirable

to introduce the sound pulse into the component at various angles. It is also necessary to consider other factors in making probe selection such as type of material to be tested, the thickness involved and weld geometry and welding process, when welding inspection is involved. The following refracted angles are usually suggested ⁽¹⁸⁾:-

<u>Material Thickness</u>	<u>Probe Angle (degrees)</u>
½" (12.5 mm) and less	70 - 80
Over ½" (12.5 mm) to 1½" (37.5 mm)	60 - 70
Over 1½" (37.5 mm) to 2" (50 mm)	45 - 60
Over 2" (50 mm)	45

Obviously the choice of angle probe is not dependent on material thickness alone. Although it is desirable to employ several probes of different angles the real criterion for probe selection is often a matter of economics rather than good practice ⁽³⁶⁾.

Improvements to defect measurement in conventional tests are possible by careful choice of probes, keeping the beam as narrow as possible and selecting probes from the range of high performance models commercially available ⁽⁴⁾. It has also been shown experimentally that with a proper choice of angle probe, the source of background signals can be minimised if not completely avoided. In addition, the use of shear waves at small angle of incidence offers advantages; accuracy and resolution are almost doubled and because of the small angle, the amplitude is very sensitive to probe displacement. A slight lateral displacement will

cause a sharp drop in amplitude. This makes it easy to determine the exact probe position for maximum amplitude (37). Another problem area is the mis-match between the ultrasonic set and the probe. This has been stressed by Jackson (38), who claimed that many difficulties stem from mis-matching. Selecting probes which have been designed to match the ultrasonic set can overcome these problems and will provide optimum sensitivity, a narrow dead zone due to reduction of "ringing" of the probe, clearer time-base and optimum resolution.

Meyer (39) and Gericke (40) claimed that an improvement in the detection of defects and in size evaluation can also be achieved by reducing the test frequency which gives increased beam spread. Ridder (36) also confirmed the use of lower frequencies in order to obtain a wider divergence of the reflected sound beam would be advisable. However, this will result in a decrease in resolution and the detection of small defects (whose diameter $< \frac{1}{2}$ wavelength) is a problem. A determination of frequency dependence of the defect echo amplitude will yield information on the defect geometry, since the reflection of ultrasonic energy from a defect depends on the ratio of the defect size to the ultrasonic wave length (39). A variety of procedures for processing reflected ultrasound waves and their variations with probe angle and frequency are being sought as a means to identify defect parameters (41). There are trends which indicate that through thickness sizing is more accurate with lower angles and higher

frequencies ⁽⁴⁾. It is also important to consider the material in selecting the test frequency, since although it may be desirable to increase the frequency this will often result in increased attenuation. Consequently, if it becomes rather difficult to penetrate the material, it may be necessary to lower the frequency ⁽³⁶⁾.

2.3 Reflection of Ultrasonic Shear Waves at Air Gap in Steel and Mode Conversion

An ultrasonic beam travelling through a solid body is almost totally reflected when it encounters an air gap. This is shown in Figure 1, where a beam of shear waves S strikes a boundary between steel and air at angle α to the normal. A part of the incident beam is reflected back into the steel as a beam S of shear waves at an angle α to the normal. Another part of the incident beam is converted into a beam of compression waves C at a bigger angle β , i.e. mode conversion.

Mode conversion occurs at incident angles between 0 to 30.7 degrees ^(42,51). The relative intensities of these two reflected beams depend on the angle α and are shown graphically in Figure 2. These intensities of shear and compression wave components after reflection are shown as curves S and C respectively. The value of compression wave angle for a particular incident angle α is obtained from the curve marked B.

The fall of S takes place until $\alpha = 30.7$ degrees (i.e. critical angle for shear wave). At this point, the S

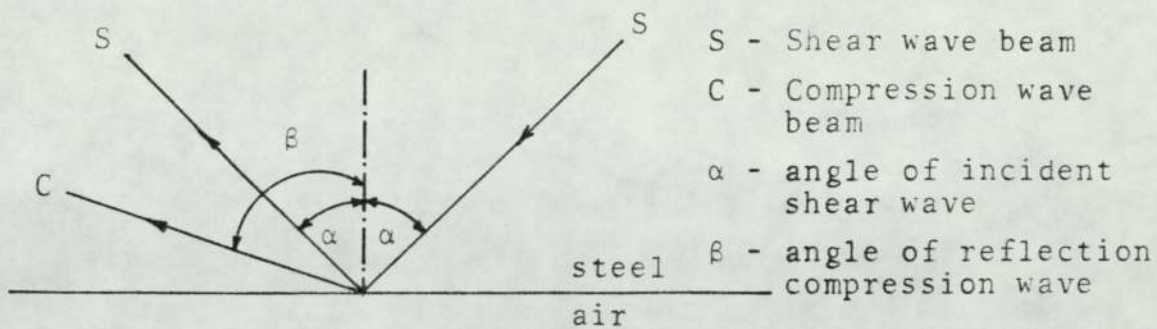


FIG. 1: Reflection of incident shear wave with partial conversion into compression wave at steel/air boundary

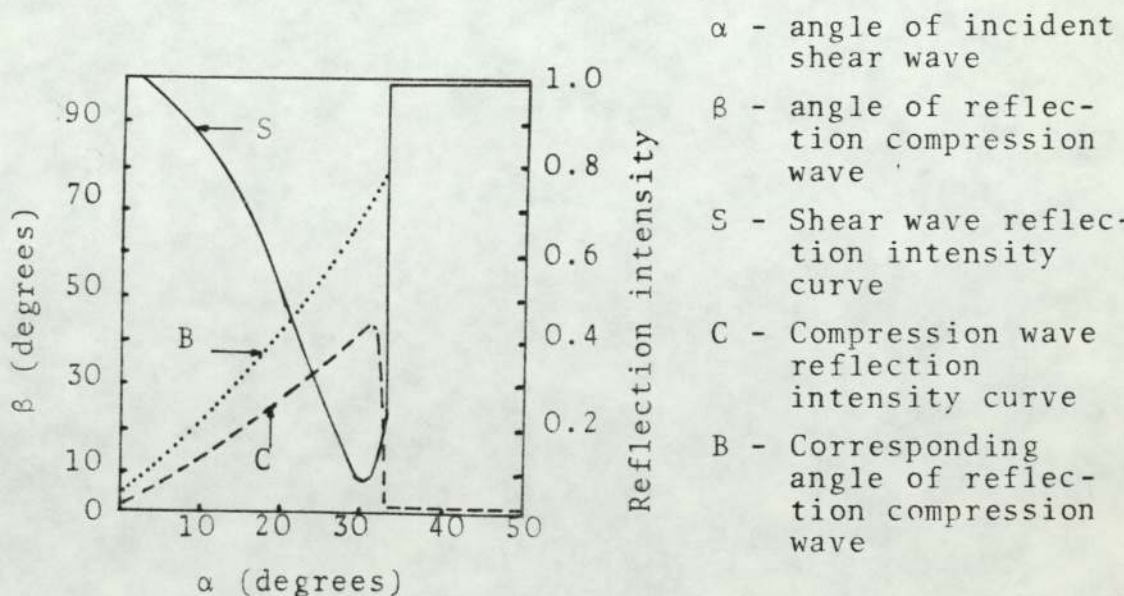


FIG. 2: Relative intensity of shear and compression wave component after reflection of shear wave beam

intensity turns upwards until $\alpha = 33.5$ degrees, where there is a sudden total reflection of S without any conversion into C (7,51).

A significant amount of energy can be converted from the 60° shear wave mode to the longitudinal when waves undergo double reflection at the surface of the sample and the intersection of a perpendicular planar defect such as fatigue crack. Since the compression reflection angle is different from the incident angle, the energy converted to longitudinal wave does not return to the probe (29). This is shown in Figure 3, where the incident angle is 30° , which is less than the critical angle for shear waves (30.7 degrees) and the reflected beam is therefore a mixture of shear and longitudinal waves (43).

The weak response from a 60° probe has been recognised by a number of investigators and is related to the mode conversion (29,44,45,46). There is, therefore, some risk of under-estimating the size of a crack or even missing it altogether. This has been stressed by Doyle (30), who claimed that it is possible for a reflected pulse to disappear altogether at suitable angles due to mode conversion. This emphasises the caution needed in applying the pulse-echo technique.

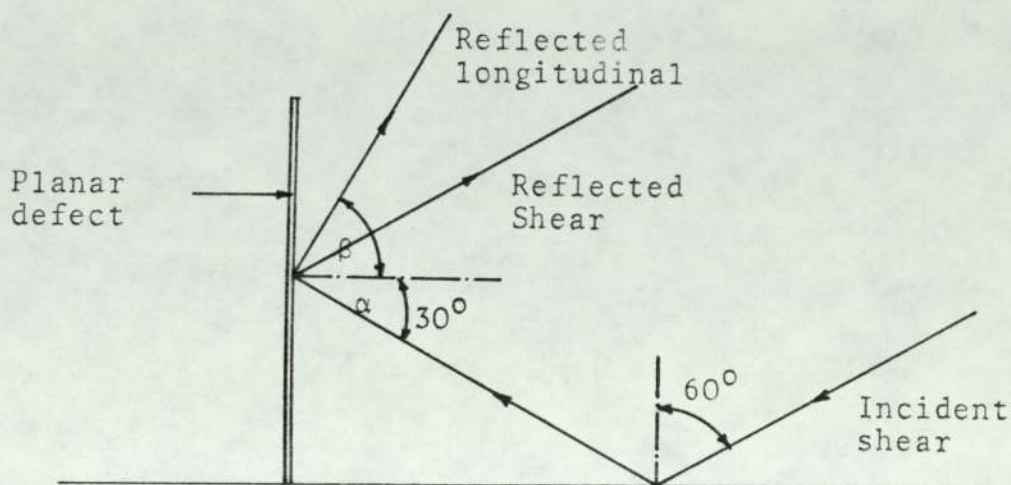


FIG. 3: Shear waves from 60° probe are incident on a vertical planar defect at 30° and are reflected as a mixture of shear and compression waves, after double reflection

2.4 Limitations of the Pulse-Echo Techniques

The limitations of present-day NDT methods are recognised in many publications (47,48,49), but there is no doubt that techniques will improve to allow the detection of smaller defects. This could well produce a rise in weld repair costs which at some point no one could afford (50). What is needed now most of all is a better understanding of the limitations of ultrasonics in detecting and measuring defects, particularly planar defects. This will bring about important changes in the defect acceptance standards used to judge the fitness for purpose of components (52). There is consequently a need to broaden our ultrasonic capabilities, so that size, shape and orientation of defects can be determined. In order to achieve this a better understanding of the interaction of ultrasound with defects is needed (41).

During the past few years there has been a move away from the employment of reflected pulse amplitude to estimate the size of defects. A number of techniques based on the use of surface waves in a time delay mode have been proposed, such as those of Cook (53) and Hudgell et al (54). Spectrographic techniques have also been proposed (55,56), although as yet these do not appear to have made much impact on practical defect sizing. Both time domain and spectrographic analysis offer potential advantages over attempts to use amplitude in quantitative manner. They are less prone to the effects of variations in coupling, reflectivity, defect geometry and interference. All these

factors modify the reflected pulse amplitude in a manner unrelated to defect size ⁽⁵⁷⁾. Nevertheless, the amplitude based system is still the procedure most used in the field today ⁽⁵⁸⁾.

In the pulse-echo technique it is customary to regard the presence of a signal as indicative of the existence of a defect and the amplitude of the signal as related to defect size. The ultrasonic amplitude technique as currently used is, however, limited by its non-quantitative capabilities. In this sense non-quantitative implies that current technology is capable only of producing a signal that indicates the presence of a defect, but it can say very little about the characteristics of the defect. This limitation has been brought into sharp focus in recent years with the advent of fracture mechanics as a major structural design and maintenance philosophy ⁽⁵⁹⁾.

One of the most severe limitations of current amplitude techniques is that they are not capable of giving the size, shape and orientation of a defect which lies in a stressfield. A fully satisfactory answer will require a thorough study of the morphology of defects and the reflection of the ultrasound waves from them ^(52,59,60).

In manual inspection probes are used singly in the pulse-echo mode, and several beam angles are necessary to increase the probability of detecting the specular reflection from smooth cracks, or the weak diffuse scatter from a rough jagged crack. The signal's strength depends on

the amount of sound transmitted into the component and, more fundamentally, on the reflecting properties of the defects. Research is therefore required to indicate the smallest number of probes which provide the required level of confidence in the test (60).

The use of ultrasonics for the detection of welds has increased considerably during the last few years, but it still has not gained the level of acceptance that it should have (36). It is clear from the voluminous literature published in recent years on defect sizing and characterisation that a universal solution to the problem does not exist and may be never will (61).

Ultrasonic holography, ultrasonic spectroscopy and focussed ultrasonic probes have each been used in specific 'one-off' type situations for providing further information on sizing and identification, particularly for buried or relatively inaccessible defects. However, combination of their cost, early stage of development and lack of conclusive understanding of their behaviour have so far restricted their use. Significant advances in this field can be expected over the next few years (61). Increased sophistication of equipment has led actually to a less accurate assessment than would have been afforded by simple manual testing (1,4).

There are many variables which affect the conventional ultrasonic inspection of defects and reproducibility of results. The most important variable is the procedure. The next most important variable is the quality of the

personnel. The problem of reliability of defect detection is receiving increased attention in the United States. An example of this interest is that over \$1,000,000 of research monies are being spent on the detection and evaluation of stress corrosion cracks in stainless steel piping (62).

Ultrasonics can be a rapid means of examining thick weld sections and gives one the advantages of being able to quickly obtain the defect depth as well as its length. It may not be possible to determine the type of the defect by attempting to interpret information presented on the screen alone. A skilled operator can use his knowledge of the weld geometry, the type of welding process used, the type of material, the condition of the material and the position of the defect and its ultrasonic response to make a logical decision. Until such time as ASME code accepts ultrasonic methods as well as radiography for examining specific weld joint configurations, ultrasonic methods should at least be used to supplement radiographic examination to give engineers greater confidence. It is not in any way intended or suggested that ultrasonics be used as a total replacement for radiography. However, there are many instances where this technique could be used to good advantages (63).

2.5 The Influence of Compressive Stress on the Ultrasonic Response from Fatigue Cracks

For a number of years it has been suspected that the ultrasonic response from cracks may be altered considerably by

the application of stress and there is some published evidence to support this view (32,64,65,66,67). Although fatigue cracks grow under tensile loads, they may be in residual compression when examined. Such tight cracks could present a small enough gap width to permit significant transmission and hence poor reflectivity, thereby prejudicing both detection and sizing (61). Examples have been seen in the literature (54,66,68,69).

A compressive stress generally decreases the amplitude of the echoes from cracks and increases the signal transmitted through the crack. Consequently echoes from tight cracks may not be appreciably larger than those from small inclusions making it difficult to detect the cracks in the pulse-echo technique.

There are situations where a component may be subject to fatigue during service at high temperature or pressure, and yet during shut-down the resultant stress may be compressive (6). It is also known that the capability of detecting cracks is improved by the application of tensile stress (67,70).

However, the few results on the effects of compressive stresses on fatigue crack detection which are available seem to be limited to small fatigue cracks in aircraft wings (Chang et al, 1973 (64)) and compressor blades (Lake et al, 1975 (71)).

In 1980, Fiat investigated the defect detection capability using ultrasonics, radiography and dye-penetrants for

detecting cracks in aluminium alloy plates for the European Space Agency. The results for ultrasonics were found to be the worst of the three NDT methods. This was thought to be related to the compressive stresses across the walls of some cracks, which may have caused them to become transmitting and so not detectable by the technique ⁽⁷²⁾. This is also confirmed by Chang et al ⁽⁶⁴⁾ who found that compressive loading tended to hold fatigue cracks together and diminish their ultrasonic response.

Ultrasonic shear wave measurements do not measure the true depth of a crack but only the depth for which the crack opening displacement is greater than some critical amount. Thus when stressing the crack the apparent indicated crack depth increases under tension and decreases upon compression. The change in intensity of echo signals with applied stress is related to the change in the effective crack opening, which in turn is a function of the stress intensity at the crack tip ^(32,67).

When a crack is compressed the dominant effect is a steady reduction in echo amplitude caused by the increase in actual area of solid contact between the crack faces ⁽⁶⁾.

Residual compressive stresses particularly in welds and castings will lead to defects being undersized by ultrasonics. Such stresses, however, also reduce the likelihood of fatigue crack growth. These stresses are usually variable and largely unknown ⁽⁶⁾. There is a need for more

measurement of residual stresses. Although considerable effort and money are put into the measurement of static tensile properties, parts rarely fail because of non compliance with the requirements for yield or ultimate tensile stress. They fail primarily because of fatigue, or in the case of high strength aluminium alloys, stress-corrosion. However recognition of the presence of stresses, let alone their measurement, is seldom included in procurement specifications (73).

2.5.1 Fatigue Cracks Surface Topography

For a given material, the minimum detectable fatigue crack size appears to be dependent on the maximum fatigue load and the sequence of load application. These two features affect the ultrasonic response via residual closure stress, which in turn affects the crack opening. There appears to be a direct correlation between maximum tensile load and crack surface roughness. However, more work is needed to relate ultrasonic response to crack surface topography (65).

Crack detection using ultrasonics is not solely dependent on the overall crack orientation, because a crack tends to have a jagged irregular surface. Though the entire side of a crack may not be in a plane perpendicular to the sound beam, many small facets of this surface are, and these facets reflect the sound back to the probe. This reflection behaviour of a crack or what is called "reflectivity" is an important factor in estimating the size of a crack (34,74). If a crack is tight and does not have many reflecting facets it may be quite difficult to detect (69,75). The overall response from a crack appears to be composed of elements

from small facets on the surface. Experiments have demonstrated that the ultrasonic response from cracks is greatly modified by defect roughness (4).

Preferentially oriented facets of a crack surface gives spikes in the response which in turn give a reflected pulse proportional to their height. It is possible, therefore, for a first approximation to consider a surface of this type as a large number of facets each reflecting independently. Hence the probability of detecting such a crack can be enhanced over a smooth crack by the occurrence of the occasional facets at near normal incidence to the incident beam. It is thus necessary to study crack topographies for the occurrence of facets as a function of both size and orientation relative to the mean direction of the crack (75).

The nature of the reflective surface of a crack depends upon the fracture process. Fatigue cracks have relatively smooth surfaces, whereas creep cracks and stress-corrosion cracks can present a very rough profile to ultrasonic beams and scatter it in a very different way. Sound reflected from a rough surface, like many crack faces, has two components; a coherent component which is reflected in the specular direction, and incoherent component scattered diffusely into a wide solid angle. The ratio of diffuse to specular scattering increases rapidly when the root-mean square roughness exceeds one eighth of the sound wave length (18).

Fatigue cracks usually grow in a plane perpendicular to the main principal stress at least as long as the crack growth rate is low. At faster crack rates the growth direction remains perpendicular to the maximum principal stress, but the plane of the fatigue fracture will be at an angle of 45° with that stress for several materials⁽⁷⁶⁾.

The reflected energy from a fatigue crack surface is generally not symmetrical about the beam axis, because its distribution depends not only on the incident energy but also on the geometry and reflectivity of the crack surface. The upper portion of the crack near to the surface reflects more energy per unit area than the rest of the crack. Consequently, the incident energy required to detect a signal reflected from the tip (bottom) of the crack is generally greater than that from elsewhere on the crack surface. Failure to recognise this geometrical effect on the reflected energy would lead to an under-estimate of the actual depth⁽⁴⁴⁾.

2.5.2 Fatigue Crack Closure

Fatigue crack size estimation has been shown to be dependent upon the applied stress and hence if compressive stresses are present the crack size is under-estimated due to crack closure^(32,66,67). Ultrasonic energy transmission is possible if the crack is closed. However, a mechanically closed crack is not the same as an "acoustically" closed crack⁽⁷⁶⁾. This is because crack closure under compressive stress is imperfect, as the area of

contact depends on the compression of surface roughness peaks. The size of the surface irregularities relative to the acoustic wave length is an important parameter and in some instances complete "ultrasonic transparency" has been reported at stress levels of only 20 MN/m^2 (29,37). The difference between an "acoustically" open and closed crack is only of the order of micrometers (44).

The ultrasonic response of a closed crack differs from that of an open crack in two characteristics; first, the signal amplitude is much lower, second, closure makes the crack semitransparent to ultrasonic beam. Because of the low amplitude from the closed crack and the high noise background, a signal may approach the noise level and become undetectable (37).

Mechanical crack closure can be caused by plastic deformation left in the wake of the growing fatigue crack. It should be expected that material with a high yield stress will form a small plastic zone and thus show less crack closure. However, small plastic zones can still leave sufficient residual deformation and stress to cause closure (76).

2.6 Ultrasonic Inspection of Austenitic Weldments

It is assumed that ultrasonic waves can travel through the material to be tested substantially without hindrance, but in certain types of engineering material however there are fundamental difficulties, simply in propagating the wave. These difficulties arise whenever the grains in the material

are not small compared to the wave length of sound. In this situation a high level of scatter arises at the grain boundaries and can mask signals from even quite large defects. The difficulties are especially present in cast or welded Inconel and austenitic steels and are described in several recent papers and reports (77,78,79, 80,81,82,83).

In recent years considerable use has been made of austenitic stainless steel welds and castings, particularly in the chemical industry and in nuclear power plants. Such components have been regarded as uninspectable by ultrasonics and have relied on radiography. There is a need however to demonstrate that such welds and castings are free from significant defects. Defect size measurement is very difficult and special techniques need developing, since the usual pulse-echo methods are not applicable (52). Adequate defect identification and characterisation are inhibited (82).

Ferritic castings may sometimes exhibit the same effects where there has been no heat treatment to refine the as-cast structure. There is no practical grain-refining heat treatment for austenitic materials and the as-cast structure inevitably persists. Forging does modify the structure, but austenitic forgings still often contain large grains which make ultrasonic penetration difficult. For welds the situation is particularly bad, because preferential grain alignment along the thermal gradients during welding makes the completed weld elastically anisotropic. When this happens the ultrasonic beam may be grossly distorted and skewed

away from the forward direction. The consequent loss of signal strength makes the detection of small defects impossible. The need to establish suitable ultrasonic techniques for austenitic weld inspection has become of great importance due to the extensive use of austenitic materials in the construction of power stations, and particularly nuclear power plants. Conventional ultrasonic shear wave techniques commonly used on ordinary carbon steel welds are not directly applicable to welds in austenitic stainless steel as their microstructure dominates the wave propagation response (81).

In any weld, when the first run of weld metal is deposited, columnar grains grow along the maximum thermal gradients as the metal cools. Growth in this direction is faster than in others and this leads to the rapid disappearance of unfavourably oriented grains. Deposition of subsequent weld metal, reheats the bead and, although in the case of ferritic weld, the columnar grain structure is destroyed by the austenite-ferrite phase transformation, no such transformation occurs in the austenitic alloys, and consequently, the columnar grain structure survives, and the grains continue to grow as the weld is built up. The result is a weld which contains long columnar grains spanning many weld runs which have a dendritic structure and tend to grow with $\langle 100 \rangle$ crystallographic axis parallel to the crystal axis (82). The finished weld is highly anisotropic, and the velocity of sound within it depends strongly on the direction of propagation.

It has been established that sound attenuation is high both parallel and perpendicular to the grains, but low at an angle of 45° . This is now known to be a general property of textured columnar structures in F.C.C. metals and has been observed in a wide range of austenitic welds (18).

It has also been established that ultrasonic velocity is strongly dependent on the angle made by the direction of wave propagation and the axes of columnar grains existing in the weldments (81,84,85,86). A ~~min~~imum occurs at approximately 50° , and two distinct minima occur when the direction of the waves is parallel to the grain axis (0°), and when perpendicular to them (90°), the former being the lower in value. Sound waves which propagate in these weldments are skewed during their passage through the weld metal/parent metal interface due to the angular variation of velocity, and tend to be refracted towards the direction of maximum velocity (87). These effects of velocity and attenuation and the consequent beam skewing, present serious difficulties in the inspection of these weldments by conventional shear wave probes. However, A. Juva and J. Lieto (46), B.S. Gray et al (88), E.R. Reinhardt (89), and C.J. Abrahams (90), have all found that pulse-echo shear ultrasonics is a viable volumetric inspection technique, when certain conditions, such as plate thickness, weld geometry, size of grains structure, are met.

Of the two techniques currently available for the assessment of internal weld quality, namely radiography and ultrasonics, the latter is more sensitive to the most critical type of defects, and is also applicable to a wider range of configuration. Certain joint configurations, e.g. butt-welds in relatively thin sections, can be examined by radiography. Other, such as branch or stub welds onto vessels, are geometrically unsuited for radiography and require the use of ultrasonics for examination of the full weld section. The likelihood of a much increased use of austenitic materials in future power generation plant, and the higher standard of plant integrity that will be called for, make the establishment of reliable ultrasonic techniques for welds in these materials of prime importance. A number of papers have been published on testing austenitic welds, but different opinions have been expressed on the usefulness of ultrasonic examination. An optimistic view is taken by Grebennikov and Sotnickenko ⁽⁹¹⁾ who claimed that $\frac{1}{2}$ inch (~ 12.5 mm) thick welds in 18/8 stainless steel can be satisfactorily tested using a relatively low frequency probe with beam focussing to improve the signal/noise ratio. In the literature there is little guide to the size and position of defects that can be confidently detected in welds. Such information is essential before ultrasonic testing can be specified on austenitic joints. The use of compressional wave angle probes appears to show much improvement in both attenuation and spurious signal characteristics ⁽⁹²⁾. Good results have been

achieved in the angle probes using longitudinal waves, often by means of transmitter/receiver technique. One difficulty in the practical application of these special probes is presented by the shear waves which accompany longitudinal waves at an oblique angle, i.e. mode conversion, and the shear wave component can be the cause of spurious indications.

3. EXPERIMENTAL TECHNIQUE

3.1 Mild Steel and Aluminium Alloy

3.1.1 Ultrasonic Testing

The ultrasonic flaw detector type PA.1020 and the probes used throughout this study were all manufactured by Baugh and Weedon to avoid mis-matching thus achieving optimum performance.

A number of preliminary tests were carried out to assess the characteristics and performance of both ultrasonic set and the probes most commonly used. These tests included:-

1. Determination of probes characteristics (Table 1)
2. Assessment of probe beam spread (Fig. 4).
3. Determination of the responses of the probes to artificial reflectors:-

(i) The 100 mm curved quadrant of the IIW calibration block, where the same sound path distance (range) can be achieved for different angle probes (Fig. 5).

(ii) Drilled holes, machined slots and then fatigue cracks (Figs. 6a and 6b).

Hence detectability and sensitivity were established.

All the probes were set to obtain the maximum echo height possible from both artificial reflectors and fatigue crack surfaces by moving the probe forwards and backwards and by

rotation. After obtaining the maximum echo signal for either $\frac{1}{2}$ skip or full skip scanning position, the ultrasonic sensitivity level was adjusted by bringing down the signal to a reasonable height on the screen using the calibrated attenuator. The sensitivity level used throughout the tests was set to bring the maximum echo signal to 80% full screen height (F.S.H.), which corresponds to 5 cm height on the screen. This was found to be adequate for all the range of crack depths and the testing conditions used.

For fatigue cracks to be tested under compression using the 3-point bending jig of the Vibraphore fatigue machine, shown in Fig. 7b, good coupling was necessary, hence the use of silicone grease and plastic insulation tape to strap the probe carefully in position. Reference defects were not required as fatigue cracks of known depths were involved. Calibration was done using either the V_1 or V_2 blocks for mild steel and a minimum of two echo signals. In the case of the aluminium alloy specimens, a machined block from the same alloy was prepared which corresponded to the international V_2 block dimensions.

The most significant probe parameters, e.g. beam angle, frequency and scanning positions were varied in order to establish the most effective combination of probe angle and frequency for inspecting fatigue cracks. 45° , 60° and 70° probes, 2 and 5 MHz frequencies were used at $\frac{1}{2}$ skip, and full skip scanning (Fig. 7a) whenever possible, depending on the length of test bars.

The same procedure was applied when testing fatigue cracks in both the QT.35-welds and in the 316 austenitic stainless steel weldment. Accurate calibration was found to be essential in the detection of fatigue cracks in the austenitic weldment, especially when propagating the sound through the weld metal, and continuous checks of screen calibration were maintained throughout the tests. Only the $\frac{1}{2}$ skip scanning position was used in order to minimise the considerable attenuation which is found in austenitic welds.

3.1.2 Preparation of Fatigue Cracks

Three specimens from each alloy whose mechanical properties are given in table 4 were machined to bars of dimensions 200 x 25 x 25 mm for mild steel and 225 x 25 x 25 mm for NP8. All specimens were finished by grinding. A V-notch of 60° included angle and 2 mm deep was cut in all the bars as a crack starter. 2, 4 and 6 mm fatigue cracks were propagated in both mild steel and NP8 bars using a 2-ton Amsler Vibraphore fatigue machine. The V-notches were then machined off and the surfaces finished by grinding. Table 5 indicates the fatigue cracking conditions for both initiation and propagation stages for mild steel and the NP8 alloy specimens.

This procedure was adopted throughout this study, with different fatigue cracking conditions for QT.35-welds and the 316 austenitic weldment as indicated in tables 9 and 13.

3.1.3 Compression Testing

The specimens containing fatigue cracks of known depths

were placed in the Amsler 3-point bending jig. This was done after the probe had been securely bound to the sample for maximum echo signal height with the specified sensitivity. Static compression was applied by having the crack downwards, as shown in Fig. 7b. The resultant compressive stresses were kept below the yield strength of the material under test for two reasons:

1. bending theory only applies up to the yield stress of the material, and
2. to avoid permanent bending of the specimens, as bending will affect the echo signal from the crack.

The elastic bending loads were introduced in small increments and the amplitude of the echo signal was recorded in dB, keeping the signal height at 80% F.S.H. for each load increment. This procedure was continued until the pre-determined load was reached. This was treated as the loading cycle. The applied load was then reduced in small increments of the same magnitude as in the loading cycle and the echo amplitude was recorded for each increment until zero load was reached, which indicated the end of the unloading cycle.

In the case of fatigue cracks in QT.35-welds and 316 austenitic steel weldment the same procedure was used, but applying different pre-determined loads, which depended on the yield stress of each material.

3.2 QT35 Steel

3.2.1 Preparation of QT35 - Welded Plate

The 1 inch (25 mm) thick QT35 steel plate of composition shown in table 7 was first cut to the required welded plate dimensions of 275 x 375 mm. For uniformity, this plate was then cut, so that the rolling direction would be parallel to the welding direction. A double V-butt joint with 6 mm root face and 60° included angle was then prepared for welding.

The welding procedure consisted of tacking the positioned plate at both ends and run-on and run-off plates were used. After a number of trial runs satisfactory welds were produced under the following conditions using submerged arc welding process:

Current	600 amps
Voltage	30 volts
Welding speed	20 in/min (500 mm/min)
Filler Wire Dia.	4 mm
Flux	Lincoln No. 1

A multirun weld was made and to avoid lack of root penetration, which has proved to be a problem using the submerged arc welding process, the following welding procedure had to be adopted. After the first weld run, the plate was allowed to cool, and then the reverse side of the joint was ground out so that the weld deposit was well exposed along the whole length of the weld. The second weld run was then made after the exposed surface had been thoroughly scratch-brushed and degreased. After two weld runs, the plate was

again turned over to be partially welded from other side to avoid bending due to distortion. The required number of weld runs on each side of the joint was then completed. Radiography indicated that the weld was "defect free".

It was decided to investigate the response of fatigue cracks to compressive stresses in welds in three conditions:

- (i) as-welded,
- (ii) stress-relieved, and
- (iii) normalised.

Hence, the welded plate was cut into three equal sized plates and the weld reinforcement was machined off from both sides of the plates. Two of these plates were heat treated as follows:

stress-relieving - 600°C for 1 hour - air cool
normalising - 950°C for 1 hour - air cool

3.2.2 Preparation of Fatigue Cracks in QT35 Welds

The welded QT35 steel plates representing the three conditions, having mechanical properties listed in table 8, were machined to bars of dimensions 250 x 25 x 25 mm. All specimens were finished by grinding. A V-notch of 60° included angle and 2 mm deep was cut along the weld centre line as a crack starter. 2, 4 and 6 mm deep fatigue cracks were propagated using a 2 ton Amsler Vibraphore fatigue machine. The V-notches were then machined off and the surfaces were finished by grinding. Table 9 indicates the fatigue cracking conditions for both the initiation and propagation stages.

3.3 316 Austenitic Stainless Steel

3.3.1 Preparation of the 316 Austenitic Steel Weldment

The 25 mm thick 316 austenitic weldment was provided by Mr. B.J. Lack of NEI John Thompson Ltd., Advanced Technology Division, Wolverhampton. Details of parent plate composition and welding details are shown in tables 10 and 11. The double U-joint weld was made by the manual metal arc (MMA) process and the root area was ground out to sound metal from one side and then filled up in accordance with table 11.

3.3.2 Preparation of Fatigue Cracks in HAZ of 316 Austenitic Weldment

The welded plate having mechanical properties listed in table 12 was machined to bars of dimensions 300 x 22.5 x 31 mm and finished by grinding. Using a V-notch of 60° included angle and 2 mm deep fatigue cracks were prepared in the HAZ of the weld, using a 2 ton Amsler Vibraphore fatigue machine. Table 13 indicates the fatigue cracking conditions for both initiation and propagation stages.

PROBES CHARACTERISTICS

Nominal angle (degrees)	Actual angle (degrees)	Nominal frequency (MHz)	Actual frequency (MHz)	Beam spread (degrees)	Probe dia (mm)
45	45	5	5.00	3,3	15
60	61	5	4.00	3,3	15
70	70	5	4.50	3,3	15
45	43	2	1.90	5,5.5	15
60	61	2	1.65	5.5,6	15
70	69	2	1.95	6,6.5	15

TABLE 1: BAUGH AND WEEDON PROBES CHARACTERISTICS IN STEEL

MILD STEEL AND NP8

Alloy	Analysed Composition Weight Percent					
	Fe	C	Si	Mn	P	S
Free cutting Mild steel	Bal	0.10	Trace	0.88	0.021	0.23

TABLE 2: ANALYSED COMPOSITION WEIGHT PERCENT OF FREE CUTTING MILD STEEL

Alloy	Specific Composition Weight Percent								
	Al	Mg	Cu	Si	Fe	Mn	Zn	Cr	Ti
Al-alloy (NP8)	Bal	4.5-5.5	0.10	0.50	0.4	0.05-0.2	0.1	0.03 0.2	0.06 -2.0

TABLE 3: SPECIFIED COMPOSITION WEIGHT PERCENT OF ALUMINIUM ALLOY (NP8)

Alloy	Tensile strength MNm^{-2}	Yield strength MNm^{-2}	%Elong ⁿ	% Red ⁿ in area	Hardness HV
Mild steel	510	470	36	57	203
NP8	330	200	29	24	87

TABLE 4: MECHANICAL PROPERTIES OF BOTH MILD STEEL AND NP8

MILD STEEL AND NP8

Stages	Mild Steel Specimens				Al alloy Specimens			
	Main Load		Resonating Load		Main Load		Resonating Load	
	Ton	N	Ton	N	Ton	N	Ton	N
Initiation	0.6	6000	±0.4	4000	0.2	2000	±0.18	1800
Propagatation	0.4	4000	±0.25	2500	0.15	1500	±0.14	±1400

TABLE 5: FATIGUE CRACKS INITIATION AND PROPAGATION CONDITIONS IN BOTH MILD STEEL AND NP8

Nominal Probe angle in steel	Calculated Probe angle in Al	Geom.range (mm)	Ultrasonic range (mm)		
			Cracks		
			2mm	4mm	6mm
45°	43°	29	30	31.25	31.5
60°	56°	36	37	37	37
70°	63°	46	51	51	51
80°	69.5°	61	86.5	85	84

TABLE 6: SCREEN RANGE/GEOMETRICAL RANGE VALUES OBTAINED FROM FATIGUE CRACKS IN NP8, FOR 5MHz PROBES AT ½ SKIP SCANNING POSITION

QT35-STEEL

Alloy	Specific Composition Weight Percent										
	Fe	C	Mn	Si	S	P	Ni	Cr	Mo	V	Al
Welded plate (QT35)	bal	0.10	0.93	0.16	0.023	0.014	1.05	0.81	0.34	0.11	0.005
Filler wire (S ₃ Mo)	bal	0.14	1.52	0.23	-	-	-	-	0.46	-	-

TABLE 7: SPECIFIED COMPOSITION WEIGHT PERCENT OF BOTH QT35-STEEL WELDED PLATE AND FILLER WIRE

Alloy	Yield strength MN/m ²	Tensile strength NM/m ²	%Elong ⁿ	% red ⁿ in area	Hardness Hv
Parent metal (QT35)	556	669	28	70	250
<u>Welds</u>					
As welded	568	766	23	50	260
Stress relieved	408	531	25	60	230
Normalised	309	488	29	55	225

TABLE 8: MECHANICAL PROPERTIES OF QT35-STEEL PARENT METAL AND WELDS

QT35-STEEL

Stages	QT35-welded			
	main load		resonating load	
	Tons	N	Tons	N
Initiation	0.76	7600	±0.70	±7000
Propagation	0.60	6000	±0.50	±5000

TABLE 9: FATIGUE CRACKS INITIATION AND PROPAGATION CONDITIONS IN QT35-STEEL WELDS

316 AUSTENITIC STEEL

Material	Thickness	C	Cr	Ni	Mo	Ti	Method of manufacture
316 S.S.	25 mm	0.029	16.8	11.39	2.28	0.033	Rolled plate

TABLE 10: DETAILS OF AUSTENITIC STAINLESS STEEL PARENT PLATE MATERIAL

Material Thickness	Weld Preparation	Electrode size & current		Electrode Type	Heat input
		Root runs	Fill-up		
25 mm	Double-U	10 swg 100/110 amps	10 swg 100/110amp	316 Stain- trode 63.30	Mini- mum

TABLE 11: WELDING CONDITION DETAILS FOR THE AUSTENITIC STAINLESS STEEL

Alloy	Yield Strength (MN/m ²)	Tensile Strength (MN/m ²)	%Elongation	%Reduction in area	Hardness Hv
Weld metal	333	655	76	66	317
Parent metal	309	605	67	58	282

TABLE 12: MECHANICAL PROPERTIES OF BOTH AUSTENITIC STAINLESS STEEL PARENT PLATE AND WELD METAL

316 AUSTENITIC STEEL

Stages	Austenitic stainless steel weldment			
	Main load		Resonating load	
	Tons	Newtons	Tons	Newtons
Initiation	0.76	7600	±0.70	±7000
Propagation	0.60	6000	±0.50	±5000

TABLE 13: FATIGUE CRACK INITIATION AND PROPAGATION CONDITIONS IN THE HAZ OF AUSTENITIC STAINLESS STEEL WELDMENT

Probe angle in degrees measured in mild steel and stainless steel		Probe frequency (MHz)	Max. echo amplitude in dB	Geometrical range (mm)	Screen range (mm)	
Parent metal	mild steel	S.S.				
	43	41				2
61	59	2	58	39	40	
69	66	2	56	56	58	
45	42	5	47	31	33.5	
61	56	5	36	36	37.5	
70	67	5	30	55	57	
Weld metal	43	41	2	46	37	41
	61	59	2	40	44	47
	69	66	2	42	48.5	52
	45	42	5	7	36.5	38.5
	61	56	5	6	44	46
	70	67	5	4	52	52

TABLE 14: SCREEN RANGE/GEOMETRICAL RANGE VALUES OBTAINED FROM AN 8 mm FATIGUE CRACK IN THE HAZ OF A 316 AUSTENITIC STAINLESS STEEL WELDMENT (DOUBLE-U)

4. RESULTS AND DISCUSSION

Defect size estimation by pulse/echo technique depends on the amplitude of the ultrasonic beam reflected back to the probe. This is indicated as an echo height on the screen of the ultrasonic flaw detector. This height is proportional to the reflected energy received from the defect. This is influenced by factors such as defect size, orientation, shape and surface roughness. It is also influenced by ultrasonic technique employed (30). These facts were borne in mind throughout this study.

4.1 Preliminary Tests

A number of preliminary tests were carried out before proceeding to study the response of fatigue cracks to compressive stresses, mainly to assess the characteristics and performance of both ultrasonic set and the probes most commonly used, i.e. the 45° , 60° and 70° probes at 2MHz and 5MHz frequencies, hence detectability and sensitivity can be established. The results of these tests are shown in Figs. 4, 5 and 6 and Tables 1 and 6. The ultrasonic reflected signal strengths measured in terms of the maximum echo-amplitude in dB shown in Fig. 5 were obtained using the curved 100 mm quadrant of the IIW calibration block V1, as the reflection surface, hence giving the same sound path distance for all the probes to eliminate the possibility of any variation due to the attenuation losses. These results show that the probes 45° , 60° and 70° have nearly the same ultrasonic reflection intensities. This is true at both 2MHz and 5MHz frequencies. When fatigue cracks are

Material : V1 international block (11W block)

Reflector : 100 mm quadrant

Probes : 35°, 45°, 60°, 70° and 80°
Baugh and Weedon type

----- : 2MHz probes

-.-.-.-.- : 5MHz probes

X : actual probes used in this study

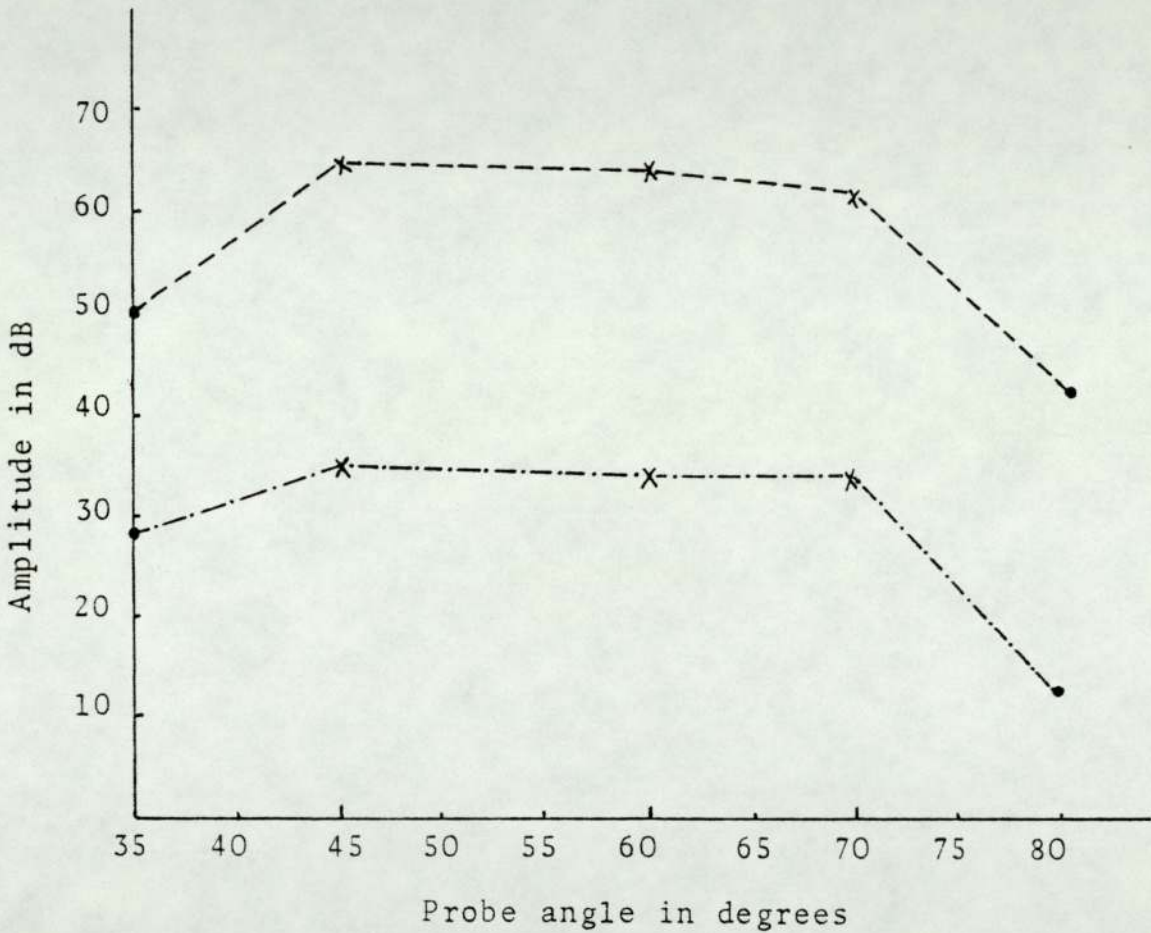


FIG. 5: Ultrasonic echo amplitude response of different angle probes from the 100 mm quadrant of the IIW block

Material : Mild steel
Probes : 35°, 45°, 60°, 70°, 80°
Scanning : ½ skip
Frequency : 5MHz

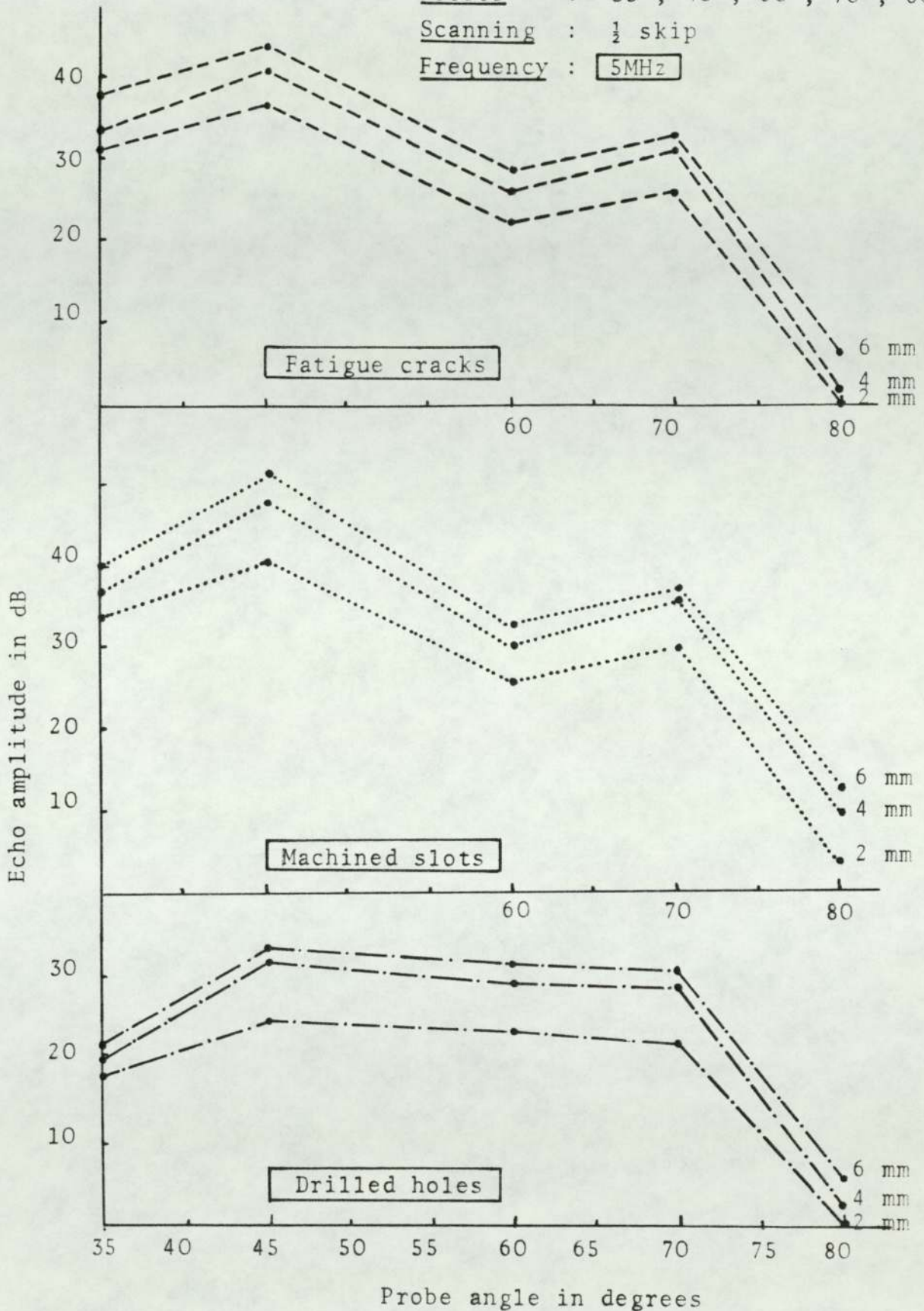


FIG 6a: Comparison between the ultrasonic responses of fatigue cracks, machined slots and drilled holes of various sizes using different angle probes at 5MHz

Material : Mild steel

Probes : 35°, 45°, 60°, 70°, 80°

Scanning : ½ skip

Frequency : 2MHz

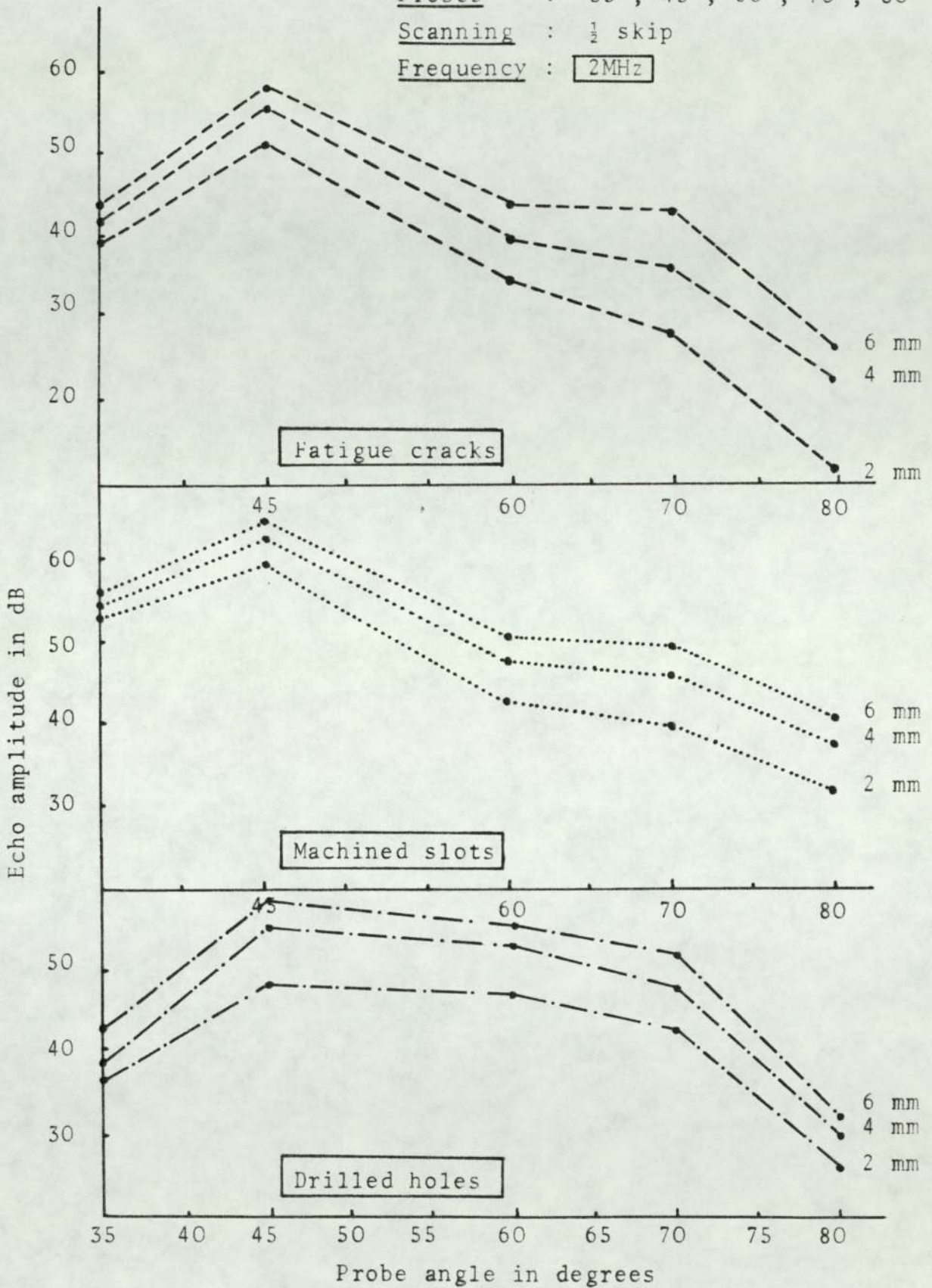


FIG. 6b: Comparison between the ultrasonic responses of fatigue cracks, machined slots and drilled holes of various sizes using different angle probes at 2MHz

considered, however, the ultrasonic reflection proved to be strongly influenced by the beam angle as shown in Fig. 6. This figure also illustrates that machined slots behave in a manner similar to fatigue cracks, with relatively higher amplitude response than fatigue cracks of corresponding sizes (depths). This is in agreement with the work of Birchak and Gardner (29) and Doyle et al (30). This was related to the poor reflection of acoustic energy by true fatigue cracks and in addition the partial transmission of energy through the crack due to the small gap opening. Hence the most accurate estimates of fatigue crack sizes were obtained using fatigue cracks as reference defects (32).

Considerable difficulties are associated with the use of artificial reference defects and many unsatisfactory results have been reported (30,31). These have been related to the many factors which influence the return signals from real cracks. For a reliable detection and sizing of true fatigue cracks when artificial reference defects are to be used, it has been found that an additional gain of 10 to 30 dB is required (29).

The results also illustrate that planar defects, i.e. fatigue cracks and machined slots amplitude response is influenced by the probe angle. However, those reflectors with curved reflecting surfaces such as drilled holes or the curved 100 mm quadrant of the IIW block are not influenced by probe angle, as shown in Fig. 5 and Fig. 6 (drilled holes section). The responses from drilled holes appeared to depend on the size (diameter) of the hole and

have considerably lower amplitudes than both fatigue cracks and machined slots. Center and Roehrs (74) related this low response to the small reflecting surface of the drilled hole, where only a thin line perpendicular to the beam reflects back to the probe. The remainder of the beam is reflected from the portion of the hole which is not perpendicular to the beam and is lost. In the case of fatigue cracks, the detection is not so dependent on orientation, this is because cracks tend to have jagged, irregular surfaces. Though the entire side of a crack may not be in a plane perpendicular to the sound beam, many small facets of this surface are, and these facets reflect the sound back to the probe.

The influence of probe frequency on the detection of fatigue cracks is well demonstrated in Figs. 5 and 6, where a higher amplitude response is achieved with the 2MHz probes compared with 5MHz probes. This may be due to the wider area of the crack covered by the sound beam, as wider beam spread is obtained from 2MHz probes compared with the 5MHz probes. This is shown in Fig. 4 which indicates that the 2MHz probes have wider beam spread and nearly twice the beam width of the 5MHz probes. The other possible reason, is that the 2MHz crystals are tuned in such a way to produce more powerful probes.

Another preliminary series of tests was carried out on fatigue cracks in NP8, and the results are shown in Table 6. These results clearly indicate that the maximum echo amplitude are obtained from the cracks surface and not from the crack corner with the specimen surface. The difference

between the geometrical and ultrasonic range illustrates the longer sound path distance travelled by the sound beam. Hence double reflection occurs. This is true for the 45° , 60° , 70° and 80° probes at $\frac{1}{2}$ skip position, and it was then found to be valid for all the cracks involved in this study.

In addition, these preliminary tests obtained from artificial reflectors and real fatigue cracks, made it possible to establish the characteristics and performance of the ultrasonic set and probes and to define adequate sensitivity levels for the subsequent examination of the fatigue cracks.

4.2 Fatigue Cracks in Mild Steel and Aluminium Alloy

The first series of tests carried out was on fatigue cracks in mild steel, using 45° and 60° probes, 5MHz at $\frac{1}{2}$ skip and full skip scanning positions, as shown in Fig. 7a and 7b. All the results obtained were averaged after scanning from both sides of each crack. Nearly all the cracks showed differing responses when scanned from opposite sides, both under zero load and under compressive stresses. Fig. 8 demonstrates one series of results from fatigue cracks in mild steel using a 45° probe, 5MHz scanned at full skip position. This is possibly due to the individual crack facets giving strong reflections on one side, but not on the other. This is in agreement with the work of Digiacommo et al ⁽⁴⁴⁾ which indicates that reflected energy distribution depends on geometry and reflectivity of the crack surface.

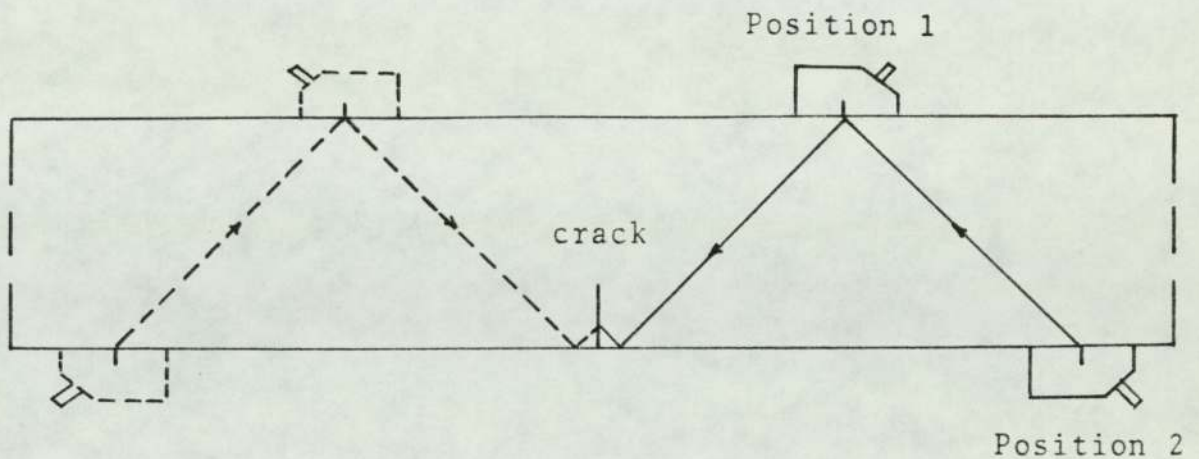


FIG. 7a: Angle probe scanning at both $\frac{1}{2}$ skip (position 1) and full skip (position 2) for maximum echo height from fatigue cracks scanned from both sides on each surface of the test bar under zero load

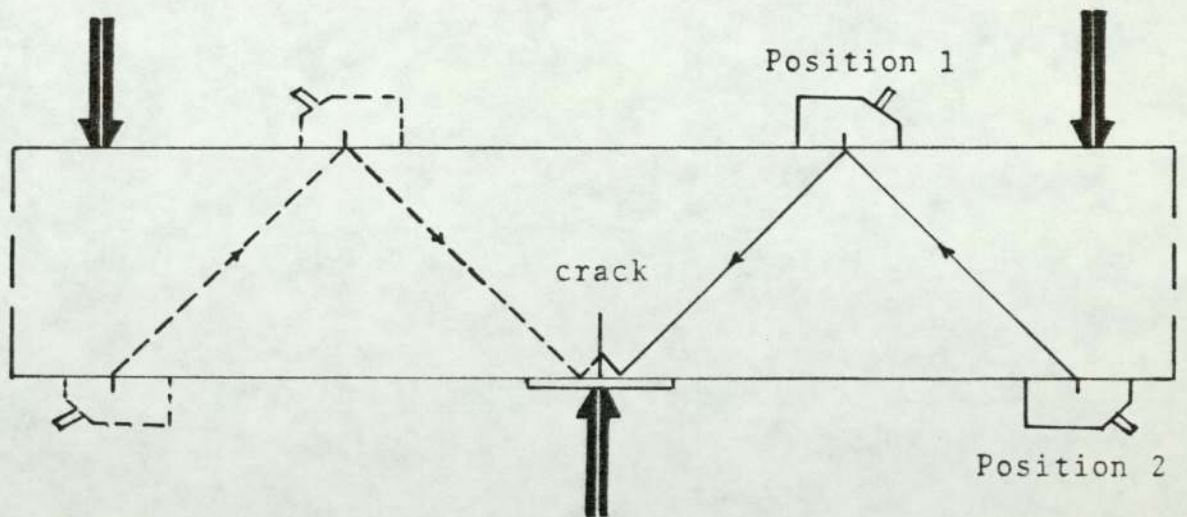


FIG. 7b: Test piece mounted on three-point bending jig for angle probe scanning of fatigue cracks under compressive loading using the maximum echo technique at both $\frac{1}{2}$ skip (position 1) and full skip (position 2)

Material : Mild steel
Probe : 45°, 5MHz (B & W)
Scanning : Full skip position
 — : Side A
 - - - : Side B

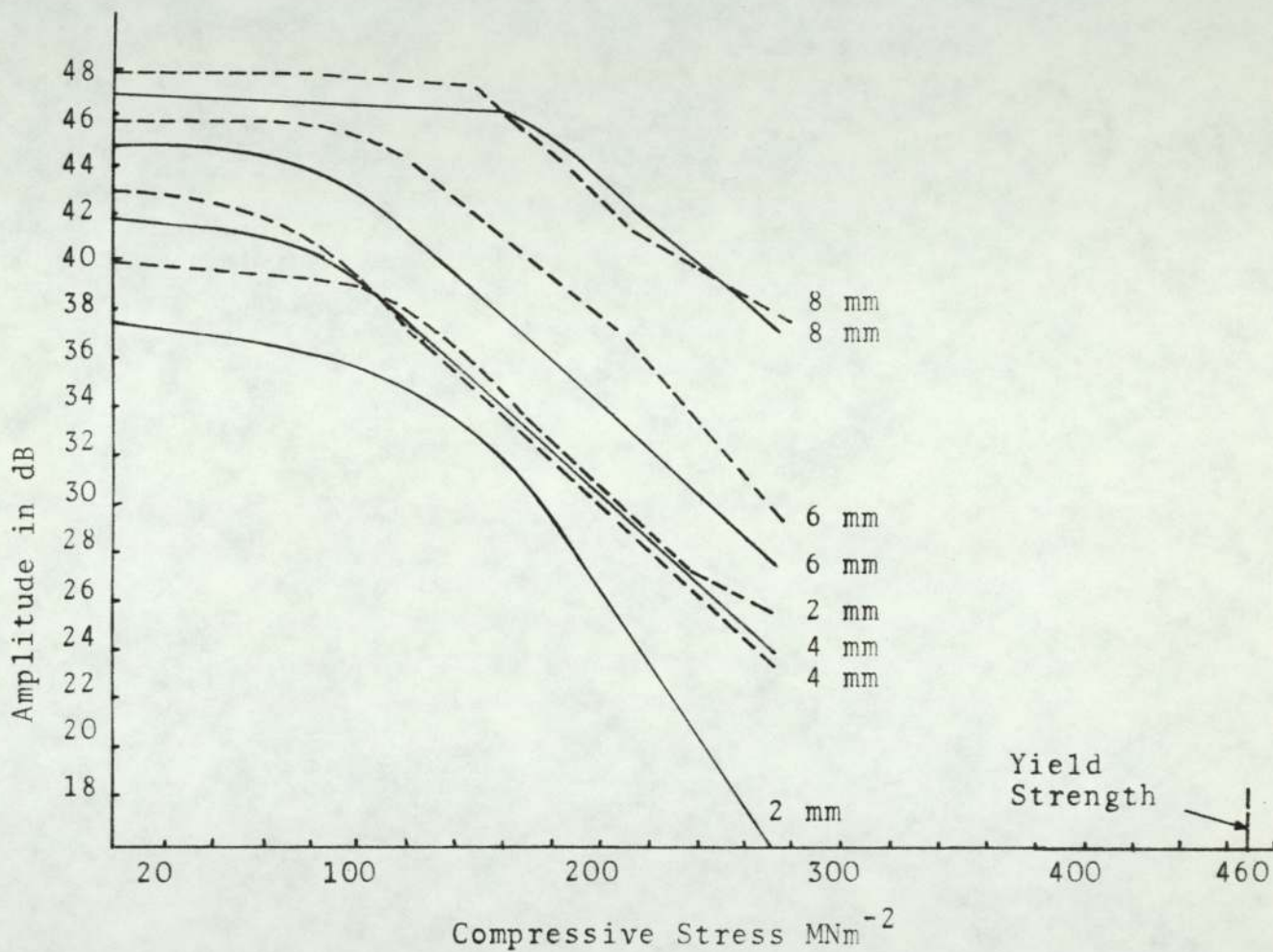


FIG. 8: The effect of compressive stresses on the response of fatigue cracks when examined from both sides

The results in Figs. 9 and 10 indicate that echo signal amplitude depends on fatigue crack size, compressive stress and probe angle for both $\frac{1}{2}$ skip and full skip scanning. There is a higher crack closure tendency when full skip scanning is applied. The 60° probe appeared to be strongly influenced by compressive stresses, but at the same time showed a weaker response to fatigue cracks at zero load.

Further work using fatigue cracks of various depths in the NP8 test bars using the 45° , 60° and 70° probes at 5MHz frequency confirmed the low ultrasonic response from the 60° probe, although again this appeared to be the most sensitive to compressive stresses, as shown in Figs. 11, 12 and 13. This weak response from the 60° probe appeared to be in agreement with a number of investigators and is related to the mode conversion (29,44,45,46). McGonnagle (42) also confirmed this idea by suggesting that when ultrasonic waves of either compression or shear type impinge on an interface between two media at angle other than at right angles, mode conversion takes place. Fig. 2 graphically represents mode conversion of shear waves which can occur at incident angles between 0 to 30.7 degrees (51). The relative intensities of shear and compression wave components after reflection are shown as curves S and C respectively (Fig. 2). The fall of shear intensity takes place until the angle of incidence = 30.7 degrees, i.e. the critical angle for shear wave and at an angle of 33.5 degrees, there is no conversion to compression waves, but total reflection of shear waves only (7). The large effect of changes in the angle of incidence on the relative amplitude response of fatigue cracks has also been reported by Baborovsky et

Material : Mild steel
Probe : 45° & 60° 5MHz
Scanning : ½ skip position
 ————— : 45° probe
 - - - - - : 60° probe

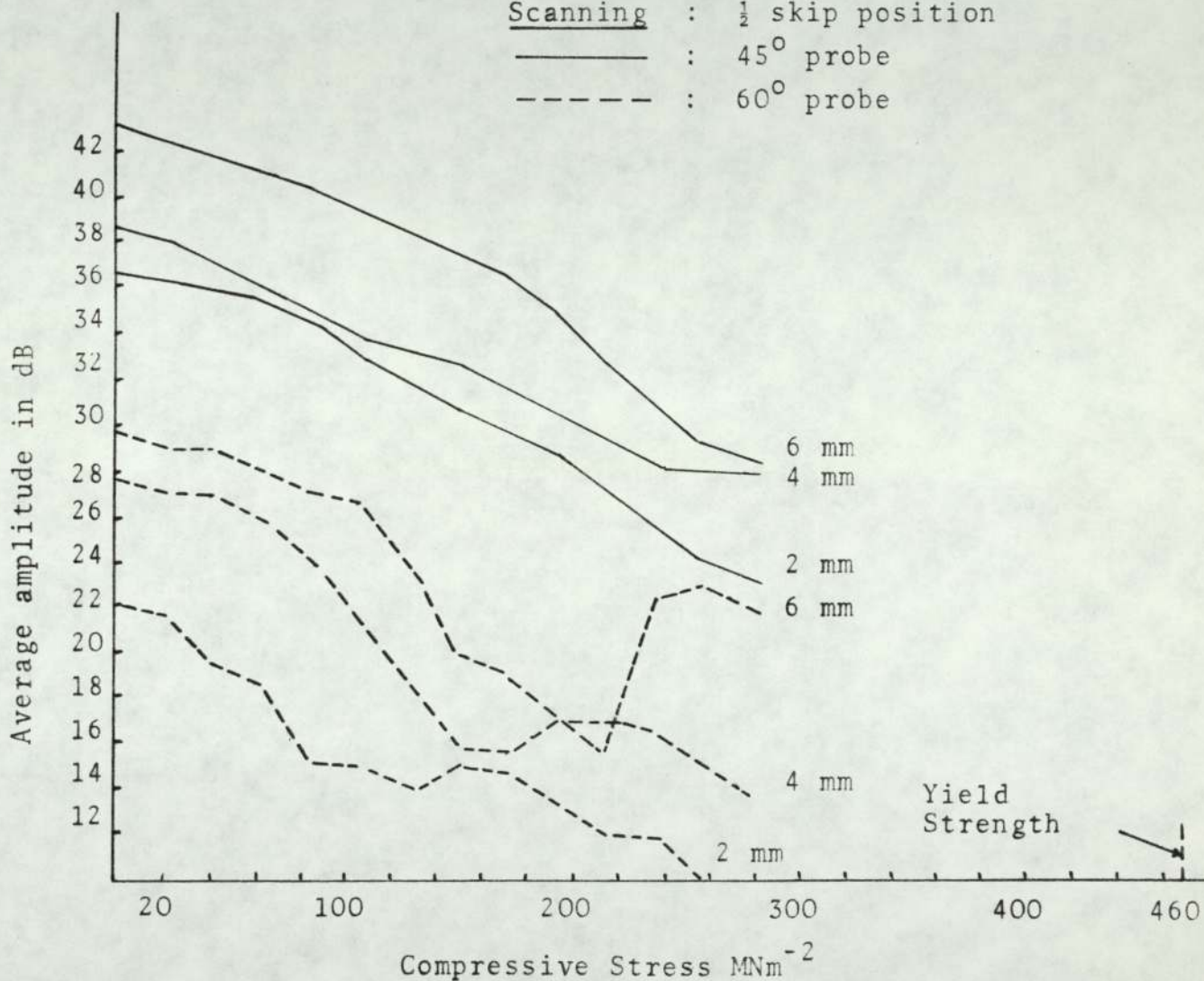


FIG. 9: Comparison between the response of fatigue cracks to compressive bending stress using 45° and 60° probes at ½ skip position

Material : Mild steel
Probes : 45° and 60°, 5MHz (B&W)
Scanning : 1 skip position
 — : 45° probe
 - - - : 60° probe

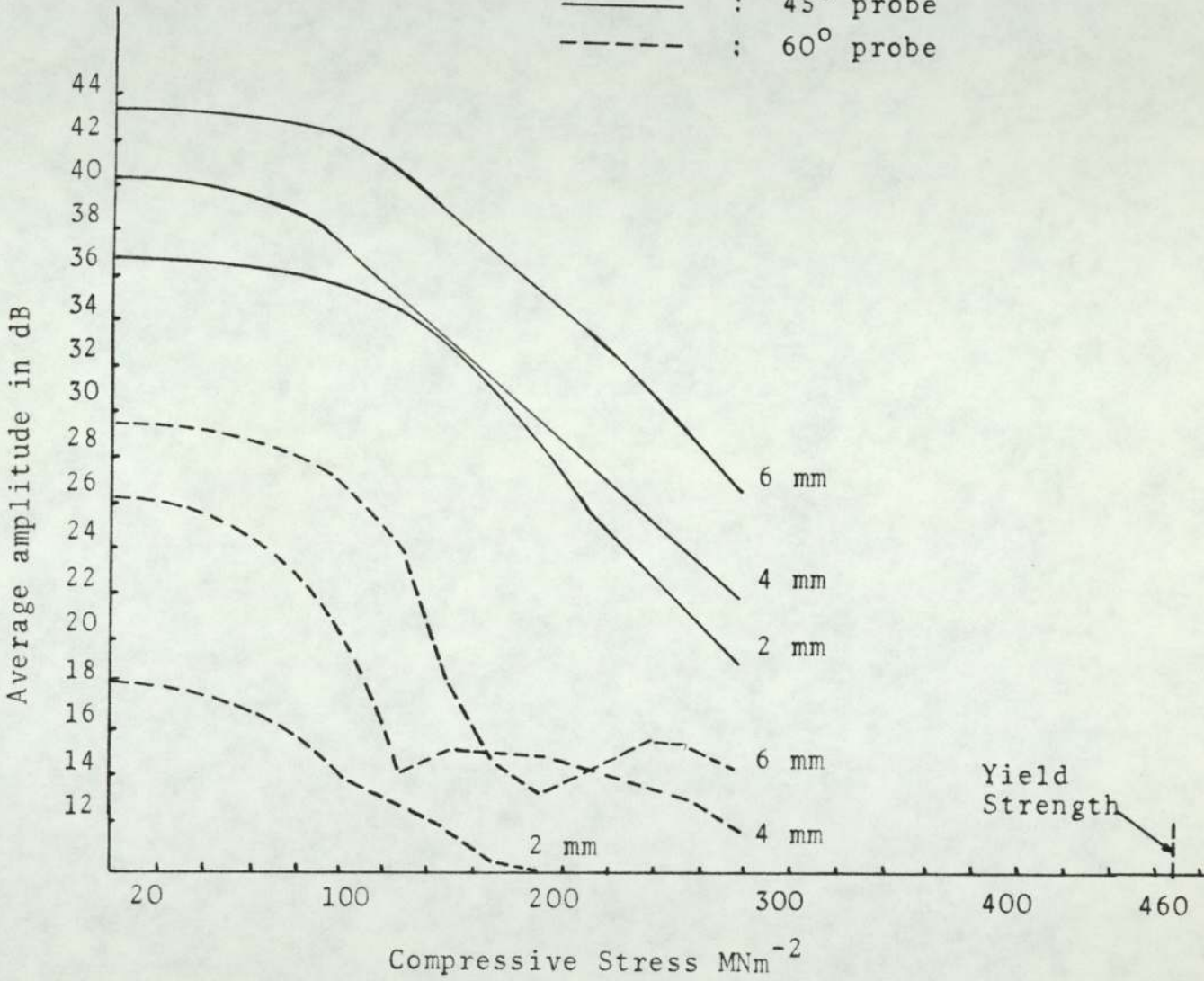


FIG. 10: Comparison between the response of fatigue cracks to compressive bending stress using 45° and 60° probes at full skip position

al⁽⁵⁾, and this is related to the different reflection mechanism involved at various angles. Hence both 60° and 70° probes (30° and 20° incident angles respectively) at double reflection mode conversion can occur. A significant amount of energy can be converted from the 60° shear wave mode to the longitudinal. This is shown in Fig. 3, where the incident angle is 30°, which is less than the critical angle for shear wave (30.7 degrees) and the reflected beam is a mixture of shear and longitudinal waves⁽⁴³⁾. The energy converted to longitudinal waves does not return to the probe⁽²⁹⁾. Hence the weak response of the 60° probe. There is, therefore, some risk of under-estimating of the size of a crack or even missing it altogether. This is clearly demonstrated in Figs. 11, 12 and 13 using the 45°, 60° and 70° probes. The 60° probe gave the lowest amplitude response with concomitant "crack closure" for both the 2 mm and 4 mm fatigue cracks at compressive stresses well below the yield stress of NP8 (45 and 125 MN/m² respectively). The 70° probe also showed the mode conversion effect, but not so markedly.

From the result obtained in this study, the 45° probe, gave the highest echo signal amplitude. This applied when cracks were at zero load and when under compressive loads. The possible explanation for the high echo amplitude achieved with the 45° probe could be related to:

- (1) absence of mode conversion as shown in Fig. 2,

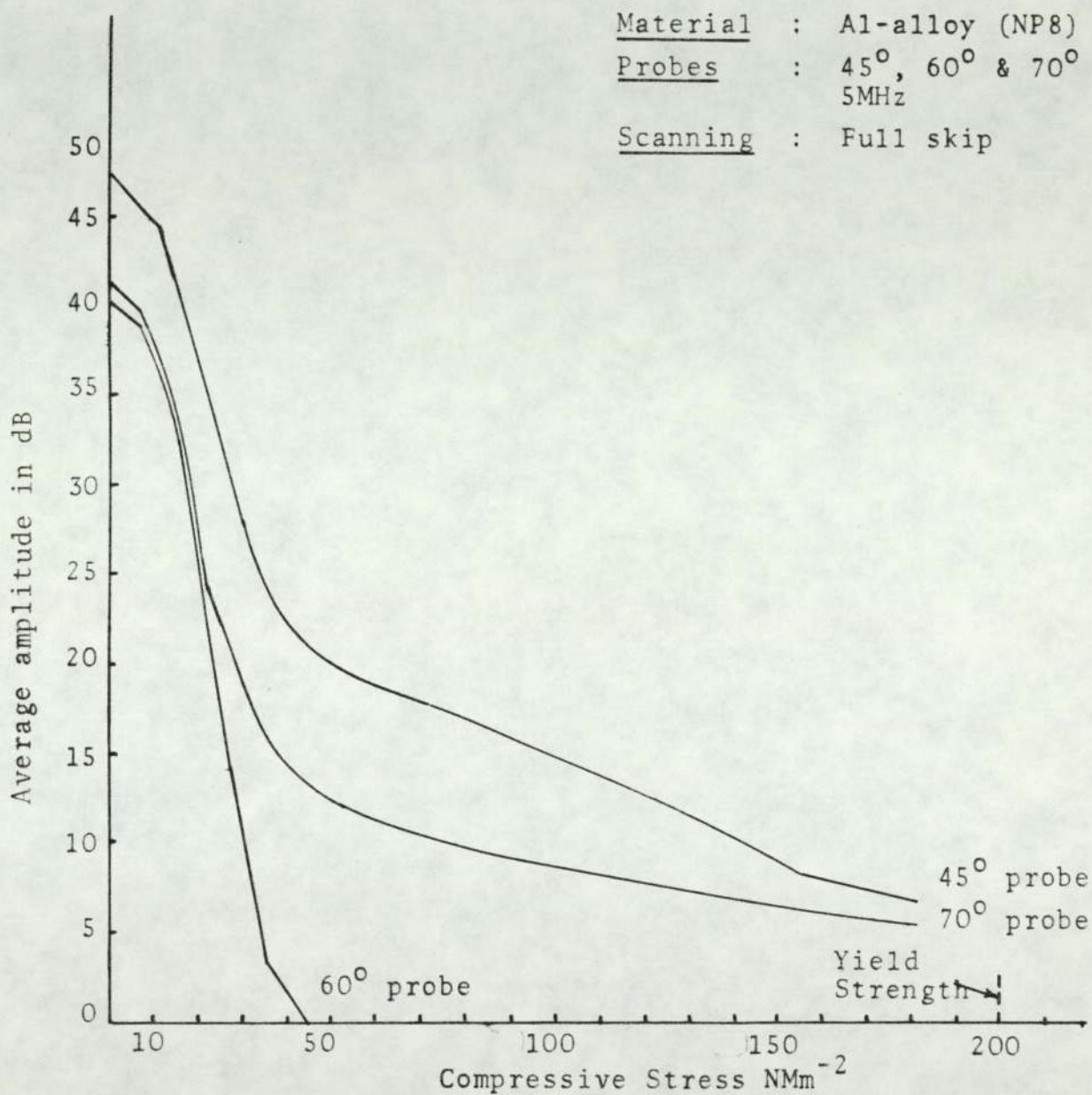


FIG. 11: Effect of probe angle on the response of 2 mm fatigue crack to compressive bending stress

Material : Al-alloy (NP8)
Probe : 45°, 60° & 70°
5MHz
Scanning : Full skip

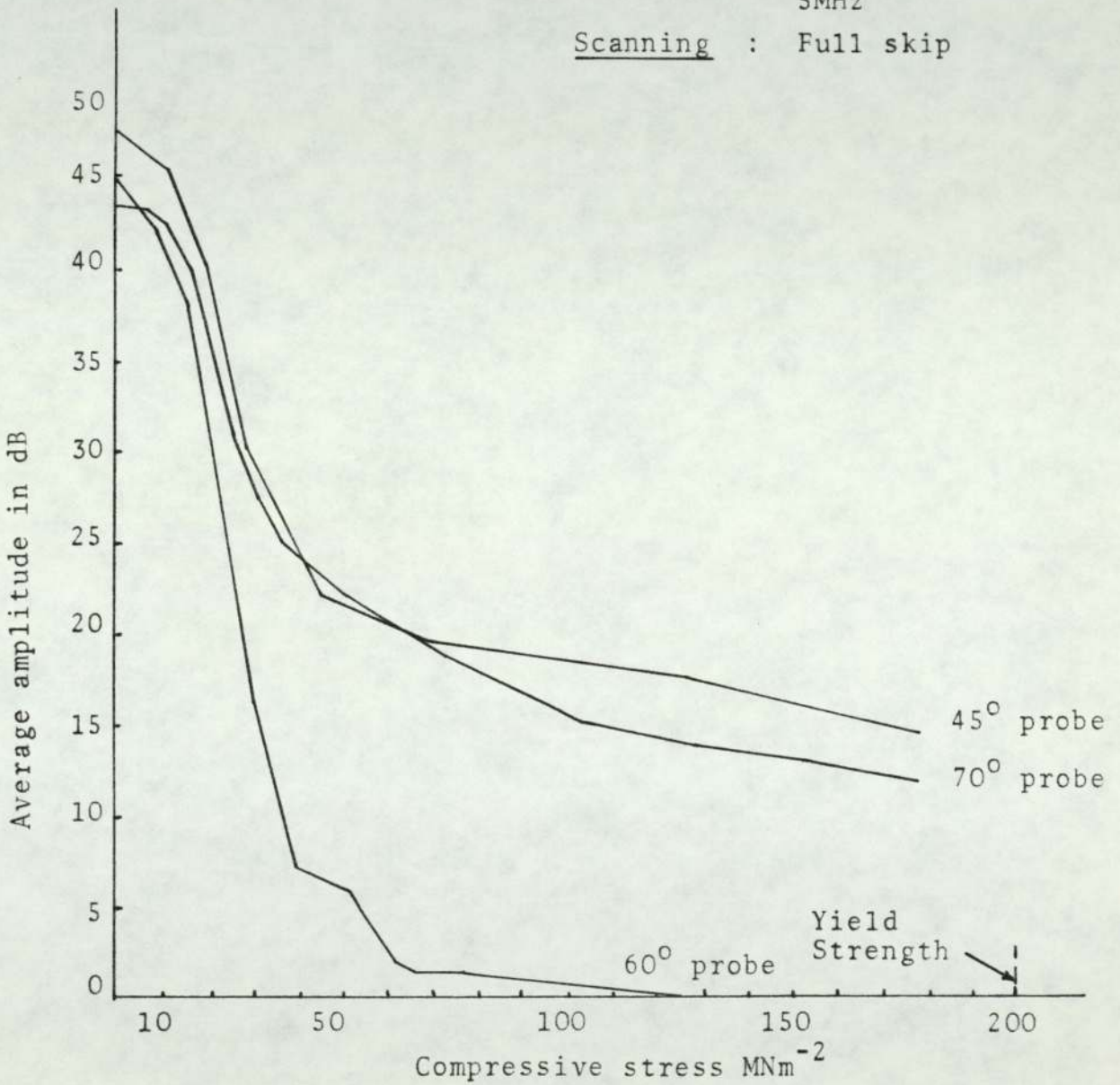


FIG. 12: Effect of probe angle on the response of 4 mm fatigue crack to compressive bending stress

Material : Al-alloy (NP8)
Probes : 45°, 60° & 70°
 5 MHz
Scanning : Full skip

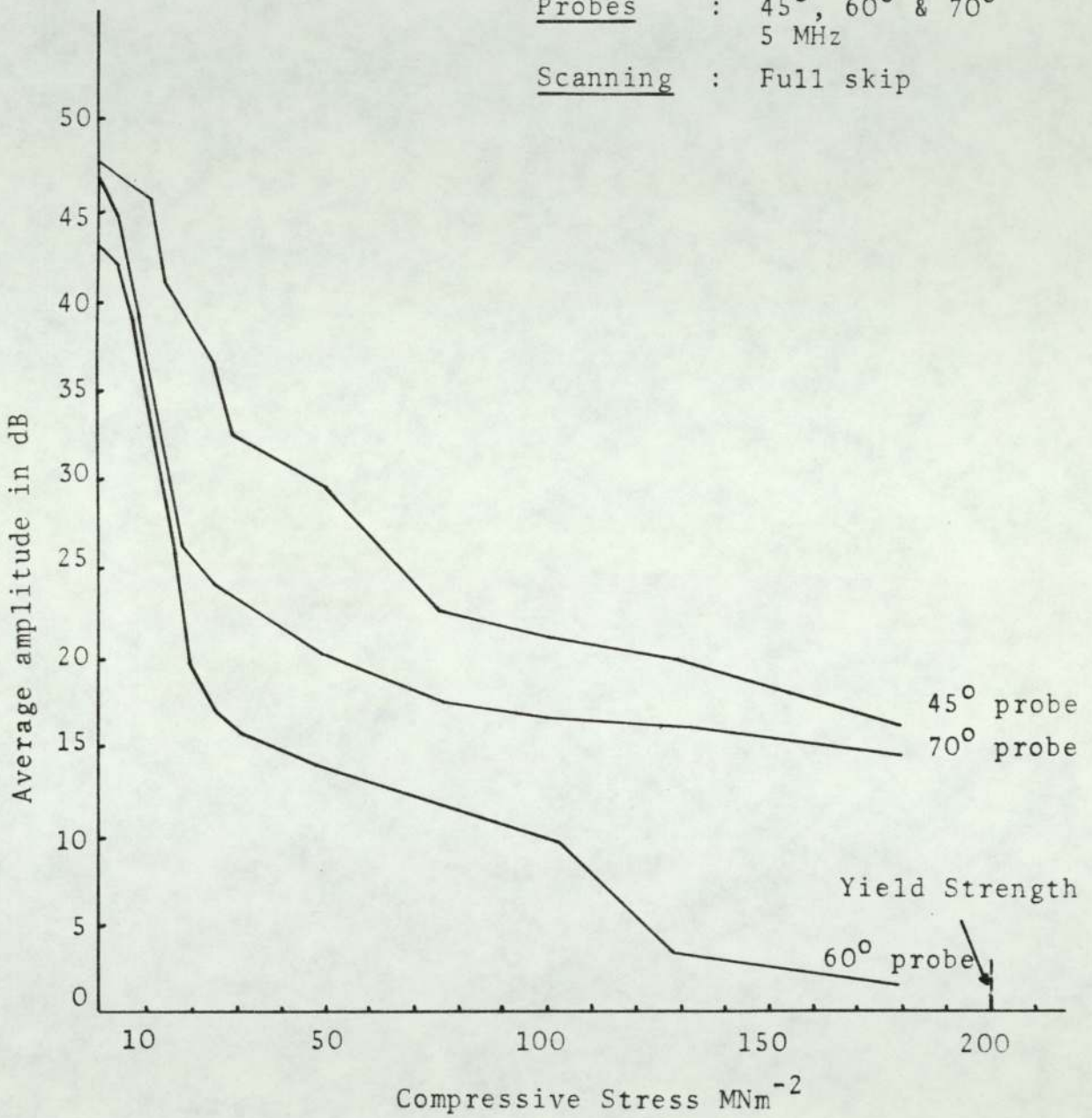


FIG. 13: Effect of probe angle on the response of 6 mm fatigue crack to compressive bending stress

- (2) fatigue crack facet orientation which could be normal or nearly normal to the incident beam direction when using 45° probe.

Some evidence for this could be seen from the fatigue cracks fracture surface profile in Fig. 17. There is a strong indication that relatively large portions of the fracture facets are oriented so that reflection from 45° probe is favoured. The 45° probe, 5MHz gave the highest overall response, but the lowest sensitivity to compressive stresses. This is in agreement with the result obtained from fatigue cracks in mild steel, as shown in Figs. 9 and 10. Thus the 45° probe, 5MHz gives the best response to fatigue cracks in both mild steel and aluminium alloy.

Further work was carried out on fatigue cracks in NP8 to investigate the performance of the 2MHz frequency probes in relation to the results obtained from the 5MHz probes. These results are shown in Figs. 18, 19a and 19b. Fig. 18 represents the response of 35° , 45° , 60° , 70° and 80° probes, 2MHz and 5MHz frequencies from unstressed fatigue cracks, again a clear high amplitude response was obtained from the 45° probes at both 2MHz and 5MHz. Fig. 18 also shows higher response achieved with the 2MHz probes. Following the results obtained from unstressed fatigue cracks shown in Fig. 18, work on the influence of compressive stresses on these fatigue cracks using the 2MHz probes was then carried out. Figs. 19a and 19b clearly illustrate the behaviour of the three most common probes and prove that the 45° probes are best suited for crack detection

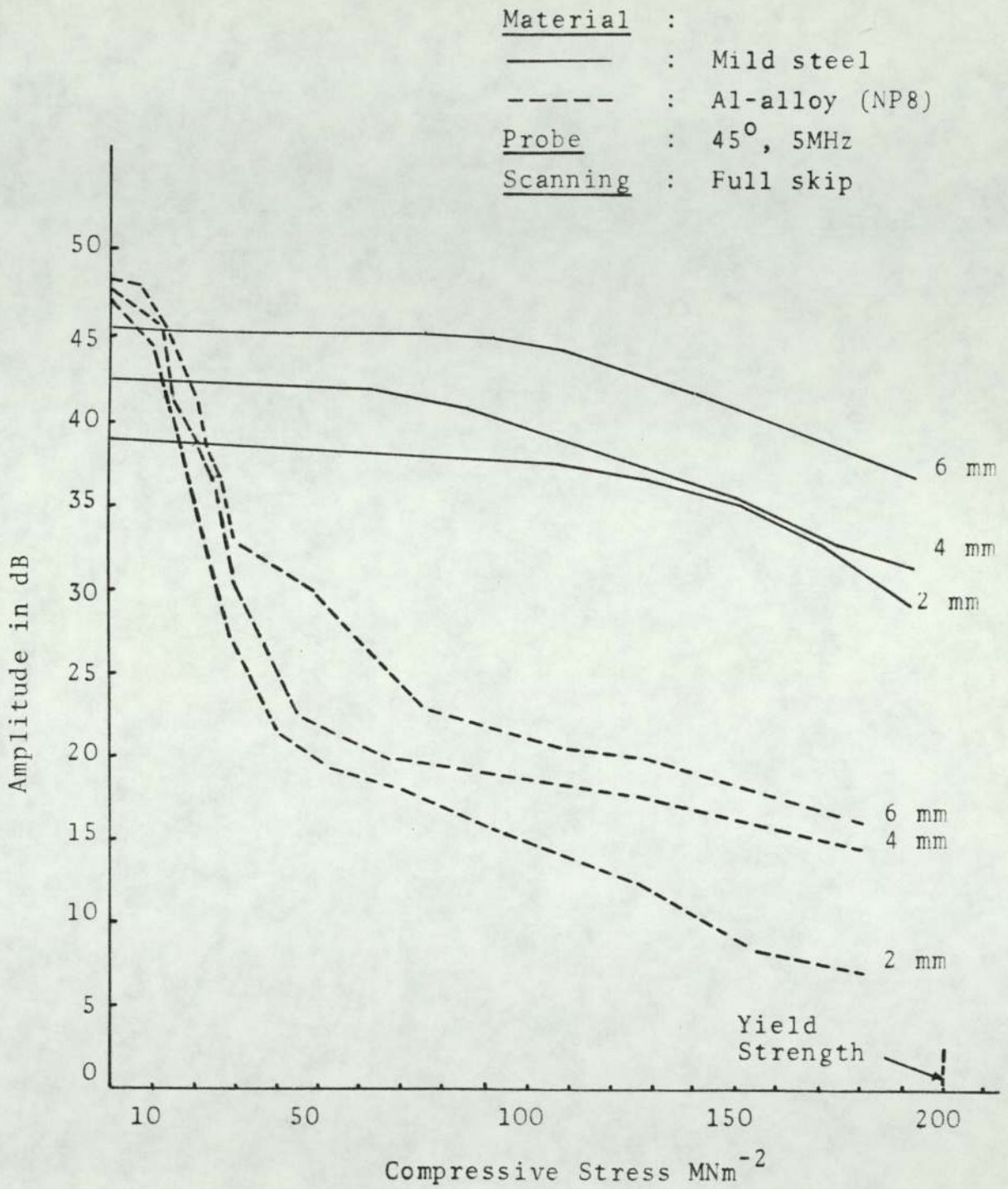


FIG. 14: Comparison between the response of fatigue cracks in mild steel and in NP8 to compressive bending stress (45° probe)

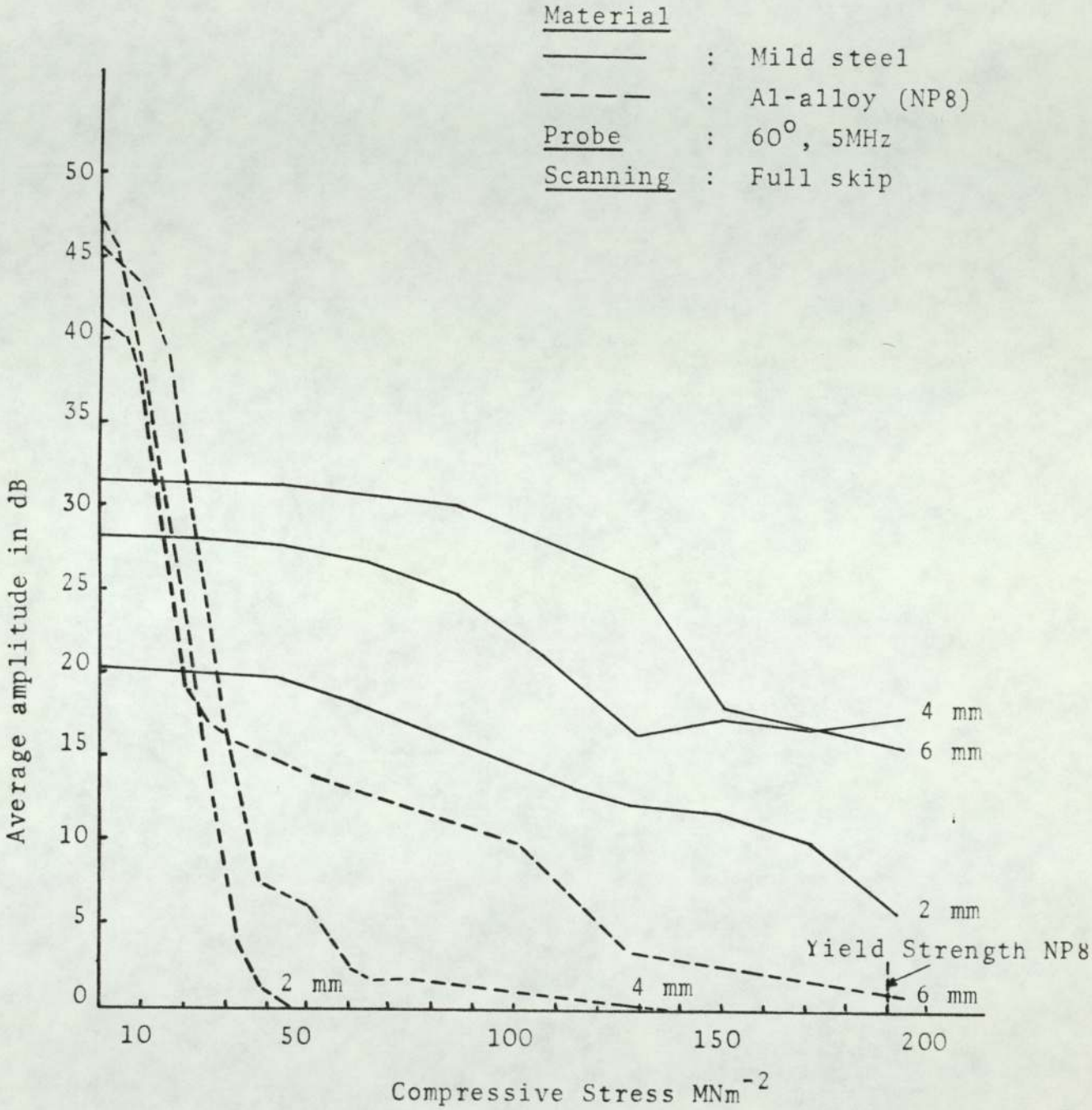
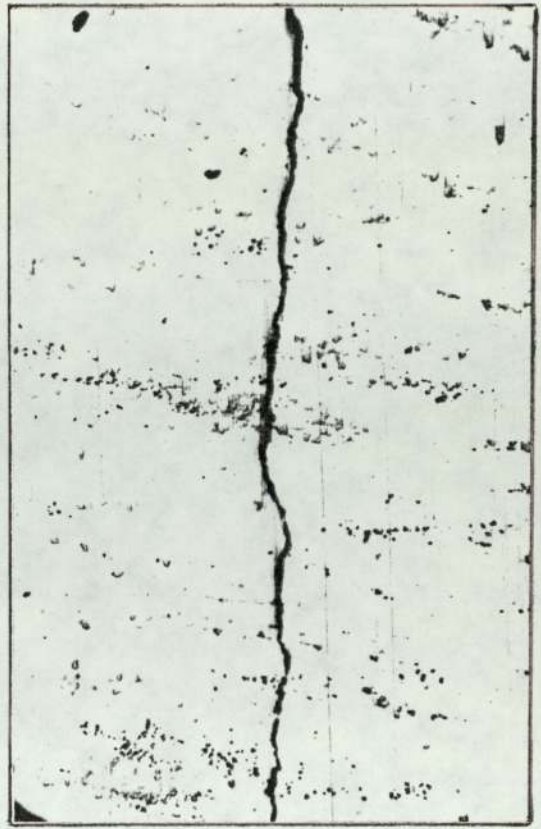


FIG. 15: Comparison between the response of fatigue cracks in mild steel and NP8 to compressive bending stress (60° probe)

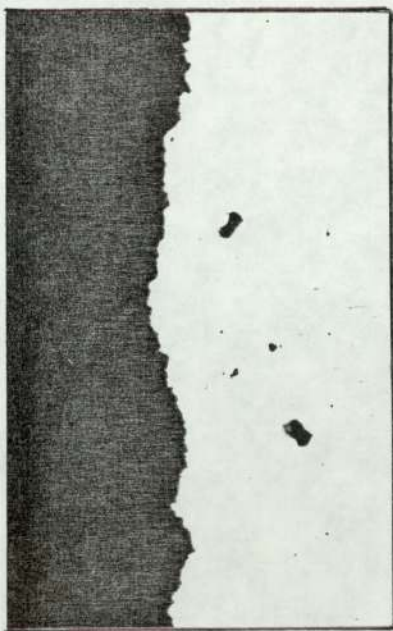


Mild Steel

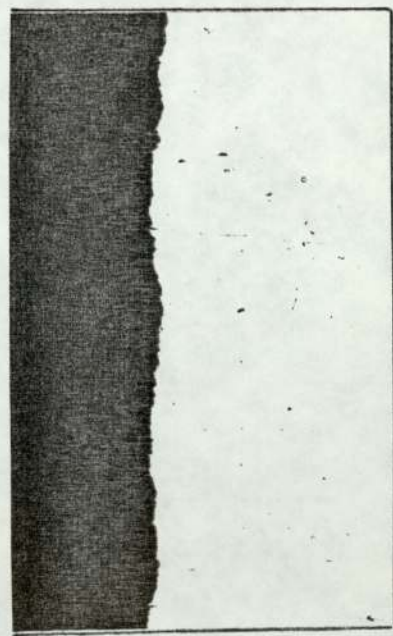


NP8

FIG. 16: Comparison between fatigue cracks opening in mild steel and aluminium alloy (x100)



Mild Steel



NP8

FIG. 17: Fatigue crack sideview profile, showing variation in crack facets roughness and orientation in mild steel and aluminium alloy (x150)

Material : Al-alloy (NP8)
Probes : 35°, 45°, 60°, 70°
 and 80°
 - - - : 1/2 skip
 : Full skip

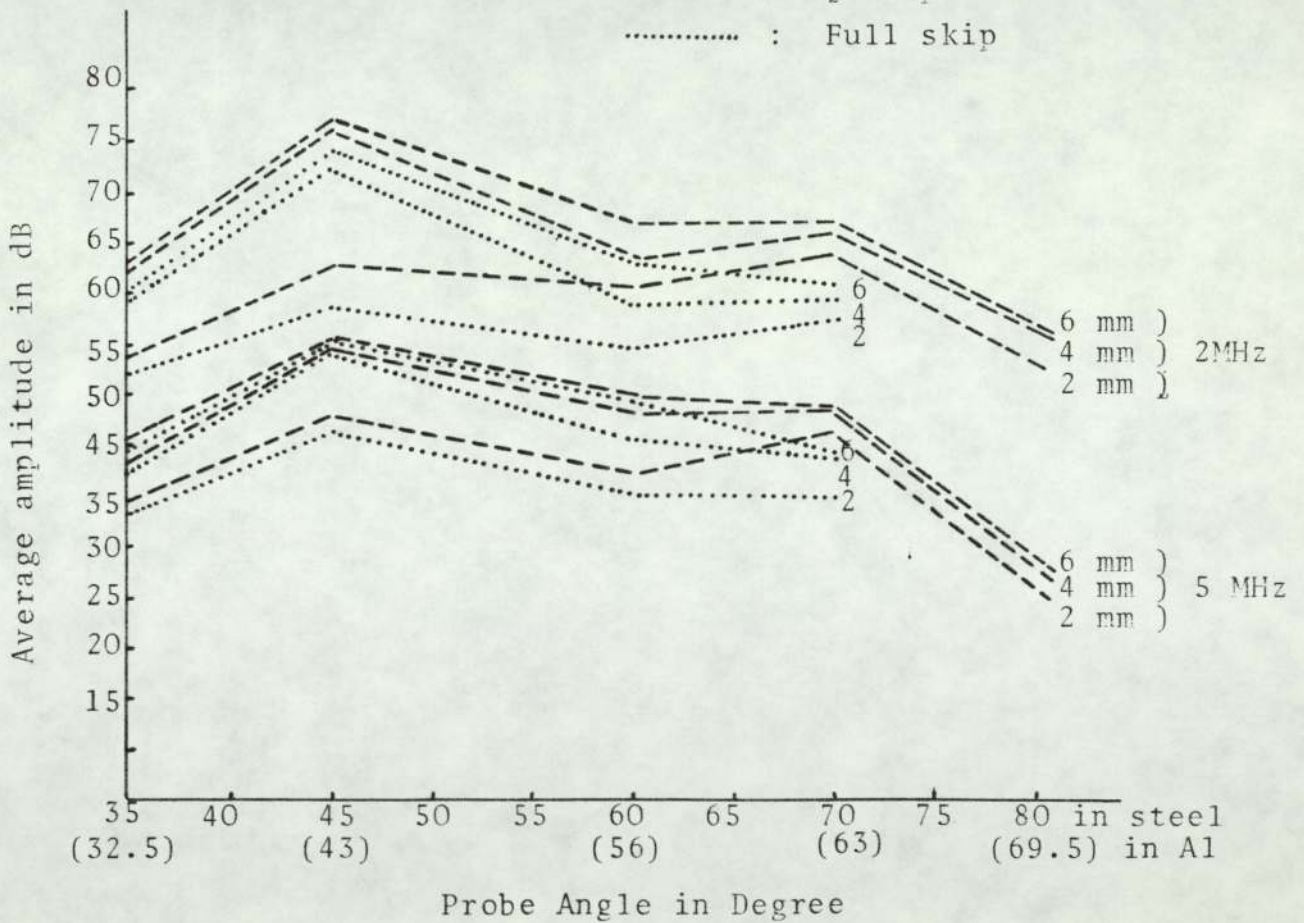


FIG. 18: Ultrasonic response of fatigue cracks of different depths under zero load to different angle probes

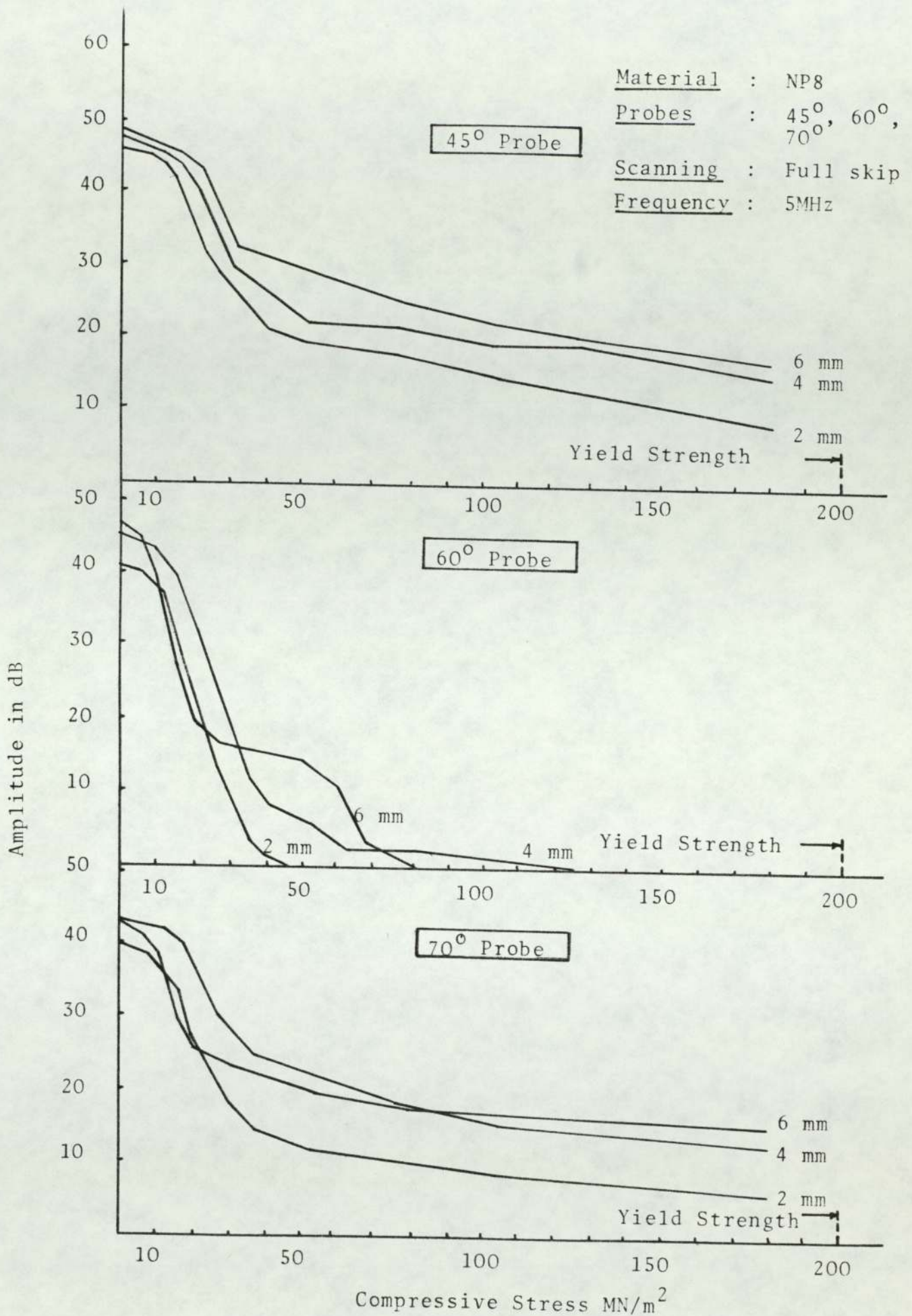


FIG. 19a: Comparison between the responses of fatigue cracks in aluminium alloy (NP8) to compressive stresses using various angle probes at 5 MHz frequency and full skip scanning

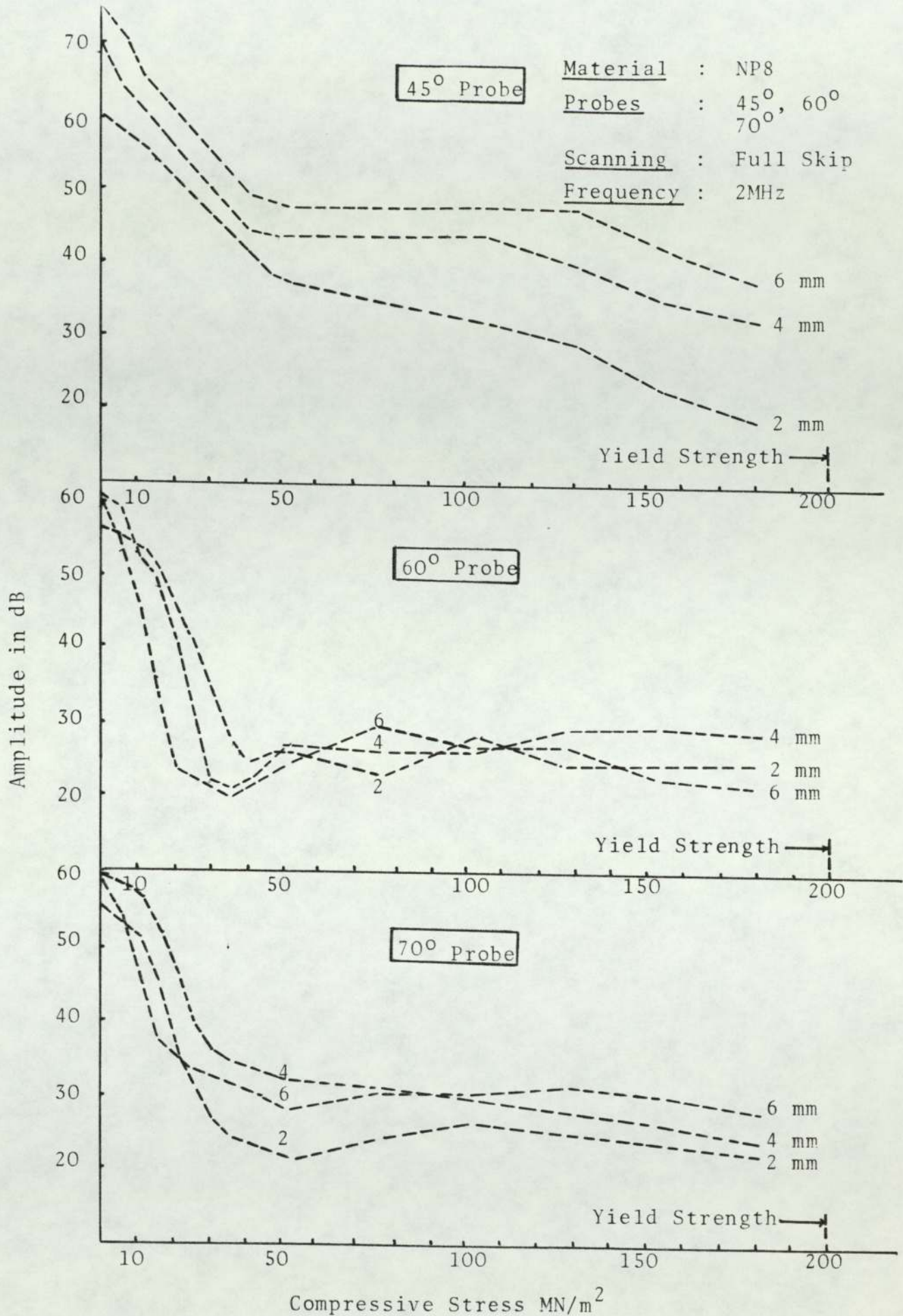


FIG. 19b: Comparison between the responses of fatigue cracks in aluminium alloy (NP8) to compressive stresses using various angle probes at 2 MHz frequency and full skip scanning

under the influence of compressive stresses, in particular when using the 2MHz probe. These figures confirm the risk in using the 60° probes for two reasons:

- (1) 5MHz probe is characterised by the high tendency to 'crack closure' under low compressive stresses well below the yield stress of the material, and
- (2) 2MHz probe is unreliable due to the scattered results performance although there is no indication of 'crack closure' (see Fig. 19b).

Figs. 14 and 15 illustrate the different responses from fatigue cracks of the same sizes in mild steel and NP8. It is clear that fatigue cracks in NP8 are more sensitive to compressive stresses than are cracks in mild steel. This sensitivity to compressive stresses is shown in Fig. 15, where fatigue cracks are seen to close rapidly. This higher closure tendency may be related to the type of fatigue crack fracture surface, i.e. cracks topography. Figs. 16 and 17 very clearly show that tighter cracks with smoother fracture surface are the characteristics of fatigue cracks in NP8, compared with wider gap crack and rougher fracture surface in mild steel. The cracks facets in mild steel and NP8 shown in Fig. 17 are both favourably oriented to the beam from the 45° probe thus reducing the effects of closure.

4.3 Fatigue Cracks in QT35-Welds

Following the results obtained from fatigue cracks in both mild steel and aluminium alloy, it was decided to carry out further detailed study on fatigue cracks in QT35-submerged

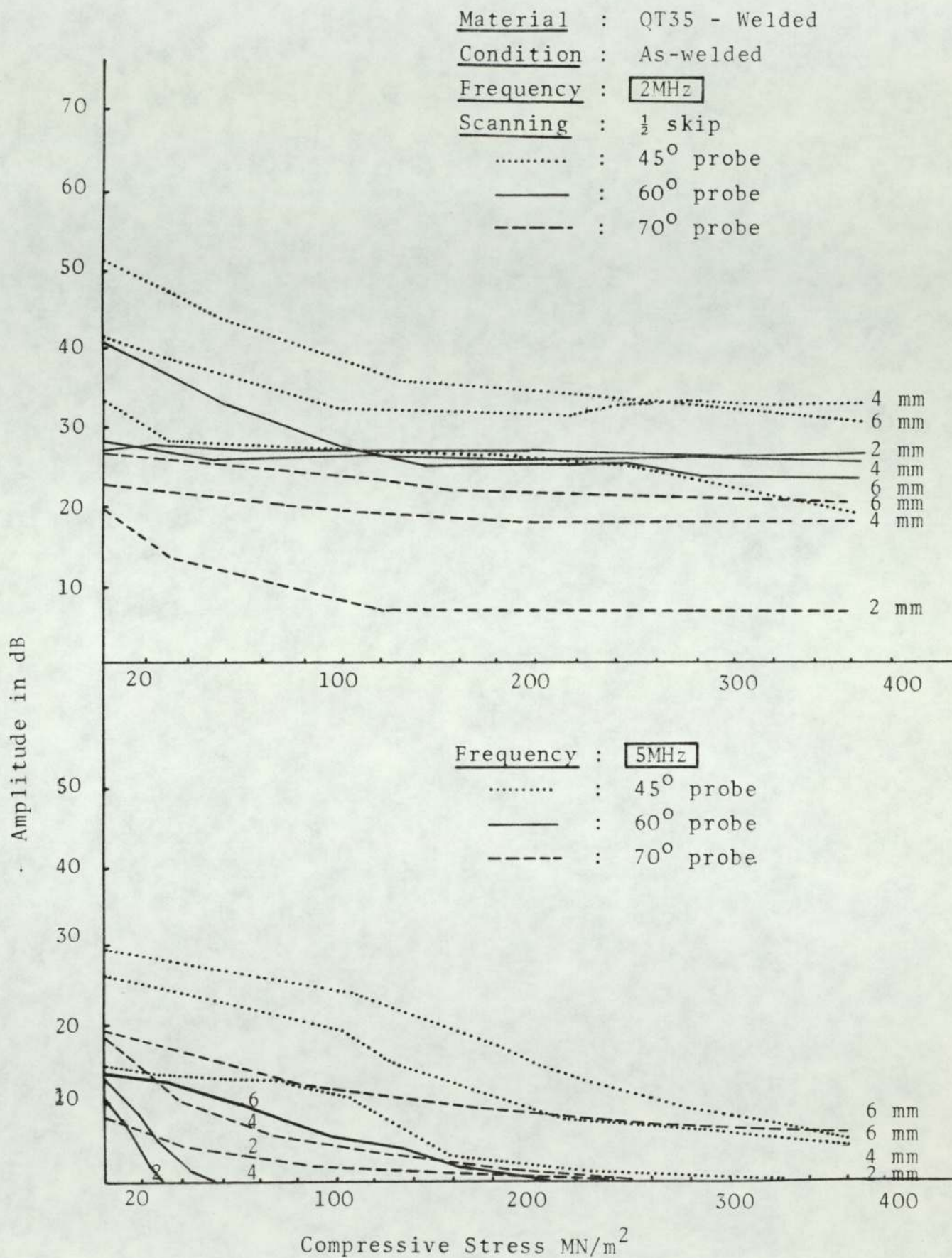


FIG. 20: Signal amplitude responses from fatigue cracks under compression using the 2 and 5 MHz probes at $\frac{1}{2}$ skip position

Material : QT35 Welded

Condition : As-welded

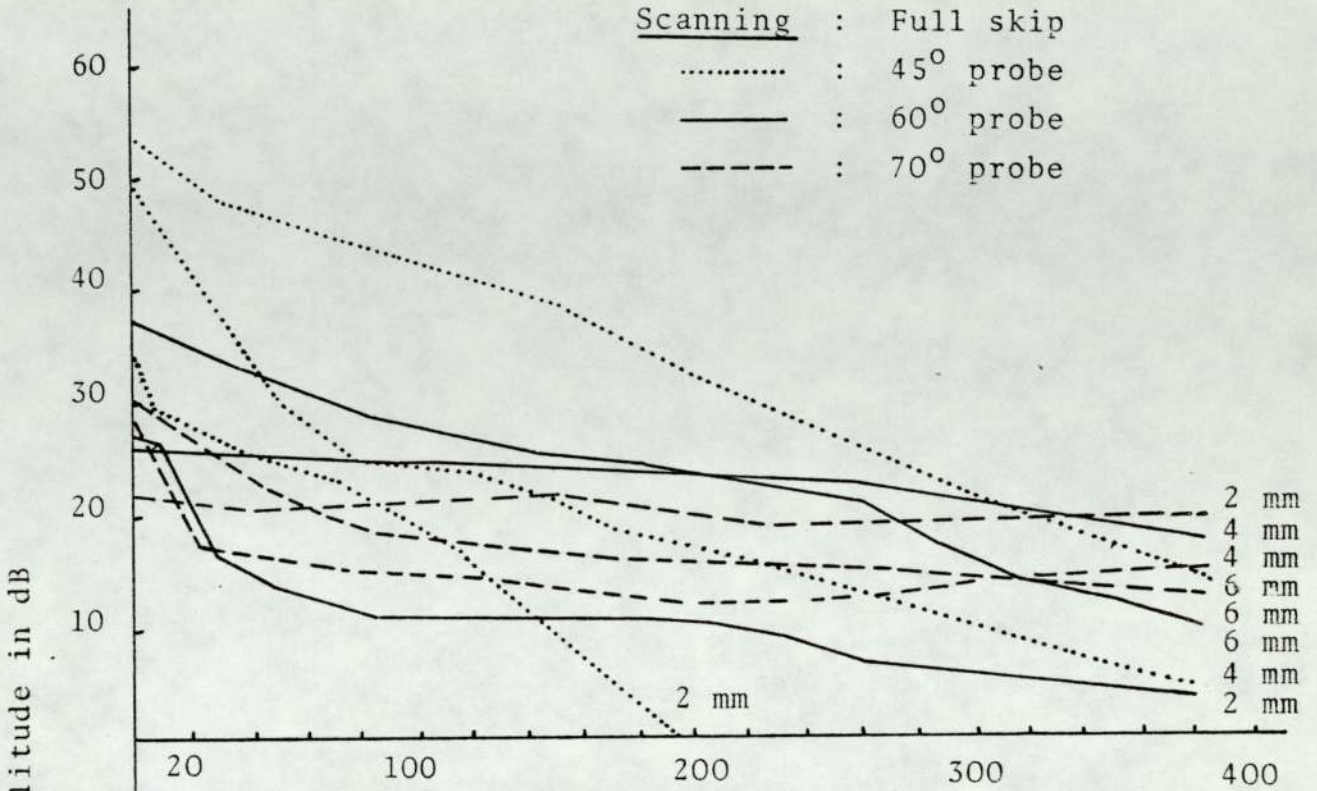
Frequency : 2MHz

Scanning : Full skip

..... : 45° probe

———— : 60° probe

----- : 70° probe



Frequency : 5MHz

..... : 45° probe

———— : 60° probe

----- : 70° probe

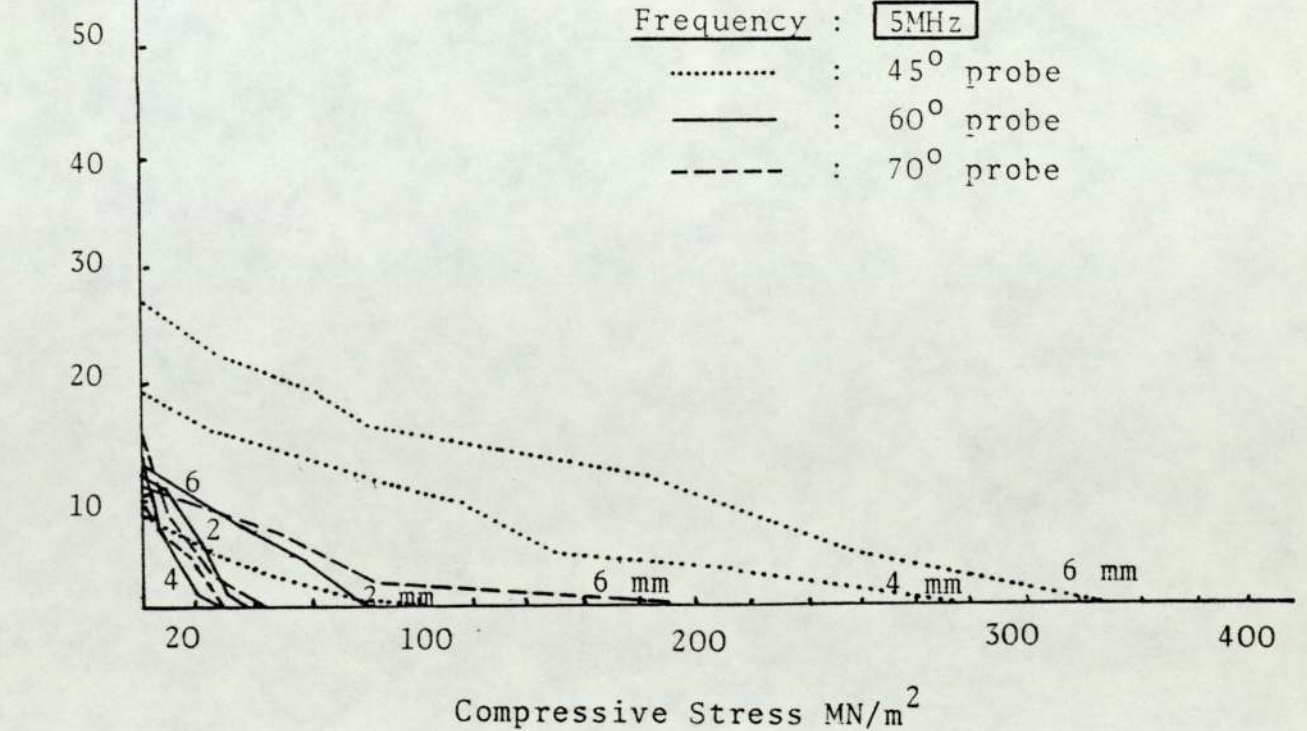


FIG. 21: Signal amplitude responses from fatigue cracks under compression using the 2 and 5 MHz probes at full skip position

Material : QT35-welded

Condition : As-welded

Frequency : 5 MHz

Scanning : $\frac{1}{2}$ skip

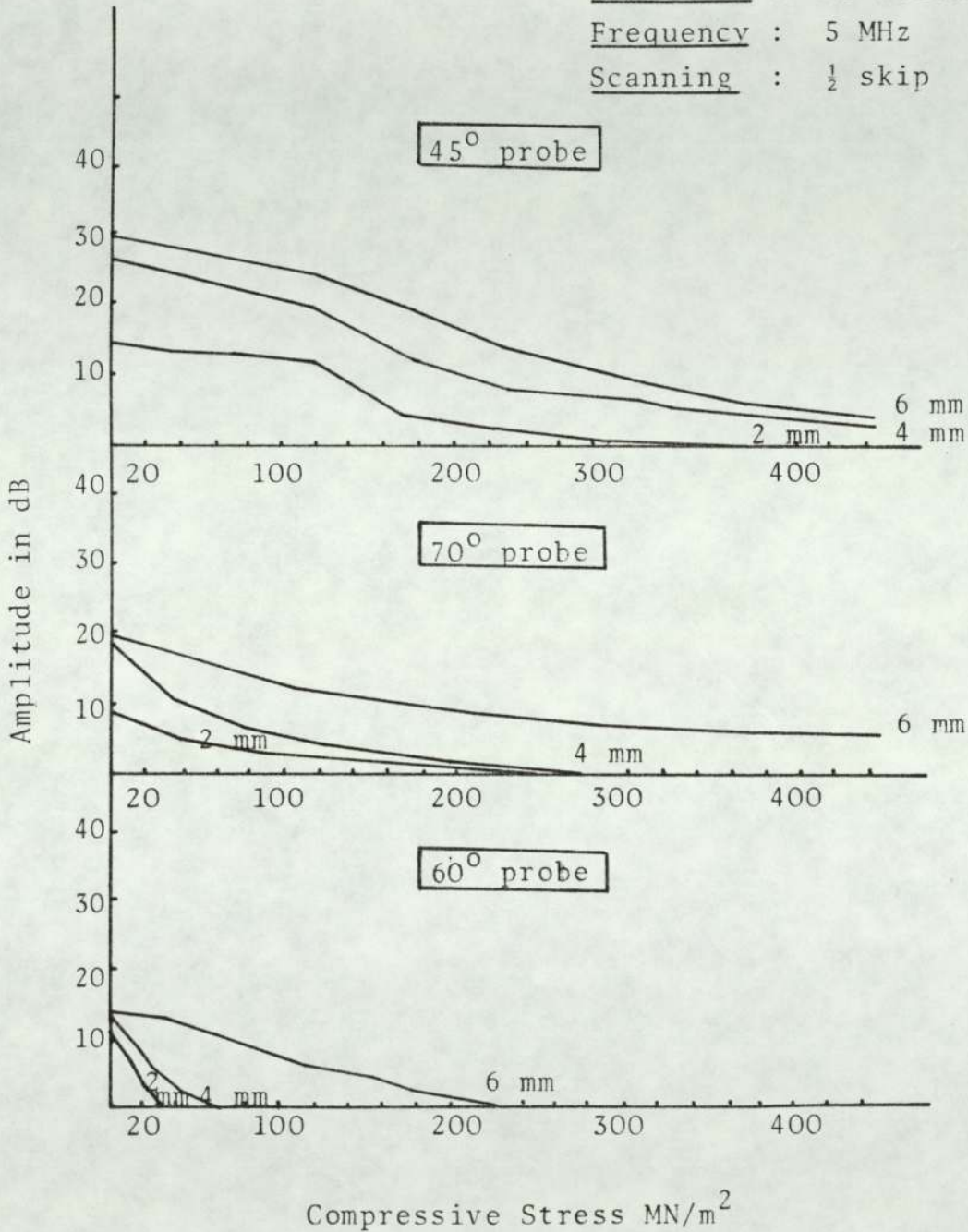


FIG. 22: Optimum ultrasonic techniques for detecting fatigue cracks under both zero load and compressive stress when using 45°, 60° and 70° probes (5 MHz at $\frac{1}{2}$ skip scanning)

arc welds. This study was done by varying all possible effective ultrasonic technique parameters, such as; probe angle, frequency and scanning positions, using the three most common angle probes, i.e. the 45° , 60° and 70° , in order to establish the most effective combination of angle and frequency for inspecting these cracks.

By varying the probe parameters and scanning positions it was possible to obtain the results shown in Figs. 20 and 21 for fatigue cracks of different depths, i.e. 2, 4 and 6 mm under various levels of compressive stresses. These results are somewhat inconsistent when the 2MHz probes are used both at $\frac{1}{2}$ skip and full skip scanning positions, especially with the 60° and 70° probes. For the 5MHz probes, the results show much better response to compressive stress at both $\frac{1}{2}$ skip and full skip positions.

Crack closure seems to be a common phenomenon when using all the three 5MHz probes at full skip scanning, although the crack closure tendency varies, as shown in Fig. 21.

The 5MHz probes at the $\frac{1}{2}$ skip scanning position were best able to differentiate between cracks of different depths, and this remained true both at zero load and under compressive stresses (Fig. 22). Fig. 22 represents the optimum condition for the echo-amplitude technique when the three most common probes, the 45° , 60° and 70° are to be considered, i.e. 5MHz, $\frac{1}{2}$ skip position. It also shows clearly why the 45° probe can be considered to

represent the best probe compared with the performance of 60° and 70° probes. Obviously, there are situations in practice where limited access may allow only the full skip techniques to be used. In this case faster apparent crack closure is to be expected if the 45° probe is to be used (Fig. 23). Figure 23 also covers other less favourable conditions for the 45° probe, and even under these conditions if compared with the performance of either 60° or 70° probes, the 45° probe can still be considered the most reliable.

The 60° probe again shows a rather weak amplitude response but at the same time proved to be the most sensitive probe to compressive stresses giving apparent crack closure at low stress levels, illustrated in Fig. 22. The performance of the 60° probe confirmed those results obtained earlier from fatigue cracks in mild steel and NP8 (93). This has been related to the mode conversion by a number of investigators (29,44,45,46).

It has been shown earlier from the results obtained in Fig. 5 that the signal strength measured in terms of the maximum echo-amplitude is of nearly the same intensity for all the probes, 45° , 60° and 70° , when the curved 100 mm quadrant of the IIW block is used as a standard reflecting surface. When fatigue cracks are considered, however, the ultrasonic reflection proved to be strongly influenced by the probe beam angle (Fig. 22). The 45° probe, 5MHz gave

Material : QT35 welded

Condition : As-welded

Probe : 45°

Frequency

$\frac{1}{2}$ skip - - - : 2 MHz
 - - - : 5 MHz

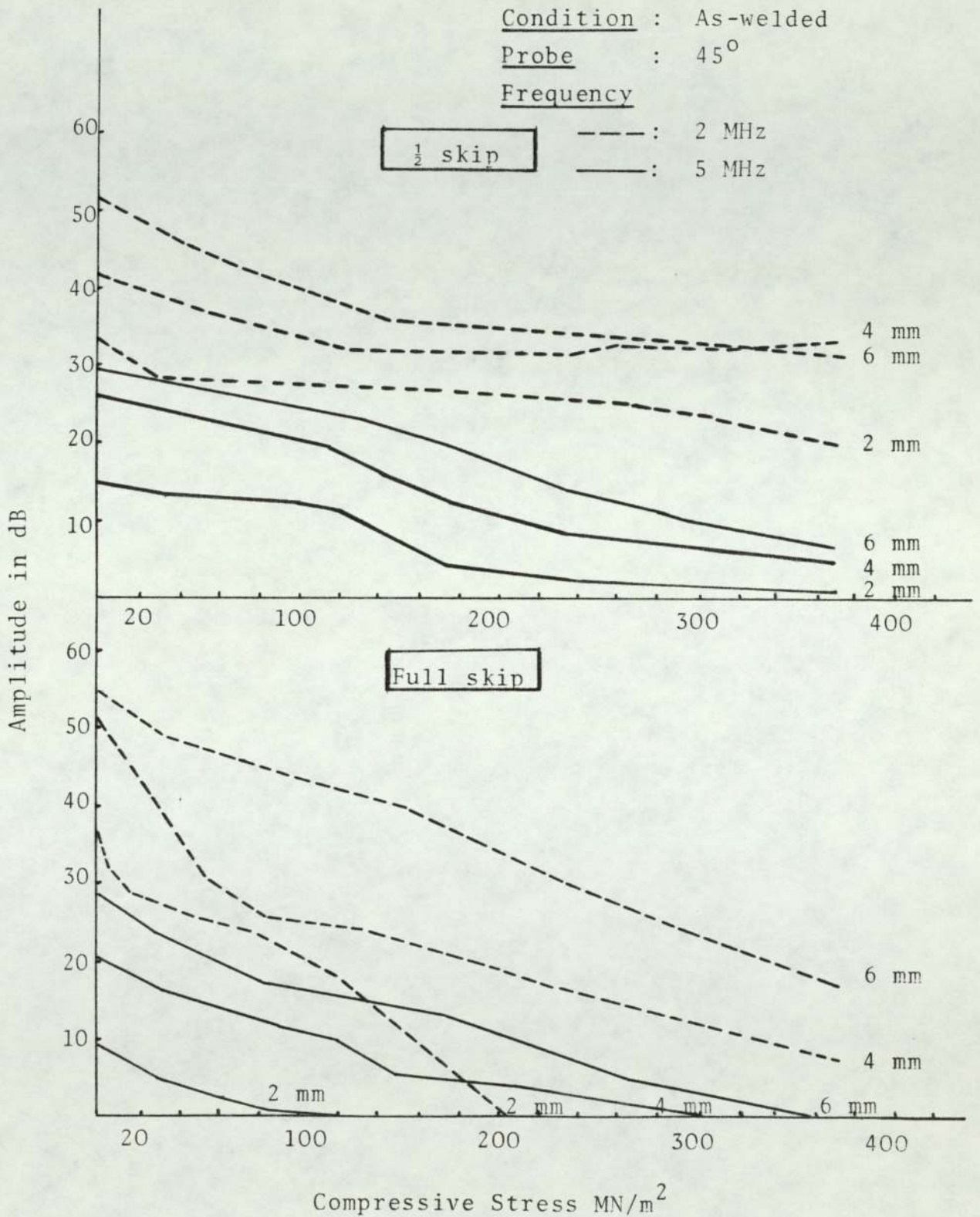


FIG.23: Ultrasonic response to fatigue cracks under compression using 45° probes at different frequencies and scanning positions

the highest overall response over the whole range of compressive stresses, whilst at the same time, this probe proved to be the least sensitive to compressive stresses. Therefore, it is possible to conclude that the strength of the signal is related to the reflecting properties of the fatigue cracks. The fatigue cracks here are in a plane which is not perpendicular to the sound beam, and they tend to have jagged irregular surfaces with many small facets, as shown in Fig. 28. Center and Roehrs ⁽⁷⁴⁾ have confirmed the presence of these small facets, and suggest that they reflect the sound back to the probe. Thus a possible explanation for the overall high echo amplitude response of the 45° probe could be related to the favourable orientation of the crack facets. Some evidence for this could be seen from the fatigue crack fracture surface profile in the as-welded condition weld in Fig. 28. There is an indication that relatively large portions of the fracture facets are oriented so that reflection from a 45° probe is favoured. Hence ultrasonic detection of fatigue cracks is influenced by the surface topography of the crack.

After establishing the most effective combination of probe angle, frequency and scanning position, i.e. 45°, 5MHz probe at $\frac{1}{2}$ skip scanning position it was possible to differentiate best between cracks of various sizes in the as-welded condition, as shown in Fig. 22. Accordingly this technique was used to study the other two weld

conditions, i.e. stress-relieved and normalised welds containing fatigue cracks of the same sizes which have been prepared under the same cracking conditions (Table 9). The results have been compared with those obtained from the original as-welded samples, and show similar trends, i.e. high echo amplitude response from the 45° probe and low response from the 60° probe (Fig. 24). This is found to be true for all the cracks in the different weld conditions. The results also demonstrate the overall low response in echo amplitude from fatigue cracks in the as-welded condition compared with those in the stress-relieved and normalised conditions. This applied to all three probes used.

The high echo-amplitude obtained from cracks of stress-relieved and normalised welds can be mainly related to the different crack topography, as shown in Fig. 28. This figure shows the as-welded condition to have relatively smooth surface with fine crack facets compared with coarser well defined facets covering a large portion of the cracks in both stress-relieved and normalised welds. These individual crack facets are oriented so that reflection from a 45° probe is favoured, especially those cracks in the normalised welds. Schijve ⁽⁷⁶⁾ has also confirmed this favourably oriented facets to the 45° probe angle, i.e. facets at near normal incidence to the incident 45° beam. He also added that fatigue cracks usually grow in a plane perpendicular to the main principal stress, but the plane of the fatigue fracture will be at an angle of 45° with that stress for several materials.

Material : QT35 welded
Probes : 45°, 60° and 70°
Frequency : 5 MHz
Scanning : ½ skip
 ----- : Normalised
 : As-welded

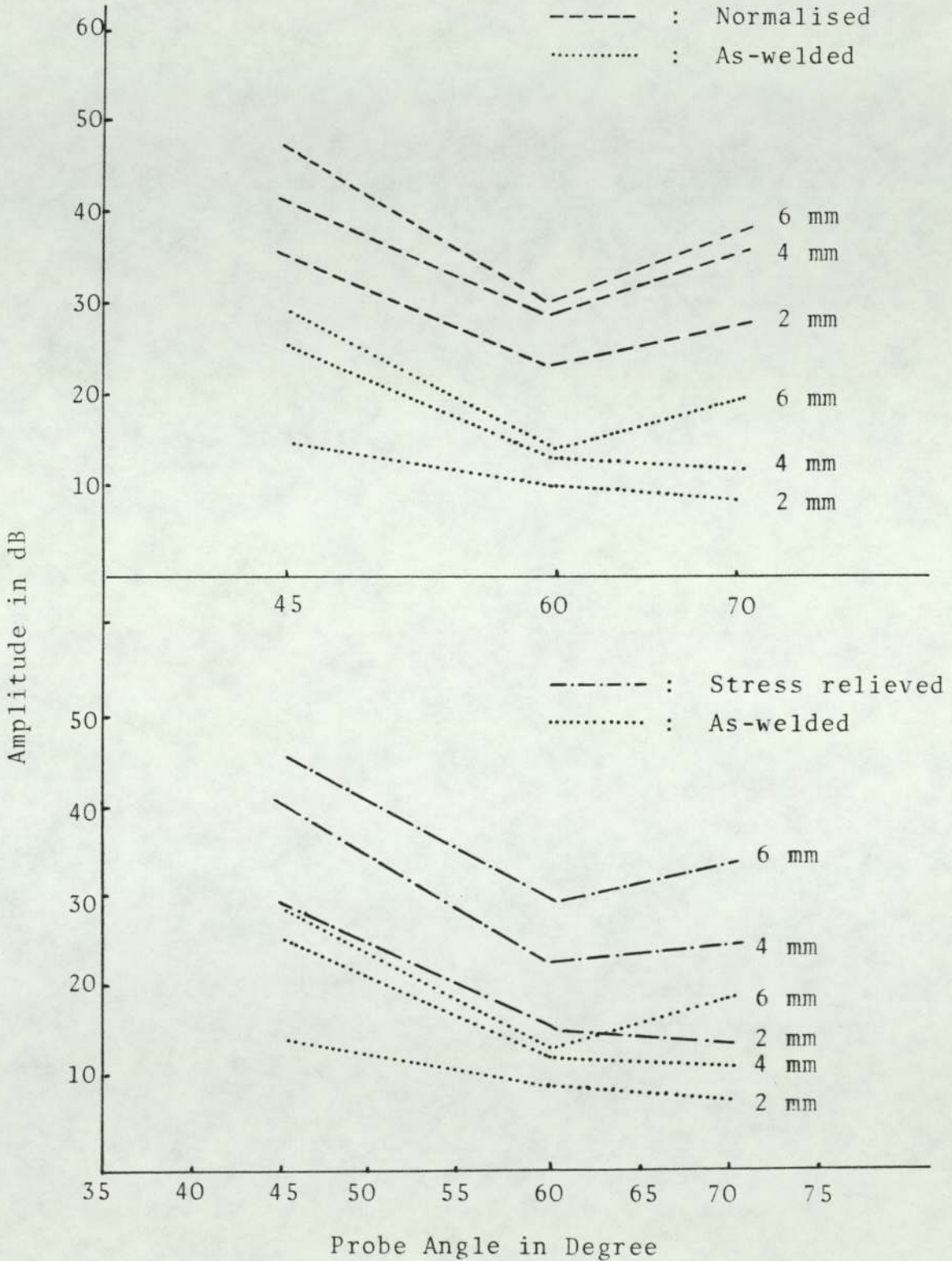


FIG. 24: Response to fatigue cracks under zero load in submerged arc welds in the as-welded, stress-relieved and normalised conditions using 45°, 60° and 70° probes, 5 MHz at ½ skip scanning

The other factor which must be considered in addition to the topography is the attenuation loss due to the possible changes in the metallurgical structure. This was found to have little or no effect, as the difference in attenuation loss between the as-welded and normalised welds for example is only 0.08 dB/mm. In addition, the material thickness involved was less than 25 mm, and only a small portion of the weld is covered by the ultrasonic beam, especially when using the 45° , 5MHz probe at $\frac{1}{2}$ skip scanning position, which represents the optimum technique in this study.

It has been shown earlier that 2MHz probes produced unreliable results compared with the 5MHz probes. Figure 26 shows the effect of probe frequency on the oscilloscope screen trace produced by the 2mm and 6mm fatigue cracks in the as-welded condition using 70° probe at 2MHz and 5MHz and $\frac{1}{2}$ skip scanning. The signals from the 2MHz probe are characterised by poor signal/noise ratio which could make small crack detection difficult if not impossible. This is possibly due to the wide beam spread (Fig. 4), which allows other reflectors to be picked up, e.g. crack corners, crack tips, far edge of specimen, surface reflection and others. This effect becomes even worse when full skip scanning is applied, since although the beam angle remains the same, the beam spread (width) increases with distance. In the case of 5MHz probes, the signals are sharper and clearer with very much less noise interference, because of the narrower beam (Fig. 4) and a switch to 5MHz might therefore prove beneficial.

Fig. 27 shows a comparison between the response of 2 mm cracks grown in the as-welded and normalised welds using 2MHz, 45°, 60° and 70° probes at $\frac{1}{2}$ skip scanning position. This figure clearly shows the weak echo-amplitude signals from the 2 mm crack in the as-welded condition compared with those from normalised weld. There is more than 20 dB difference in the amplitude response of these cracks in different weld conditions. Because of the high amplification that is needed to enhance the weak signal in the as-welded samples the oscilloscope trace becomes noisy with spurious signals from variety of sources such as; inclusions, or microcracks in the crack region. These traces and their respective amplitudes confirm the results shown in Fig. 24, which again indicate the higher response from cracks in the normalised weld.

Fig. 25 shows that if fatigue cracks were grown in post-weld treated structures, the effect of compressive stresses on ultrasonic crack closure is substantially reduced. This is due to the relatively high echo-amplitude response over the whole stress range. Hence, both post-weld treatments, i.e. stress-relief and normalising, assist in crack detection when compressive stresses are present.

The variation in the ultrasonic echo-amplitude from cracks under zero load in the as-welded, stress-relieved and normalised welds has earlier been related to the corresponding variation in their crack surface topography. Variation in crack surface topography can also explain the changes in ultrasonic response under compressive stress, which

Material : QT35 welded
Probe : 45°, 5MHz
Scanning : ½ skip
 - - - : Normalised
 ——— : As-welded

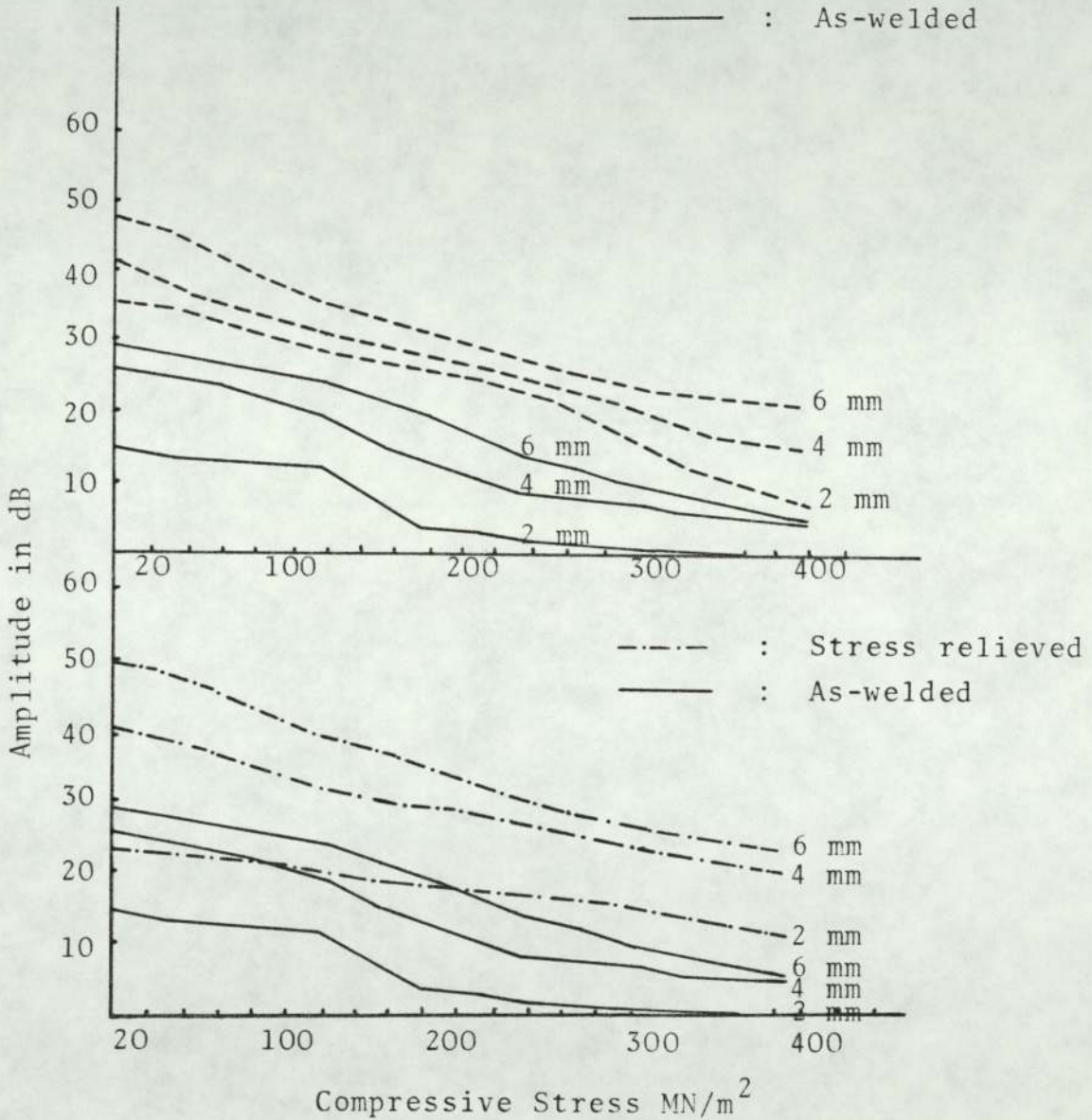
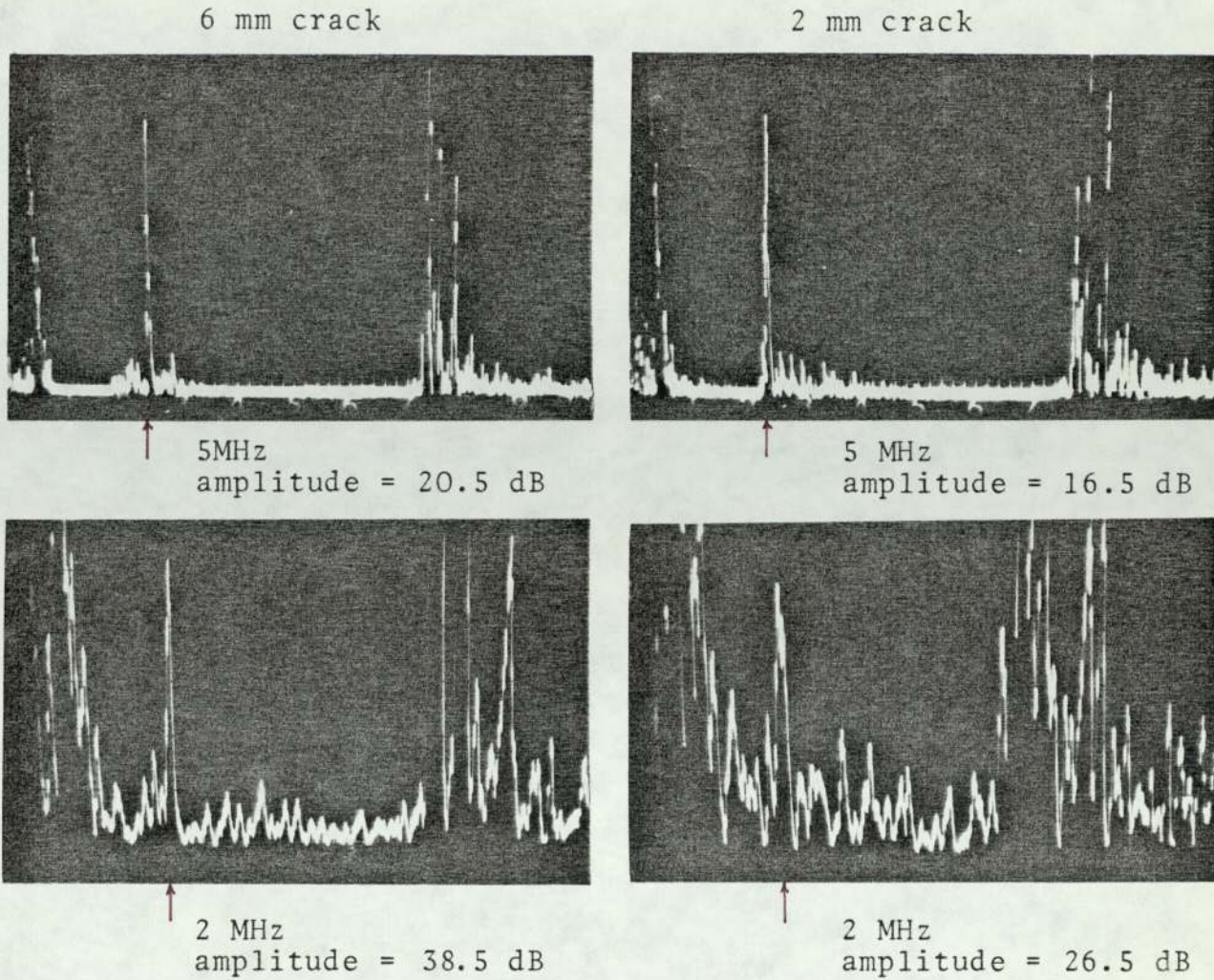


FIG. 25: Signal amplitude responses from fatigue cracks under compression in the as-welded, stress-relieved and normalised welds using a 45° probe, 5 MHz at ½ skip scanning



Material : QT35
 Condition : As-welded
 Probes : 70°
 Frequency : 2MHz and 5MHz

FIG. 26: Ultrasonic screen traces of the signals from 2 mm and 6 mm fatigue cracks using 2MHz and 5 MHz 70° probes at $\frac{1}{2}$ skip scanning position

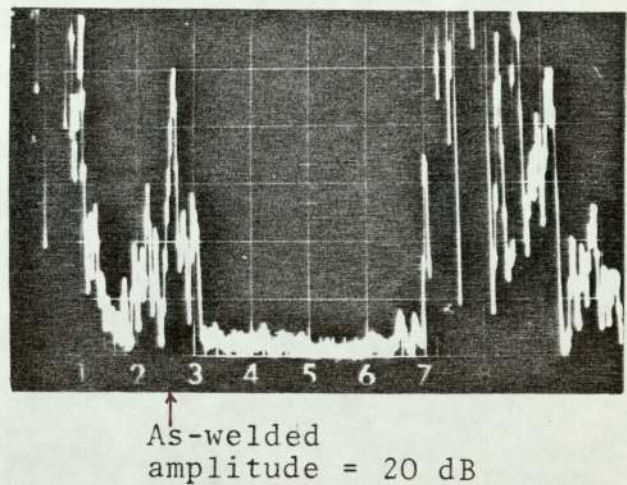
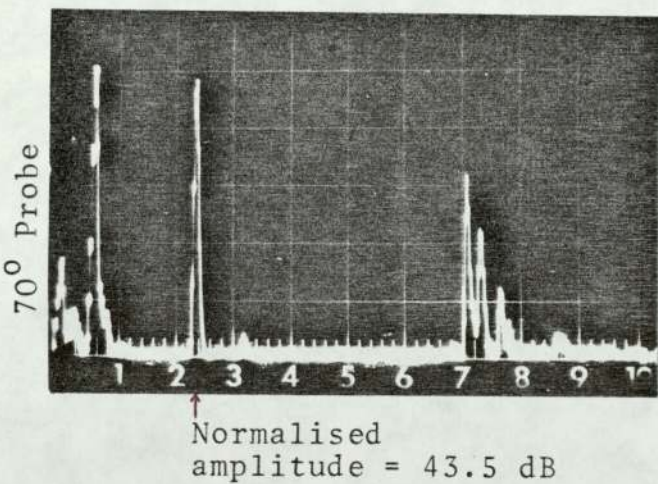
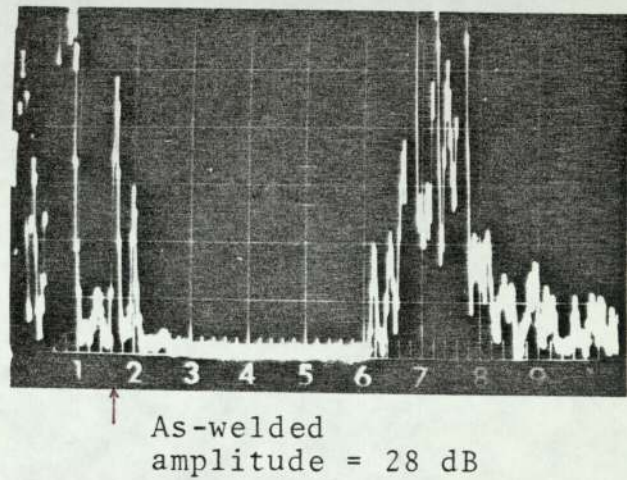
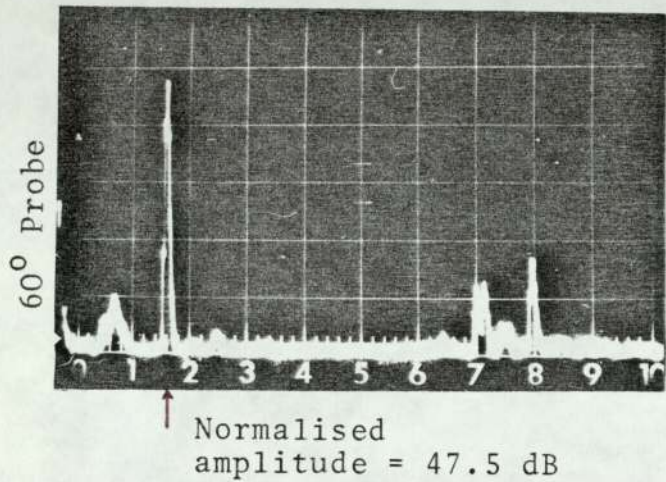
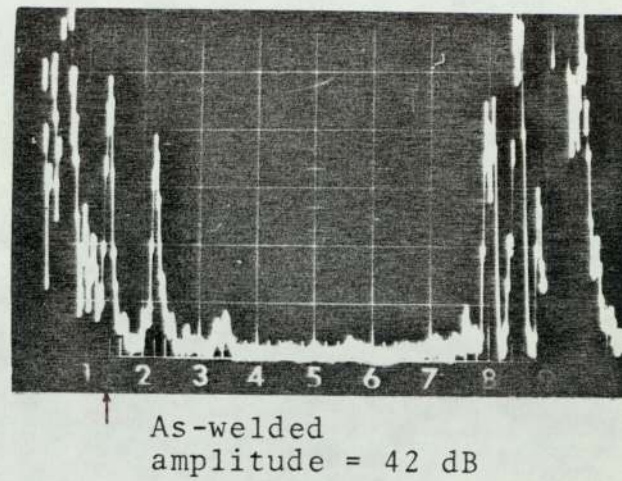
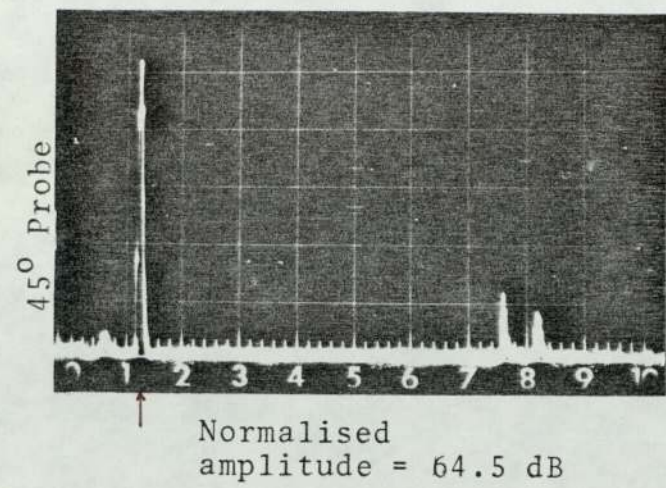


FIG. 27: Comparison between the ultrasonic screen traces of 2 mm fatigue cracks in the as-welded and normalised QT35 welds using 45°, 60° and 70° probes, 2MHz at $\frac{1}{2}$ skip scanning position

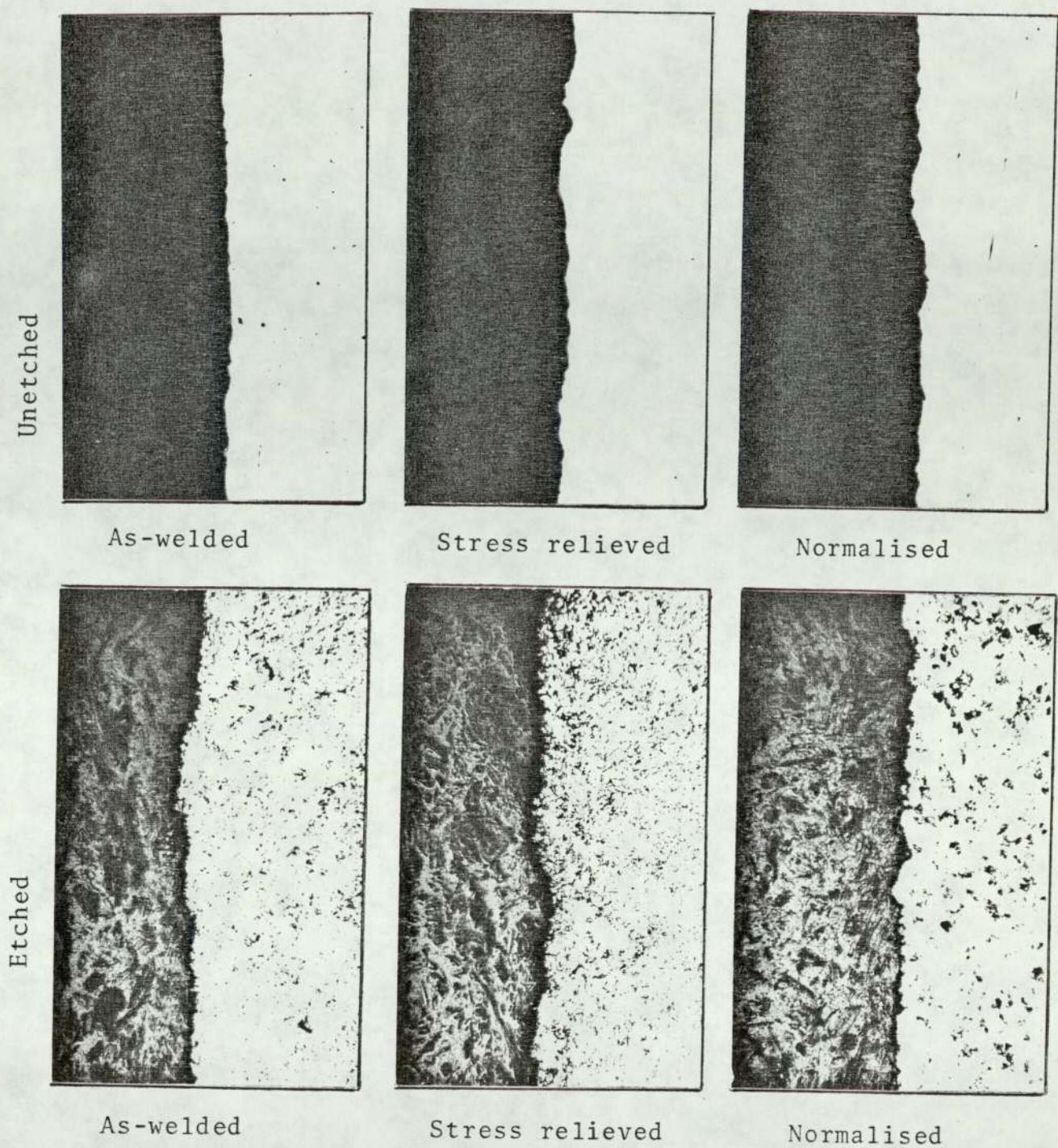


FIG. 28: Surface topography of 6 mm fatigue cracks grown in QT35 submerged arc welds in the as-welded, stress relieved and normalised conditions (x100)

occurs in the different structures. Birchak and Gardner ⁽²⁹⁾ claimed that fatigue crack closure is imperfect as the area of contact depends on the compression of surface roughness peaks. The effective displacement therefore depends on the size of the surface irregularities. It is therefore possible to conclude that crack surface topography plays an important role in acoustic crack closure which results from compressive stresses. Accordingly the relative ease of crack closure associated with the crack in the as-welded condition can be related to the smooth and fine crack facets and the relatively weak overall echo-amplitude response. The gradual and slow closure rate which is associated with the cracks in the stress-relieved and normalised welds can be related to the coarser but well defined facets, which because of their favourable orientation give a strong overall response. Presumably their coarse and well defined facets make mechanical closure difficult. Packman ⁽⁶⁹⁾ and Haines ⁽⁷⁵⁾ also found that if a crack is tight and does not have many reflecting facets, i.e. smooth cracks, it may be quite difficult to detect. In the case of a crack with a large number of facets, the probability of detecting such a crack can be enhanced over a smooth crack, especially where these facets are at near normal to the incident beam. Wooldridge ⁽⁶⁾ and Lumb ⁽⁶¹⁾ also observed the strong tendency of smooth fatigue cracks to acoustic closure under compressive stresses and the dominant effect is a steady reduction in echo amplitude caused by the increase in actual area of solid contact between the crack faces. Hence crack faces are held together permitting

sufficient transmission and consequently poor reflectivity associated with loss of echo signal strength, which makes the detection of small cracks impossible (64). Because of the low amplitude from a closed crack the high level of background noise a signal may approach the noise level and become undetectable (37,81).

4.4 The Influence of the Material Factor on the Detection and Sizing of Unstressed Fatigue Cracks

Figs. 29 and 30 represent the signal amplitude responses from the unstressed fatigue cracks of 2 mm, 4 mm and 6 mm depths in three different materials; NP8, mild steel and QT35-steel.. From Fig. 29 it can be concluded that all the probes used can differentiate between cracks of different sizes. The responses are markedly influenced by the material type containing these cracks. This could be explained in terms of crack tightness (gap opening) and surface topography, in addition to the possibility of ultrasound velocity variation through these materials. These maximum amplitude responses appear to correlate reasonably well with the crack size range involved, as shown in Fig. 30. This figure again demonstrates the effect of material type factor. The cracks in NP8 show the highest response, while the cracks in mild steel gave the lowest response. In addition, this figure illustrates the high amplitude response performance of the 45° probe at both 2MHz and 5MHz frequencies.

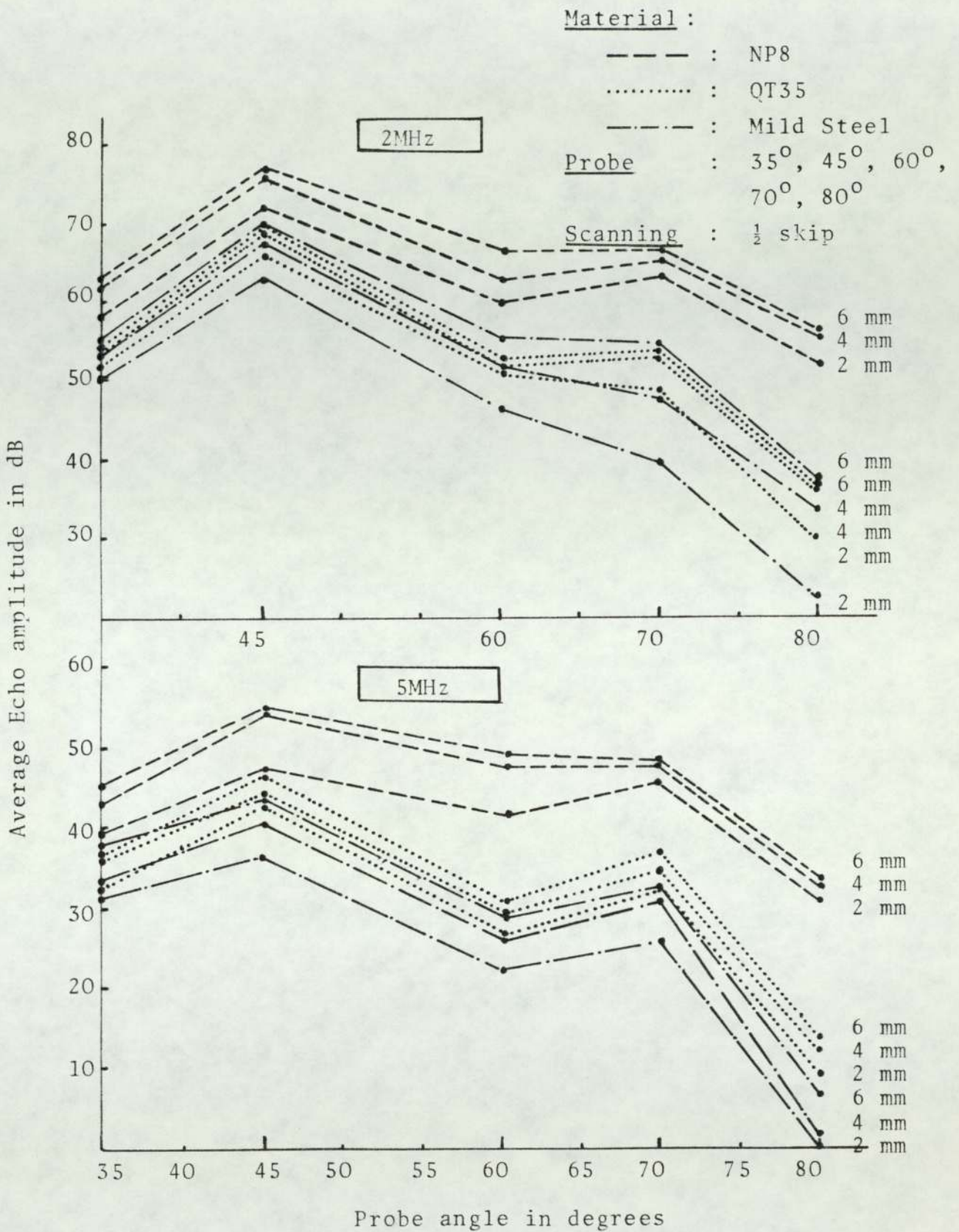


FIG. 29: Signal amplitude responses from fatigue cracks in different materials (NP8, QT35 and Mild Steel) under zero load using various angle probes at 2 and 5 MHz and ½ skip position.

Material : --- : NP8
 : : QT35
 : -.-.- : Mild steel
Probes : 45°, 60°, 70°
Scanning : ½ skip

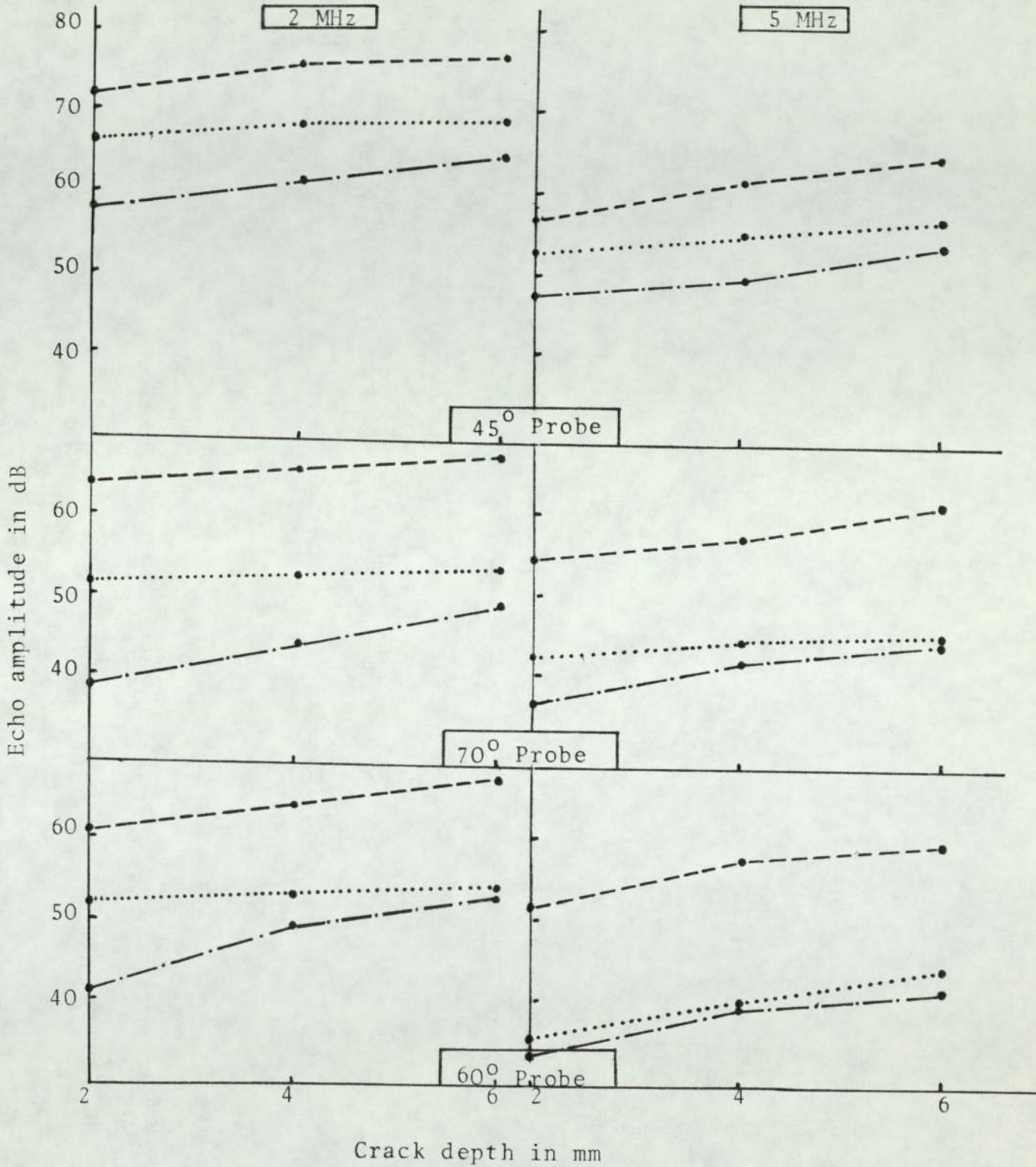


FIG. 30: Signal amplitude response from fatigue cracks in different materials (NP8, QT35 and mild steel) under zero load, using 45°, 60° and 70° probes at 2 and 5 MHz and ½ skip position

These results strongly support the idea which suggests that, if reference blocks containing reference defects are to be employed, they should be machined from the same material to be inspected for reliable results.

Finally, if all the factors which influence the fatigue crack maximum echo-amplitude, such as; crack type and material, compressive stresses and ultrasonic technique parameters, are considered thus reliable crack detection and sizing can be achieved.

4.5 Fatigue Cracks in 316 Austenitic Weldment

Previous work on surface opening fatigue cracks in ferritic steel submerged arc welds ⁽⁹⁴⁾ has shown that the optimum ultrasonic technique for detection of these cracks utilises a 45⁰, 5MHz probe at the $\frac{1}{2}$ skip scanning position. The same work also shows that the 60⁰ probe has a rather weak amplitude response, but proved to be the most sensitive probe to compressive stresses, giving an apparent crack closure at low stress levels. Comparing the above results with the HAZ fatigue cracks in austenitic weldment, it is clear that the performance of the angle probes has been drastically reversed in that 2MHz probes gave much higher and better response than the 5MHz probes. However, the 5MHz probes showed much higher sensitivity to crack closure at low stress levels (Fig. 33). In addition, unacceptable signal/noise ratios were observed when the sound waves were propagated through the bulk of the weld metal, this is shown in Fig. 36.

The 2MHz, 45° probe, when used at $\frac{1}{2}$ skip scanning position, proved to be the most efficient in detecting cracks of different sizes in the HAZ of the 316 austenitic weldment. This was true whether the inspection was carried out from the parent metal side or the weld metal side, this is illustrated in Figs. 32, 33 and 34.

Figures 35 and 36 show oscilloscope screen traces of 8 mm fatigue crack when using 45°, 60° and 70° shear angle probes, with 2 and 5MHz frequencies, at $\frac{1}{2}$ skip scanning position. It can be deduced from the traces and the respective echo-amplitude that the 2MHz, 45° angle probe appears to offer the best response from the 8 mm fatigue crack inspected from either side of the weld.

During this investigation, when the sound beam was propagated through the weld metal, differences in the values of screen and geometrical ranges were observed, with an overall increase in attenuation levels. The differences in the range values are a result of beam bending taking place when sound beam reached the parent metal/weld metal interface, this is graphically represented in Fig. 31b. This bending is dependent on the angle of approach of the sound beam, since the velocity of ultrasound inside the weld metal itself depends strongly on the angle between the weld grain axes and the sound beam direction (81,84, 85,86). This beam bending or skewing tends to be refracted towards the direction of maximum velocity (87).

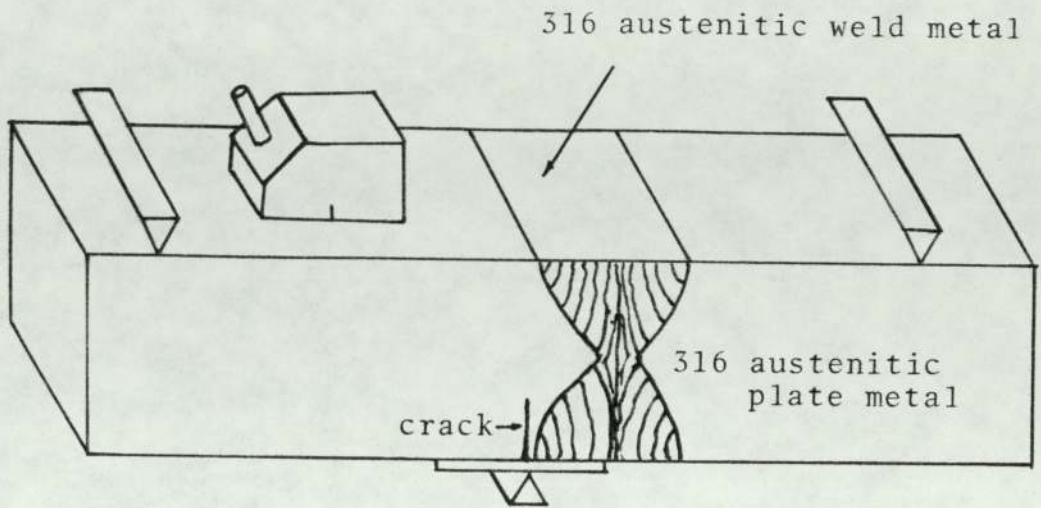


FIG. 31a: Test-piece mounted on bending jig

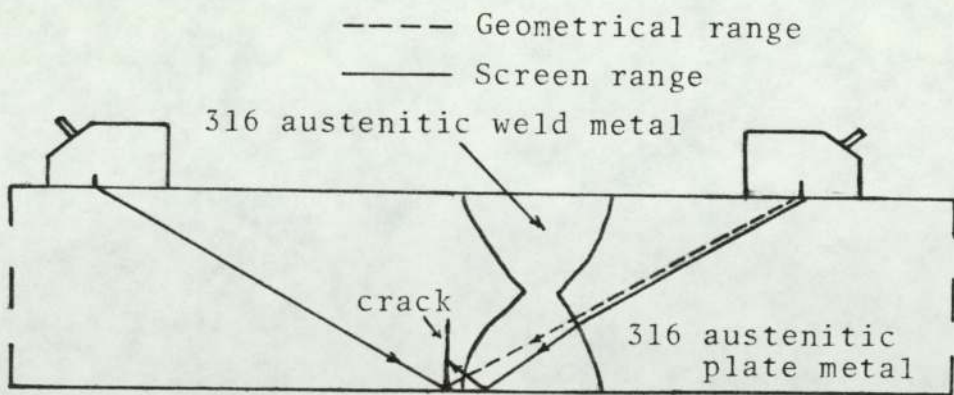


FIG. 31b: Graphical representation of the geometrical and screen ranges

HAZ Fatigue Cracks Under Zero Load

Material : 316 aust. plate welded
Probes : 45°, 60°, 70°
Frequency : 2 & 5 MHz
 --- : Parent metal
 - · - · - : Weld metal

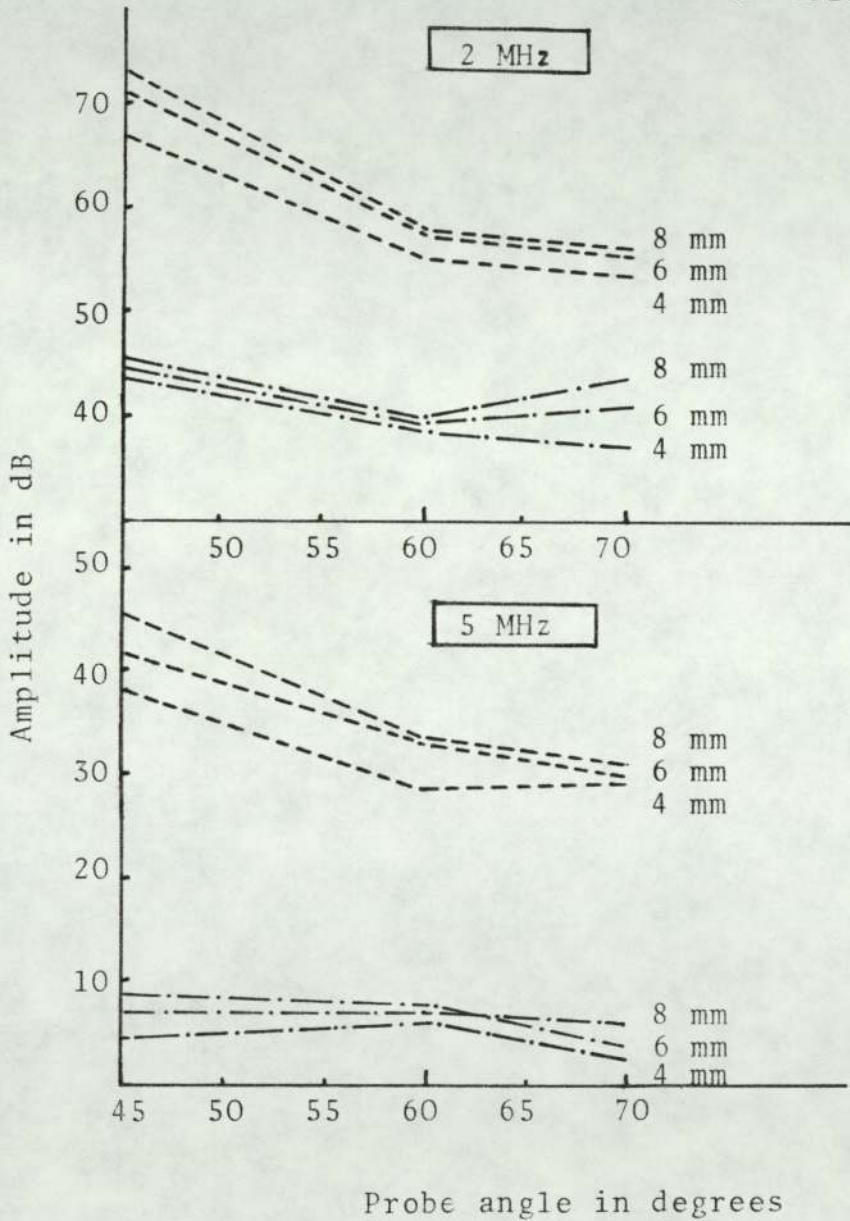


FIG. 32: Response to fatigue cracks under zero load, using 45°, 60° and 70°, 2 and 5 MHz probes, at 1/2 skip scanning position

HAZ Fatigue Cracks

Material : 316 austenitic plate welded

Probes : 45°, 60° 70°

45° Probe Frequency : 5 MHz

Scanning : 1/2 skip

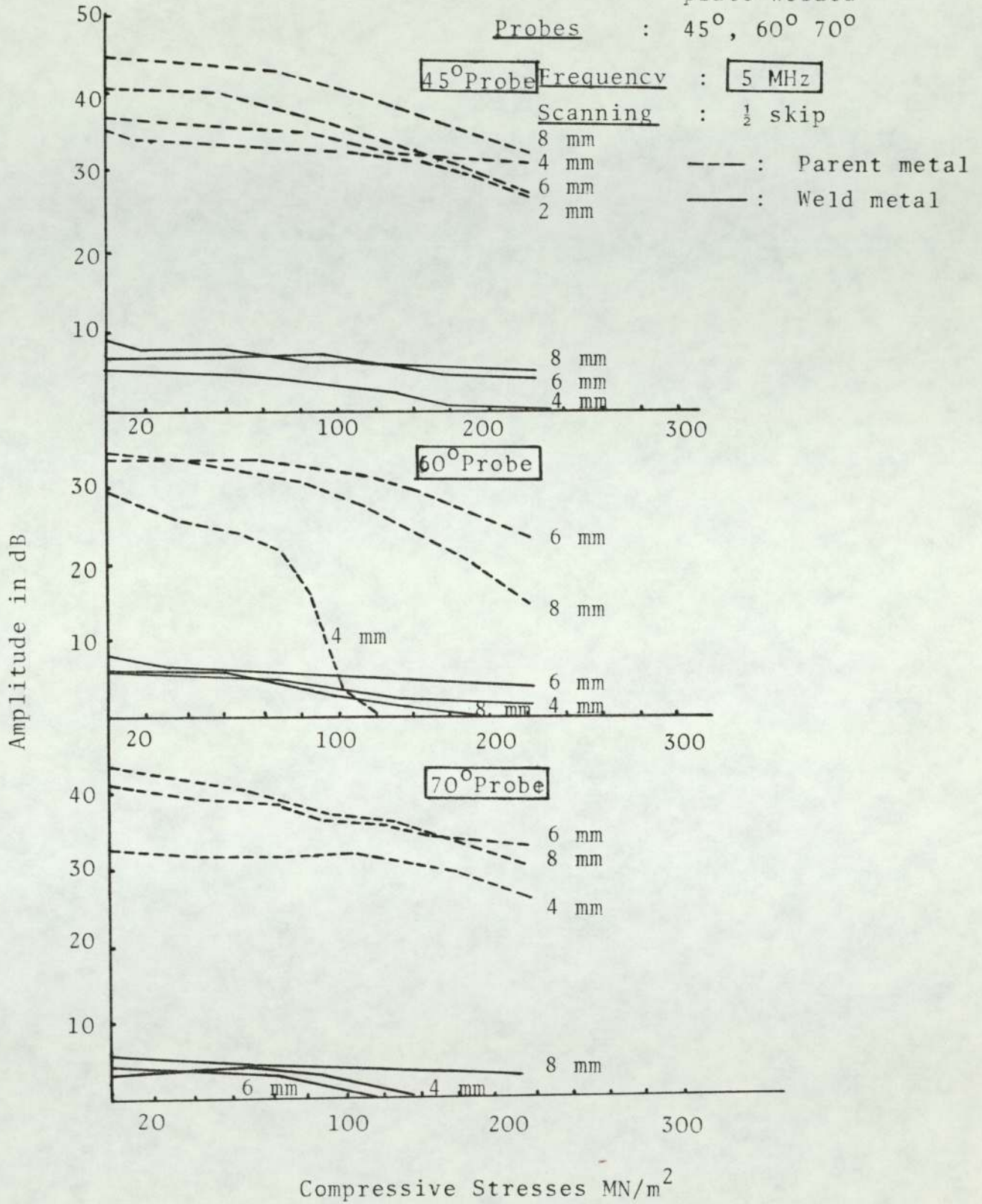


FIG. 33: Signal amplitude responses from fatigue cracks in the HAZ under compression, using 45°, 60° and 70°, 5 MHz probes at 1/2 skip scanning position

HAZ Fatigue Cracks

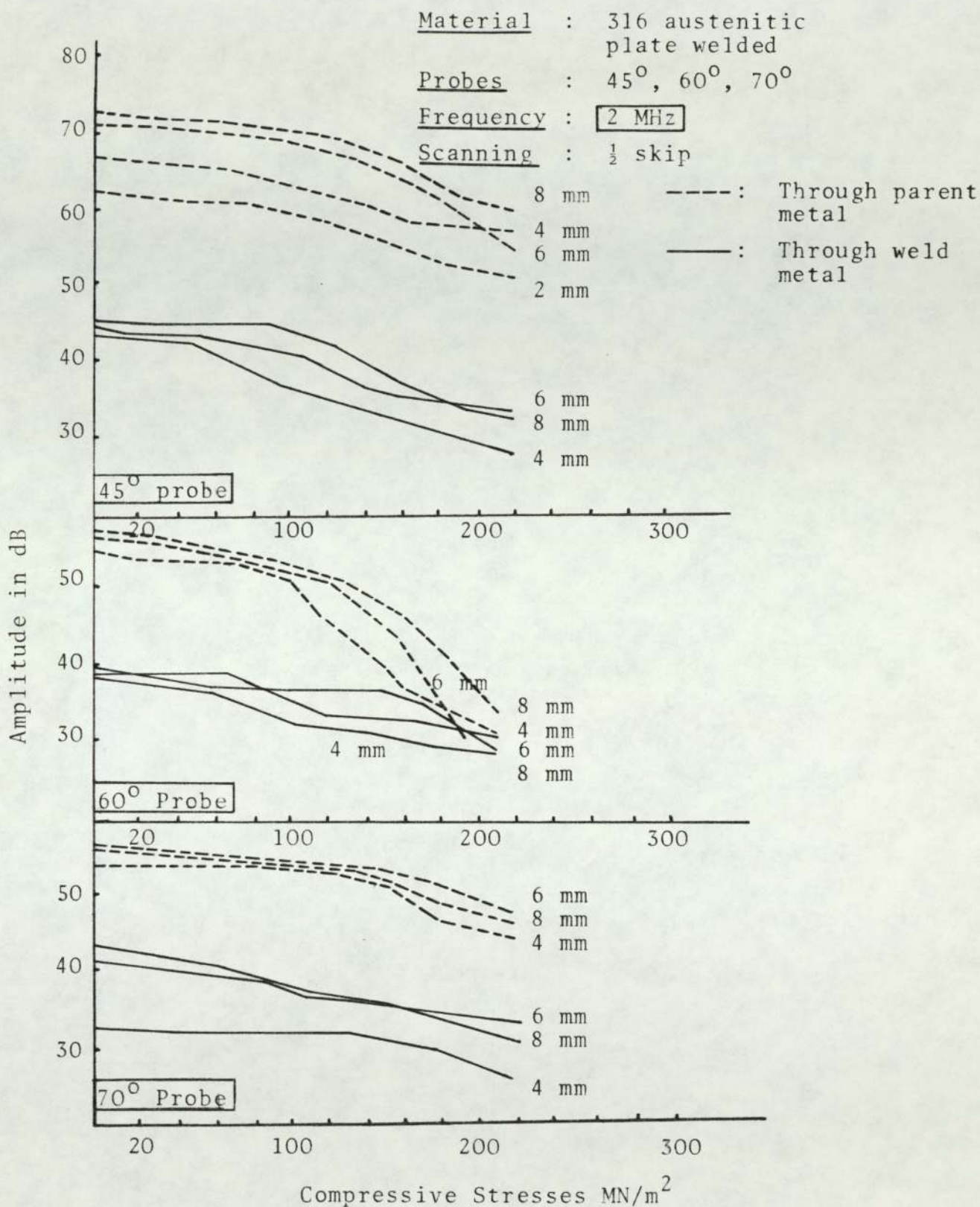


FIG. 34: Signal amplitude responses from fatigue cracks in the HAZ under compression, using 45°, 60° and 70°, 2MHz probes at ½ skip scanning position

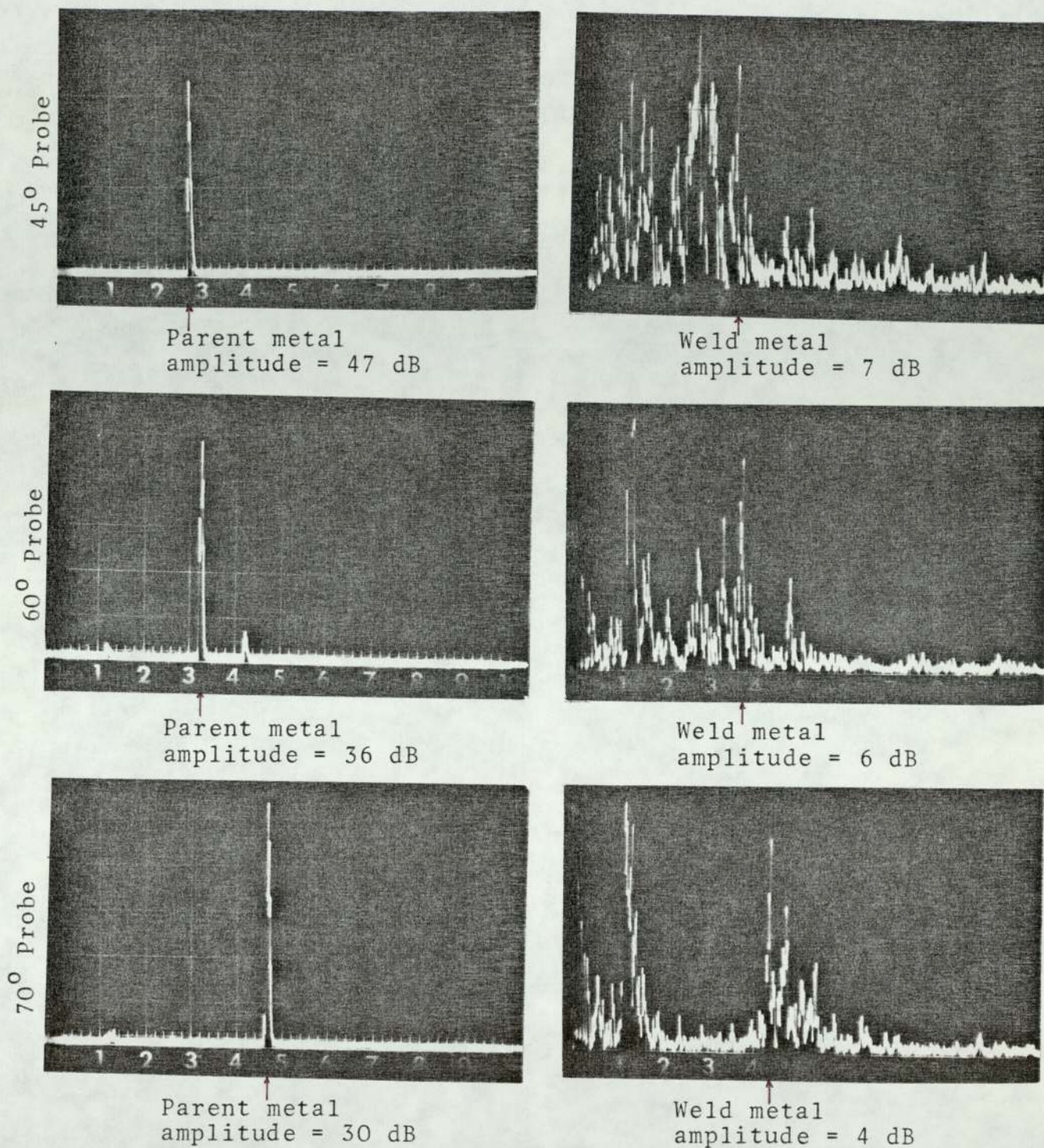


FIG. 35: Comparison between the ultrasonic screen traces of 8 mm fatigue crack in the HAZ of the 316 austenitic weldment, with the sound waves travelling through parent metal and/or through weld metal, using 45°, 60° and 70°, 5 MHz probes at $\frac{1}{2}$ skip scanning position

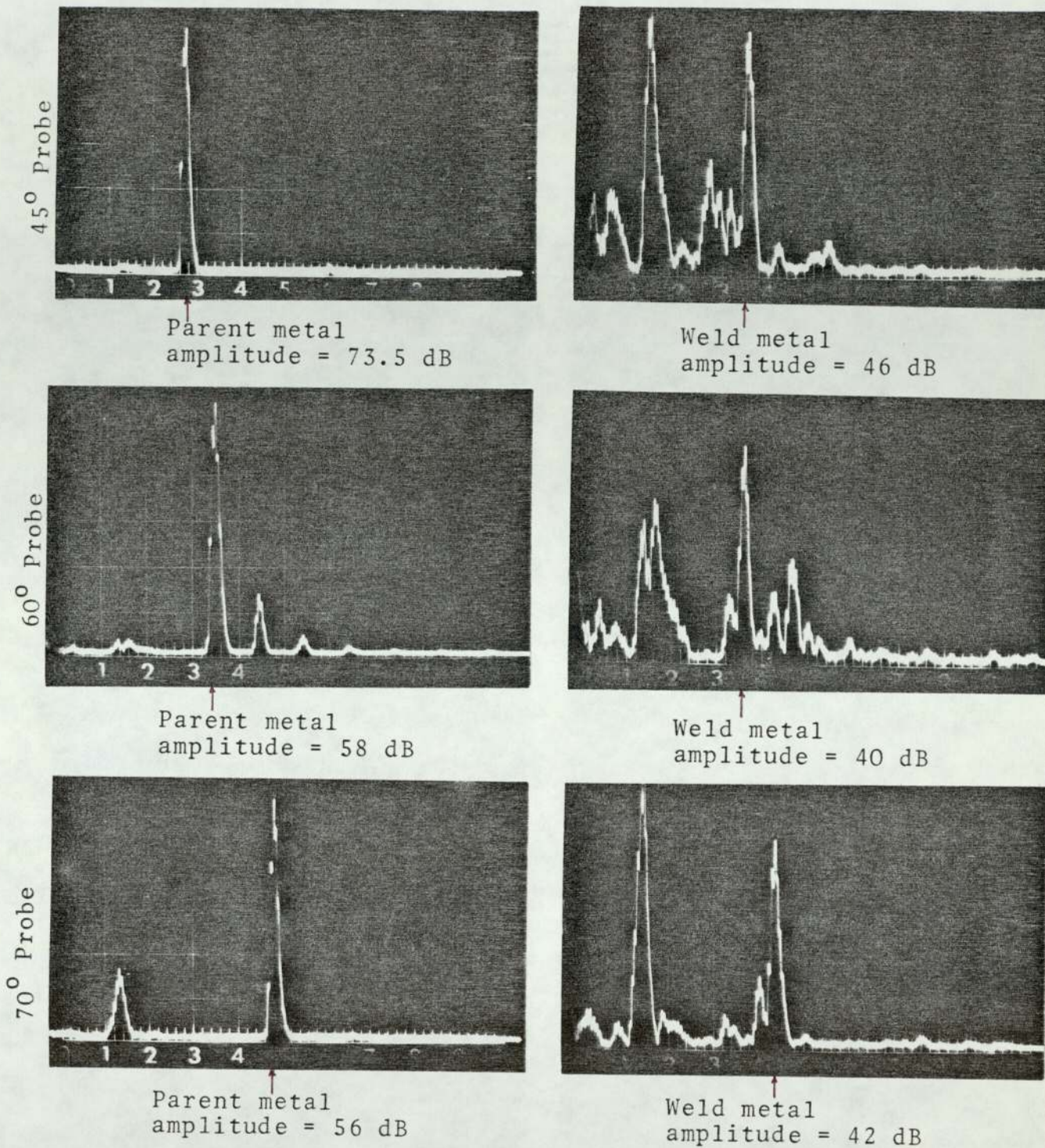


FIG. 36: Comparison between the ultrasonic screen traces of 8 mm fatigue crack in the HAZ of 316 austenitic weldment, with the sound wave travelling through parent metal and/or through weld metal using 45°, 60° and 70° 2MHz probes at $\frac{1}{2}$ skip scanning position

Table 14 gives values for the geometrical/screen range for $\frac{1}{2}$ skip scanning position, through parent metal and through weld metal. When the beam passes through weld metal it can be seen that the 45° probes produce the biggest differences in geometrical and screen ranges. This could be explained by the fact that when the 60° and 70° probes are used the velocities in the parent metal and weld metal are similar, thus reducing the bending effect.

Beam deviation, mode conversion at grain boundaries and grain boundary scattering are suggested as the main factor for the increase in attenuation levels. The $\frac{1}{2}$ skip scanning position is considered to be the most suitable because it minimises the additional attenuation that a sound beam would suffer when travelling longer distances.

The traces in Fig. 35 also demonstrate the difficulty of deciding which of the signals is coming from the crack, in the case of the 5MHz probes when the beam is passing through the weld.

The results were very encouraging in that fatigue cracks situated in the HAZ of these austenitic weldments, were readily inspectable with high signal amplitude and at an acceptable signal/noise ratio, using both 2MHz and 5MHz shear angle probes. The 2MHz, 45° probe which is considered to give the best results for inspecting these cracks, could detect a 2 mm fatigue crack in the HAZ when scanning at $\frac{1}{2}$ skip from the parent metal side, and a 4 mm crack when

scanning from the weld metal side (Fig. 34). With the same conditions, the 5MHz, 45° probe could detect the 2 mm from the parent metal side (Fig. 33), but from the weld metal side the performance was reduced to unacceptable levels of sensitivity and signal/noise ratio, with the addition of many spurious signals. From the weld metal side, it was only under the application of elastic compressive stresses that the signals returning from the crack using 45°, 60° and 70° probes were identified with a degree of certainty, and even then the 4 mm and 6 mm cracks exhibited closure when interrogated with the 70° probe at low stress levels. The 4 mm crack also exhibited similar behaviour with the 45°, 5MHz probe.

The difficulties in identifying signals coming from the fatigue cracks under static compression illustrate the unreliability of the 5MHz probes for use when the ultrasound is propagated through the austenitic weld structure. It also emphasises the need for accurate screen calibration and beam plotting if the 2MHz probes are to be used to propagate ultrasound through the austenitic weld metal.

The superiority of the 2MHz probes over the 5MHz was demonstrated during the tests and, at the same time, the advantages of using 45° angle probe instead of 60° and 70° were seen.

5. CONCLUSIONS

The results obtained in this study are considered to justify the following conclusions:

(a) General conclusions:

1. Variations in the reflected ultrasonic energy are due to changes in crack topography and geometry, which are influenced by the modification of the compressive stressfield in the vicinity of fatigue cracks.
2. The crack closure tendency is strongly influenced by crack surface topography, and smoother cracks are more sensitive to crack closure under compressive stresses.
3. Examination from both sides of fatigue cracks showed variations in ultrasonic response at all stress levels.
4. The reflection of the ultrasound from fatigue cracks is a function of the probe angle. The 45° probes gave the best response at all stress levels and the 60° probes gave the lowest response, but at the same time were the most sensitive to the influence of compressive stresses. Using the 60° probe, apparent "crack closure" was found possible at low levels of elastic compressive stresses in aluminium alloy, QT35 as-welded condition and in austenitic steel weldments.

5. These results illustrate the dangers of using the returning echo amplitude as a measure of fatigue crack size.

(b) Specific conclusions:

1. Fatigue cracks in mild steel are less sensitive to the influence of compressive stresses than are those in aluminium alloy.
2. The 45° , 5MHz probe at $\frac{1}{2}$ skip scanning positions, gave the best results in detecting all crack sizes in the three QT35-steel weld conditions, i.e. as-welded, stress-relieved and normalised welds.
3. Using the 45° probe, crack reflectivity was considerably increased when fatigue cracks were grown in heat treated weld metal. This is attributed to the nature of the crack surface facets and their effect on reflection of the ultrasound in the as-welded, stress-relieved and normalised weld conditions.
4. Fatigue cracks in the HAZ of austenitic welds were readily detected using shear waves of both 2MHz and 5MHz frequencies, and 45° , 60° and 70° probe angles, provided the sound waves travelled through parent metal only.
5. When the sound beam was propagated through the austenitic weld metal, the 2MHz probes were superior to 5MHz probes.

6. The 45⁰, 2MHz probe used at $\frac{1}{2}$ skip scanning positions offers the best possibility of detecting fatigue cracks when the sound waves travel through austenitic parent metal and/or weld metal.

6. FUTURE WORK

Future work in the following areas should be encouraged:

1. Cracks, other than fatigue cracks; such as stress-corrosion and creep cracks should be studied to determine the effects of compressive stresses and crack surface topography.
2. Weld defects such as lack of penetration and lack of fusion, which are known to be detrimental to weld performance can be studied with reference to the present work on fatigue cracks.
3. A study on sizing fatigue cracks, using different angle probes and frequencies, applying the conventional sizing techniques, e.g. 6 dB and 20 dB methods, also the maximum amplitude method, to confirm the most effective combination of probe angle and frequency.
4. Detailed study of the mechanism involved in fatigue crack formation to determine whether this ultrasonic technique can be used to analyse residual stresses at fatigue cracks.
5. A study of statistical aspects of crack detection and sizing using ultrasonics would be welcome.

7. REFERENCES

1. "Ultrasonic Techniques for the Quantitative Evaluation of Weld Defects and Their Limitations", *Welding in the World*, Vol. 19, No. 1/2, 1981, pp. 7-12.
2. Renner, R.W., Greenberg, H.A., and Clarke, W.G. Jr., "Ultrasonic and Metallurgical Evaluation of Flaws in Large Rotor Forgings", *Proceedings, 5th International Conference on NDT, Montreal, Canada, 1967*, pp. 37-42.
3. Adler, L., Cook, K.V., and Simpson, W.A., "Ultrasonic Frequency Analysis", *Research Techniques in Nondestructive Testing* (Edited by R.S. Sharpe), Vol. 3, Academic Press, London, (1977)
4. "Size Measurement and Characterisation of Weld Defects by Ultrasonic Testing", *National Seminar, Coventry, 17th March 1981, The Welding Institute, Cambridge.*
5. Baborovsky, V.M., Marsh, D.M. and Mrs. Slater, E.A., "Schliern and Computer Studies of the Interaction of Ultrasound with Defects", *Ultrasonic International Conference Proceedings, 1973*, pp. 162-172
6. Wooldridge, A.B., "The Influence of Crack Growth Conditions and Compressive Stress on the Ultrasonic Detection and Sizing of Fatigue Cracks", *CEGB Report No. NW/RR/45/80, April 1980.*

7. Frederick, J.R., "Ultrasonic Engineering",
John Wiley and Son, Inc., London (1965) pp 3-5
8. Hinsley, J.F., "Non-destructive Testing"
Macdonald and Evans Ltd., London (1959), pp 165-186
9. Wood, R.W. and Loomis, A.L., Phys. Rev., 29, (1927),
373
10. Wood, R.W. and Loomis, A.L., Phil. Mag., 4, (1927),
417
11. Sokolov, S., Elek. Nachr-Tech., 6, (1929), 451
12. Desch, C.H., Sproule, D.O. and Dawson, W.J.,
J. Iron & Steel Institute, 1, (1946), 319
13. Firestone, F.A., U.S. Patent 2280226, April 21,
1942, Iron Age, (1944), 154
14. Firestone, F.A., "The Supersonic Reflectoscope
for Interior Inspection", Metal Progr., 48,
(1945), 505
15. Krautkramer, J., and Krautkramer, H., "Ultrasonic
Testing of Metals", 2nd Edition, Springer-Verlag,
Berlin, Heidelberg, New York, (1977)
16. Tenbusch, T., and Hass, R., "Non-destructive
Testing of Unfired Pressure Vessels", Rhein-Westf.
Technischer Oberwachungs-Verein, Essen, West
Germany, (1972), 11-52, pp 715-722

17. Silk, M.G., "Sizing Crack-like Defects by Ultrasonic Means", In 'Research Techniques in Non-destructive Testing' (Edited by R.S. Sharpe), Vol. 3, Academic Press, London, (1977)
18. Whittle, M.J., "Advances in Ultrasonic Flaw Detection", C.E.G.B. Research, Nov., 1979
19. Coffey, J.M., "Quantitative Assessment of the Reliability of Ultrasonics for Detecting and Measuring Defects in Thick-Section Welds", Proc. Conf. on "Tolerance of Flaw in Pressurised Components", Inst. Mech. Eng., (1978), London, pp. 57-63
20. Adler, L., and Whaley, H.L., "Flaw Characterisation by Ultrasonic Frequency Analysis", Materials Evaluation, 29, August 1971, p. 182
21. Karjorlainen, L.P., and Moilanen, M., "Detection of Plastic Deformation During Fatigue of Mild Steel by the Measurement of Barkhausen Noise", NDT International, April 1979, pp. 51-55
22. Woods, P., Ph.D. Thesis, University of Aston (1976)
23. Lundin, C.D., "The Significance of Weld Discontinuities - A Review of Current Literature", W.R.C. Bulletin 222, Dec. 1976
24. Basar, N.S., et al, "Survey of Structural Tolerance in the United States Commercial Shipbuilding Industry", Ship Structure Committee Report No. 273, 1978, M. Rosenblatt & Son Inc.

25. Santini, W., "Quality Standards and Quality Control in Shipbuilding : A Joint Task of Shipyard and Classification Society", 1976, p. 29, Inter. Conf. London, 18-20, Nov. 1975, Vol. 1, TWI, Cambridge
26. "Inspection of Welds when Fitness-for-purpose Criteria are applied - Preliminary Recommendation", Welding in the World, Vol. 18, No. 5/6, 1980, p. 119
27. Aldher, J.F., "Detection and Measurement of Cracks - Introduction" (1976), The Welding Institute, Cambridge
28. Hanstock, R.F., "The Detection of Fatigue Cracks in Metals", British Journal of App. Phys. - supplement No. 6, April 1957, pp. 48-50
29. Birchak, J.R., and Gardner, C.G., "Comparative Ultrasonic Response of Machined Slots and Fatigue Cracks in 7075 Aluminium", Materials Evaluation, Dec. 1976, pp. 275-280
30. Doyle, P.A., and Scala, C.M., "Crack Depth Measurement by Ultrasonics - A Review", Ultrasonics, July 1978, pp. 164-169
31. Weil, B.L., "Stress Corrosion Crack Detection and Characterisation Using Ultrasound", Materials Evaluation, June 1969, Vol. 27, pp. 135-144
32. Corbly, D.M., Packman, P.E., and Pearson, H.S., "The Accuracy and Precision of Ultrasonic Shear Wave Flaw Measurement as a Function of Stress on the Flaw", Materials Evaluation, May 1970, pp. 103-110

33. Webber, D., and Maddox, S.J., "Problems in the Detection and Monitoring of Fatigue Cracks in Al-Zn-Mg Alloy Fillet Welds", In 'Detection & Measurement of Cracks', Published by the Welding Institute, Cambridge (1976), pp. 16-24
34. Abrahams, C.J., "Practical Industrial Ultrasonics Examination", Ultrasonics, Jan-March, 1965, pp. 30-35
35. Bobbin, J.E., "Ultrasonic Weld Inspection", A Status Report, NDT, May-June, 1960, Vol. 18, pp. 200-202
36. Ridder, J.H., "Ultrasonic Weld Inspection - Limitations and Possibilities", Proceedings 1968 Symposium on the NDT of Welds and Material Joining, pp. 587-604
37. Golan, S., Adler, L., Cook, K.V., Nanstead, R.K., and Bulland, T.K., "Ultrasonic Diffraction Technique for Characterisation of Fatigue Cracks", Journal of Non-destructive Evaluation, March 1980, Vol. 1, No. 1, pp. 11-19
38. Jackson, B., "The Use of Edge of Beam Methods for the Assessment of Defect Size", British Journal of NDT, July 1974, pp. 114-116
39. Meyer Hans-Jurgen, "Probability of Detecting Planar Defects in Heavy-Wall Welds by Ultrasonic Techniques According to Existing Codes", International Institute of Welding Annual Assembly, 1977, Copenhagen
40. Gericke, O.R., "Determination of the Geometry of Hidden Defects by Ultrasonic Pulse Analysis Testing", Journal of the Acoustic Society of America, March 1963, Vol. 35, No. 3, pp. 364-368

41. Thompson, R.B., "Overview of Ultrasonic NDE Research", In 'Non-destructive Evaluation of Materials', (Edited by J.J. Burke and V. Weiss) 23, 1979, pp. 257-280, Plenum Press, New York
42. McGonnagle, J.W., "Non-destructive Testing", 2nd Edition, Gordon & Breach, London (1971)
43. Harris-Maddox, B., "The Identification of Weld Defects by Ultrasonic Methods", Ultrasonics, Oct-Dec. 1963, pp. 189-193
44. Digiacomo, G., Crisci, J.R. and Goldspiel, S., "An Ultrasonic Method for Measuring Crack Depth in Structural Weldments", Materials Evaluation, Sept. 1970, pp. 189-202
45. Procedures and Recommendations for the Ultrasonic Testing of Butt Welds", The Welding Institute, Cambridge, 1971, pp. 10-11
46. Juva, A., and Lieto, J., "The Ultrasonic Examination of Thin Austenitic Stainless Steel Butt-Welds", British Journal of NDT., July, 1980, pp. 191-195
47. Consideration of Fracture Mechanics Analysis and Defect Dimension Measurement Assessment for the Trans-Alaska Oil Pipeline Girth Welds", National Bureau of Standards, Vol. 1 & 2, PB-260400, PB-260401, Washington, DC, Oct. 1976

48. "Draft PD for Guidance on Some Methods for the Derivation of Acceptance Levels for Defects in Fusion Welded Joints", British Standards Institution, June 1978, London
49. Tenge, P., et al., "Acceptance Criteria for Weld Defects and Non-Destructive Inspection Procedures for LNG Tanks in Ships", Metal Construction, Vol. 7, No. 1, January 1975
50. Sandor, L.W., "A Study of the Significance of Weld Discontinuities in Shipbuilding", Materials Evaluation, Vol. 39, No. 6, May 1981, pp. 533-539
51. Schall, W.E., "Non-Destructive Testing" Machinery Publishing Co. Ltd., 1968, pp. 125-128
52. Coffey, J.M., Oates, G., and Whittle, M.J., "The Future of Ultrasonic Examination in Engineering", Phil. Trans. R. Soc. London, A 292, 1979, pp. 285-298
53. Cook, D., "Crack Depth Measurement with Surface Waves", Procs. Brit. Acoustic Soc., Spring Meeting, Loughborough, 1972, Paper 72U19
54. Hudgell, R.L., Morgan, L.L. & Lumb, R.F., "Non-Destructive Measurement of the Depth of Surface-Breaking Cracks Using Rayleigh Waves", Brit. J. NDT., 16, (5), Sept. 1974, pp. 144-149
55. Adler, L., "Some Applications of Spectral Analysis in Ultrasonic Testing", USAFC Report 73, 1973, p. 730

56. Lloyd, E.A., "Wide Band Ultrasonic Techniques", Proc. Symposium on the Future of Ultrasonic Spectroscopy, British Non-Ferrous Metals Research Association, 1970, London
57. Silk, M.G., & Lidington, B.H., "Defect Sizing Using the Time Delay Diffracted Ultrasound", in 'Detection and Measurement of Cracks', The Welding Institute, 1976, Cambridge
58. Carson, J.M., and Rose, J.L., "An Ultrasonic Non-Destructive Test Procedure for the Early Detection of Fatigue Damage and the Prediction of Remaining Life", Materials Evaluation, April 1980, Vol. 38, No. 4, pp. 27-39
59. Thompson, D.O., and Thompson, R.B., "Quantitative Ultrasonics", Phil. Trans. R. Soc., A.292, London, 1979, pp. 233-250
60. Sharpe, R.S., "Current Limitations of Non-Destructive Testing in Engineering", Phil. Trans. R. Soc., A.292, London, 1979, pp. 163-174
61. Lumb, R.F., "Defect Sizing - The State of the Art", I.Mech. E. Conference Publication, 1978, pp. 65-71
62. Lautzenheiser, C.E., Whitting, A.R. & McElroy, J.J., "Ultrasonic Variables Affecting Inspection", 3rd Conf. Periodic Inspection of Press. Components, I. Mech. Eng., 1976, pp. 107-111

63. Roehrs, R.J., "ASME Code Ultrasonic Examination of Welds: An analysis", Proceedings, 1968, Symposium on the NDT of Welds & Material Joining, The American Society for NDT., Inc., Illinois, pp. 288-357
64. Chang, F.H.S., Couchman, J.C., and Yee, B.G.W., "The Effects of Stress on the Detection of Fatigue Cracks by Ultrasonic Techniques", Proc. 9th Sump. on NDE, San Antonio, April 1973, pp. 424-433
65. Yee, B.G.W., Hagemeyer, J.W., "Stress and the Ultrasonic Detection of Fatigue Cracks in Engineering Metals", NDT, Oct. 1974, pp. 245- 250
66. Wooldridge, A.B., "The Effects of Compressive Stresses on the Ultrasonic Response of Steel-Steel Interfaces and of Fatigue Cracks", CEGB Report No. NW/SSD/RR/42/79, April, 1979
67. Sessler, J.G., "The Effect of Stress Field on Ultrasonic Energy Reflected from Discontinuities in Solids", International Advance in NDT., Vol. 5, 1977, pp. 117-131
68. Lidington, B.H., Silk, M.G., Montgomery, P., and Hammond, G., "Ultrasonic Measurement of Depth of Fatigue Cracks", British Journal of NDT., Vol. 10, June 1977, pp. 129-134

69. Packman, P.E., "The Role of Crack Topography on the Ability of Ultrasonic Shear Wave Techniques to Detect and Measure Small Cracks", Proc. 7th Conf. on NDT., Warsaw, 1973, Paper H10
70. Rummel, W.D., Todd, P.H.Jr., Rathke, R.A., and Castner, W.L., "The Detection of Fatigue Cracks by Non-Destructive Test Methods", Material Evaluation, Oct. 1974, pp. 205-212
71. Lake, Thorp, Barton and Perry, "Development of Stress Enhanced Ultrasonic Compressor Blade Inspection Equipment", Proc. 10th Symp. on NDE, San Antonio, April 1975.
72. Magistrali, G., and Sevino, F., "Evaluation of Crack Detection Methods", NDT. International, Vol. 13, No. 2, April 1980, p. 84
73. "Trends in Testing and Inspection Technology - Technology Forecast 81", Edited by Harry E. Chandler, Metal Progress, Jan. 1981, pp. 79-81
74. Center, D.E., and Roehrs, R.J., "Ultrasonic/Radiographic Examination of Heavy-Wall Pressure Vessel Weldments", Materials Evaluation, May 1969, pp. 107-117
75. Haines, N.F., "The Reliability of Ultrasonic Inspection", In 'Reliability Problems of Reactor Pressure Components', Vol. 2, Proc. Symposium, Vienna, Oct. 1977

76. Schijve, J., "Fatigue Cracks, Plasticity Effects and Crack Closure", Engineering Fracture Mechanics, Vol. 11, 1970, pp. 167-221
77. Kupperman, D.S., and Reimann, K.J., "Ultrasonic Wave Propagation Characteristics and Polarisation Effect in Stainless Steel Weld Metal", Argonne National Laboratory, ANL-78-29, March 1978
78. Kupperman, D.S., Reimann, K.J., and Fiore, N.F., "Role of Microstructure in Ultrasonic Inspectability of Austenitic Stainless Steel Welds", Materials Evaluation, 1978, 36, No. 5, P.81
79. Mech, J.J., and Michaels, T.E., "Development of Ultrasonic Examination Methods for Austenitic Stainless Steel Weld Inspection", Materials Evaluation, 1977, 35, No. 7, p. 81
80. Neumann, E., Romer, M., Just, T., Nabel, E., Mathies, K., and Mundry, E., "Development and Improvements of Ultrasonic Testing Techniques for Austenitic Nuclear Components", Presented at 2nd Inter. Conf. on Non-Destructive Evaluation in the Nuclear Industry, Salt Lake City, Feb. 13-15, 1978
81. Baikie, B.L., Wagg, A.R., Whittle, M.J. and Yapp, D., "Ultrasonic Inspection of Austenitic Welds", J. British Nucl. Eng. Soc., 1976, 15, No. 3, p. 257-261

82. Kupperman, D.S., Reimann, K.J., and Winiecki, A., "Computer-Assisted Spatial Averaging for Ultrasonic Inspection of Stainless Steel Welds", Materials Evaluation, May, 1981, Vol. 39, No. 6, pp. 527-532
83. Edelmann, X., "Application of Ultrasonic Testing Techniques on Austenitic Welds for Fabrication and In-Service Inspection", NDT International, June 1981, Vol. 14, No. 3, pp. 125-133
84. Tomlinson, J.R., et al "Ultrasonic Inspection of Austenitic Welds", British Journal of NDT., 1980, Vol. 22, No. 3, pp. 119-127
85. Kapranos, P.A., Al-Helaly, M.M.H., and Whittaker, V.N., "Ultrasonic Velocity Measurements in 316 Austenitic Weldments", To be published in the British Journal of NDT
86. Gillan, M.T., "Ultrasonic Wave Propagation in Austenitic Stainless Steel Weld Metal", Theoretical Physical Division, AERE, Harwell, Oxfordshire, Report HL80/1528, May 1980
87. Silk, M.G., "Inspecting Austenitic Welds", In 'Research Techniques in Non-Destructive Testing' (Edited by R.S. Sharpe), Vol. 4, pp. 393-449, Academic Press, London (1980)
88. Gray, B.S., "Longitudinal Wave Ultrasonic Inspection of Austenitic Weldments", OECD/CSNI Specialists Meeting on Reliability of Ultrasonic Inspection of Austenitic Stainless Steel Components, Brussels, Belgium, May 1980, pp. 29-30

89. Reinhardt, E.R., "EPRI Program to Improve Nuclear Code Inspection Methods", Materials Evaluation, May 1978, Vol. 36, No. 6, pp. 36-42
90. Abrahams, C.J., "Tube-to-Tube Butt Welds in Austenitic Steel (thin Wall), their Ultrasonic Examination using Hand-Scanning Methods", British J. of NDT., 1972, Vol. 14, No. 3, pp. 66-72
91. Grebernikov, V.V., and Stinchenko, A.L., "Influence of Ultrasonic Frequency and Focusing on the Conditions for Flaw Detection in Austenitic Welds", Welding Production, Dec. 1971, Vol. 18, No.12
92. Lack, B.J., "Ultrasonic Testing of Welds in High Alloy and Austenitic Steels", Report No. RD/P/715, Clarke Chapman Ltd., Advance Technical Division, Wolverhampton, 1979
93. Ibrahim, S.I., and Whittaker, V.N., "The Influence of Compressive Stresses and Other Factors on the Detection of Fatigue Cracks Using Ultrasonics", British Journal of NDT., Nov. 1980, Vol. 22, No. 6, pp. 286-290
94. Ibrahim, S.I., and Whittaker, V.N., "The Influence of Crack Topography and Compressive Stresses on the Ultrasonic Detection of Fatigue Cracks in Submerged Arc Welds", British Journal of NDT., Sept. 1981, Vol. 23, No. 5, pp. 233-240

95. Papadakis, E.P., "Revised Grain-Scattering Formulas and Tables", Journal of Acoustic Society of America, 1965, 37, pp. 702-710
96. Ibrahim, S.I., Kapranos, P.A., and Whittaker, V.N., "Ultrasonic Inspection of Fatigue Cracks in the HAZ of Austenitic Weldments, Using Shear Wave Probes", To be published in the British J. of NDT

8. APPENDICES

APPENDIX 1

Determination of Elastic Compressive Bending Stresses

In order to obtain the value of the compressive bending stresses, a number of assumptions were required to maintain consistency between the results:

1. The neutral axis x which runs down the centre of the non-fatigued specimen, could be altered once a fatigue crack has been opened. This is assumed not to occur.
2. The distance of the stress from the neutral axis x , was taken at the neck of the fatigue crack and not its tip.
3. No estimation of the plastic flow around the tip of the fatigue crack was included.

For the Amsler 2-ton high frequency fatigue machine, the bending stresses were calculated as follows:

From bending theory

$$(a) \text{ bending moment } M = \frac{WL}{4}$$

$$(b) \text{ Moment of inertia } I = \frac{bd^3}{12}$$

where: W = Load
 L = Distance between supported test bar,
i.e. the span
 b = Width of specimen
 d = Thickness of specimen

Also from bending theory:

$$\frac{P}{Y} = \frac{M}{I}$$

where: P = stress at a distance Y from the neutral axis which runs down the middle plane X.

$$\therefore P = \frac{MY}{I}$$

Since all the variables are known, hence P can be calculated (see appendices 2 and 3).

APPENDIX 2

Sample of three point compressive bending stresses calculations during the loading cycle in mild steel test bar.

Material: Mild steel

Specimen dimensions: 25 x 23 x 200 mm

Span: 190 mm

Load (ton)	Load (N)	Bending Moment	Moment of Inertia	Stress MN/m ³
0.1	996.4	47329	2547.92	21.47
0.1	1992.8	94658	"	42.95
0.3	2989.2	141987	"	64.43
0.4	3985.6	189316	"	85.90
0.5	4982	236674	"	107.36
0.6	5978	283974	"	128.83
0.7	6974.8	331303	"	150.31
0.8	7971.2	378632	"	171.78
0.9	8967.6	425961	"	193.25
1.0	9964	473290	"	214.72
1.1	10960.4	520619	"	236.20
1.2	11956.8	567948	"	257.67
1.3	12953.2	615277	"	279.14
1.4	13949.4	662606	"	300.6
1.5	14949	709935	"	322.10
1.6	15942.4	757264	"	343.56

APPENDIX 3

Sample of three point compressive bending stresses calculations during the loading cycle in NP8 test bar.

Material: NP8
Specimen dimensions: 25 x 21 x 225 mm
Span: 190 mm

Load (ton)	Load (N)	Bending Moment	Moment of Inertia	Stress MN/m ²
0.02	199.28	9465.8	19293.75	5.15
0.04	398.56	18931.6	"	10.30
0.06	597.84	28397.4	"	15.45
0.08	797.12	37863.2	"	20.60
0.10	996.4	47329	"	25.75
0.12	1195.68	56794.8	"	30.90
0.14	1394.96	66260.6	"	36.05
0.16	1594.24	75726.4	"	41.20
0.18	1793.52	85192.2	"	46.35
0.20	1992.8	94658	"	51.50
0.22	2192.08	104123.8	"	56.65
0.24	2391.36	113589.6	"	61.80
0.26	2590.64	123055.4	"	66.95
0.28	2789.92	132521.2	"	71.10
0.30	2989.2	141987	"	76.25
0.40	3985.6	189315	"	103.02
0.50	4982	236645	"	128.79
0.60	5978.4	283194	"	154.54
0.70	6974.8	331303	"	180.30
0.80	7971.2	378632	"	206.05

APPENDIX 4

Typical maximum echo amplitude value measurements from fatigue cracks in mild steel under compressive loading.

Material: Mild steel

Probe: 45°, 5MHz

Scanning: ½ skip

6 mm fatigue crack

Load (ton)	Stress MN/m ²	Loading cycle		
		L.H.S. dB	R.H.S. dB	Average dB
0	0	43	47	45
0.1	21.47	42	47	44.5
0.2	42.95	41.5	46.25	43.75
0.3	64.43	40.5	45.5	43
0.4	85.90	39.5	45	42.25
0.5	107.36	38.5	44.25	41.25
0.6	128.83	37.5	43.5	40.25
0.7	150.31	37	42.25	39.5
0.8	171.78	36	41	38.5
0.9	193.25	35	38.5	36.75
1.0	214.72	33	36	34.5
1.1	236.20	31.5	34	32.75
1.2	257.67	30	32.25	31
1.3	279.14	29	31.5	30.25

APPENDIX 5

Typical maximum echo amplitude value measurements from fatigue cracks in NP8 under compressive loading

Material: NP8
Probe: 45°, 5MHz
Scanning: ½ skip
6 mm fatigue crack

Load (ton)	Stress MN/m ²	Loading cycle		
		L.H.S. dB	R.H.S. dB	Average dB
0	0	55	56.5	55.75
0.02	5.15	55	55.5	55.25
0.04	10.30	54	53	53.5
0.06	15.45	52.5	50.5	51.5
0.08	20.60	51	47.5	49.25
0.10	25.75	50	45	47.5
0.12	30.90	48	43	45.5
0.14	36.05	46.5	41.5	43.75
0.16	41.20	45	40.5	42.75
0.18	46.35	43.5	39.5	41.5
0.20	51.50	42	39	40
0.30	76.25	37	38.5	37.75
0.40	103.02	32	35	33.5
0.50	128.79	28	34	31
0.60	154.54	25.5	32.5	29
0.70	180.30	22.5	31.5	27

APPENDIX 6

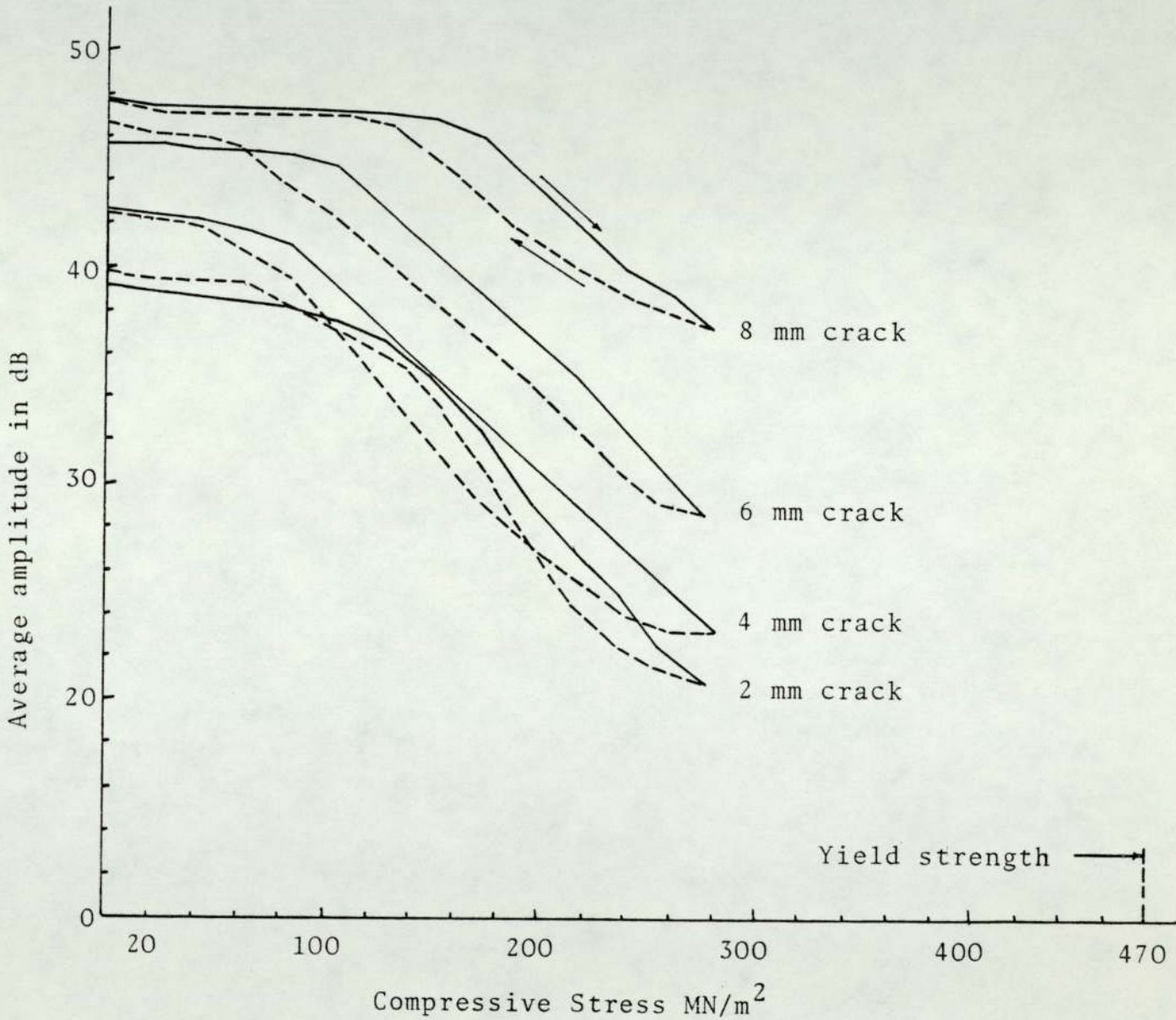
Material : Mild Steel

Probe : 45°, 5MHz

Scanning : Full skip

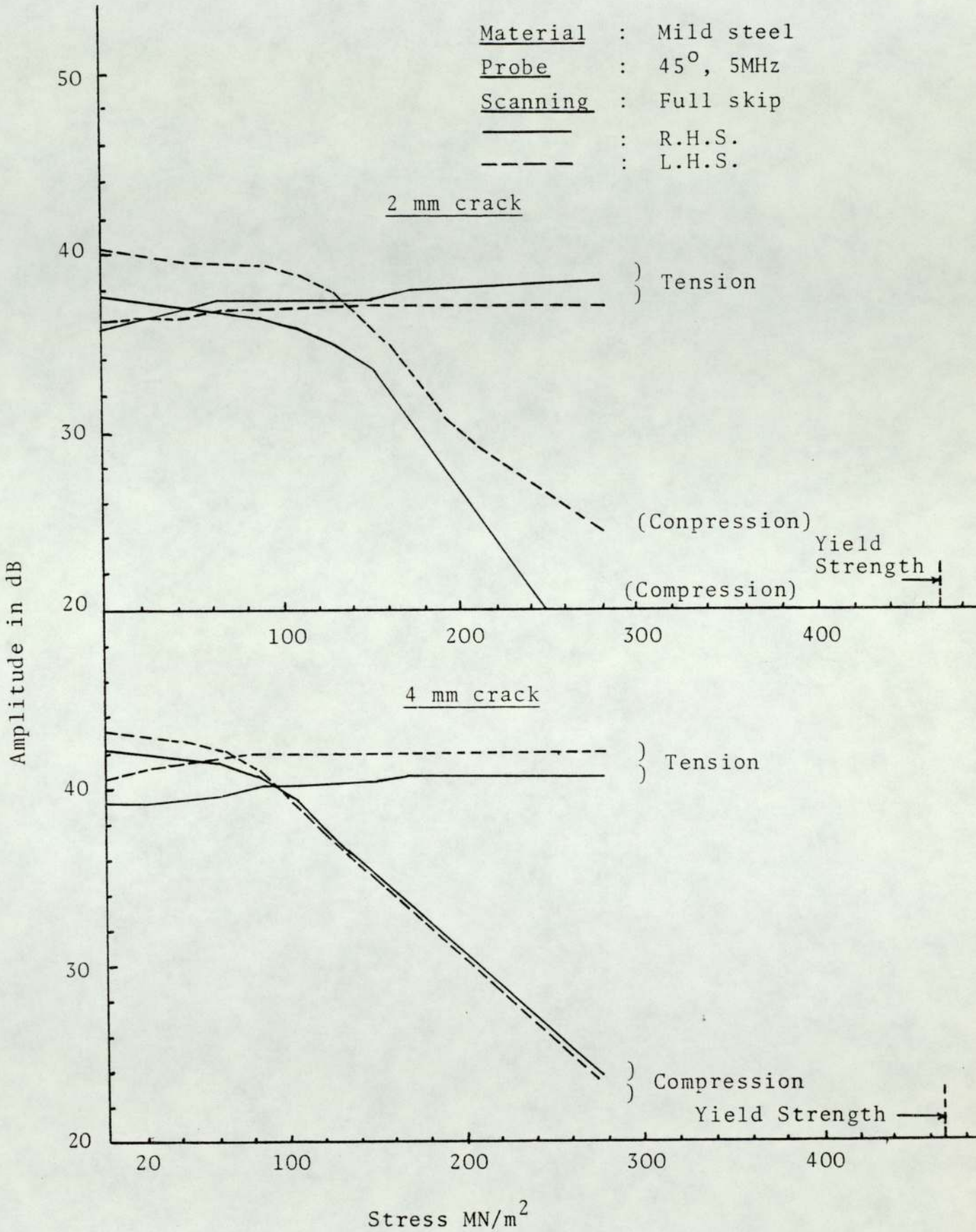
———— : Loading

----- : Unloading



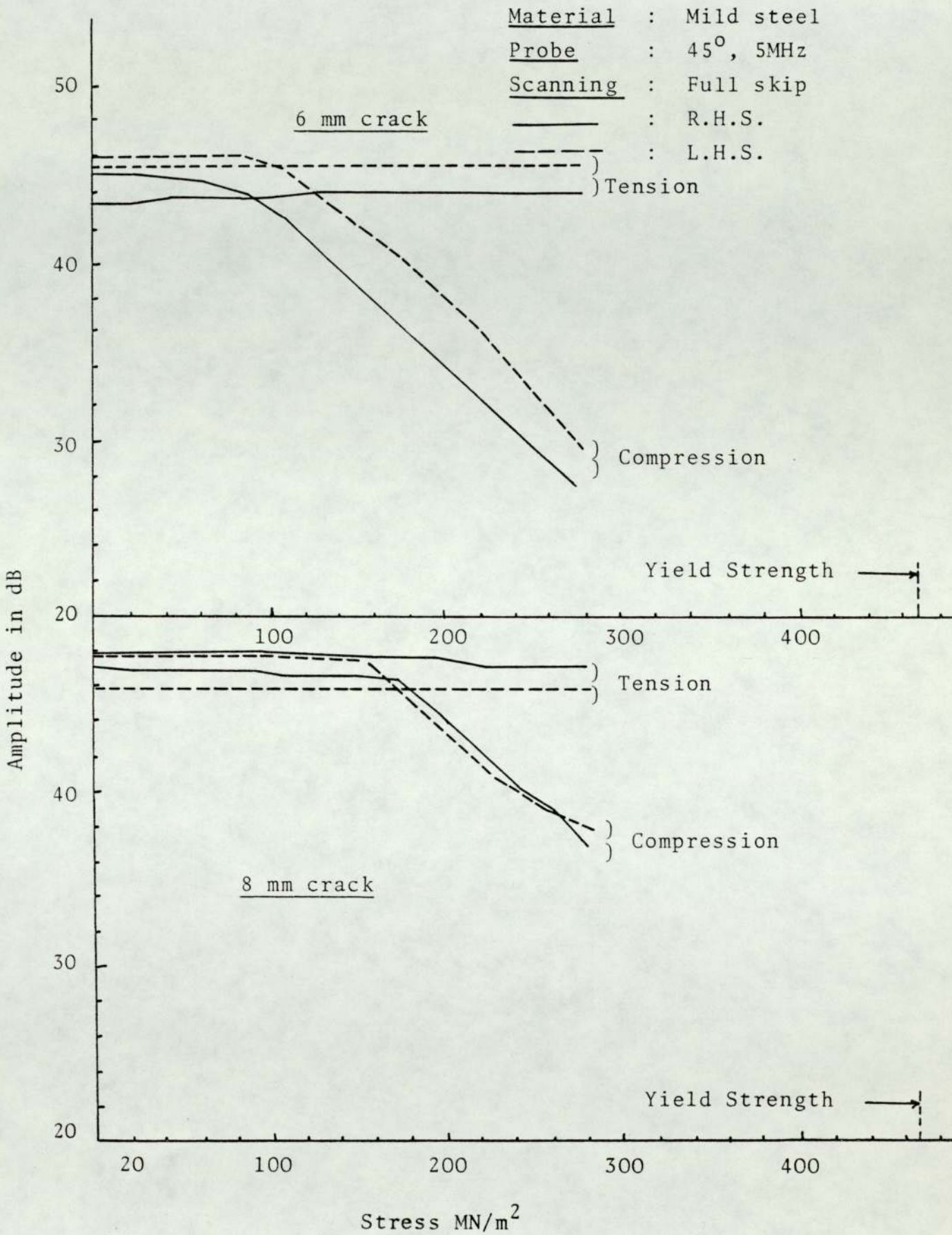
Response of fatigue cracks of different depths to compressive loading and unloading cycles

APPENDIX 7a



Response of 2 & 4 mm fatigue cracks to both compressive and to tensile bending stresses, when scanned from both sides of the cracks.

APPENDIX 7b



Response of 6 and 8 mm fatigue cracks to both compressive and to tensile bending stresses, when scanned from both sides of the cracks

APPENDIX 8

Material : Mild steel

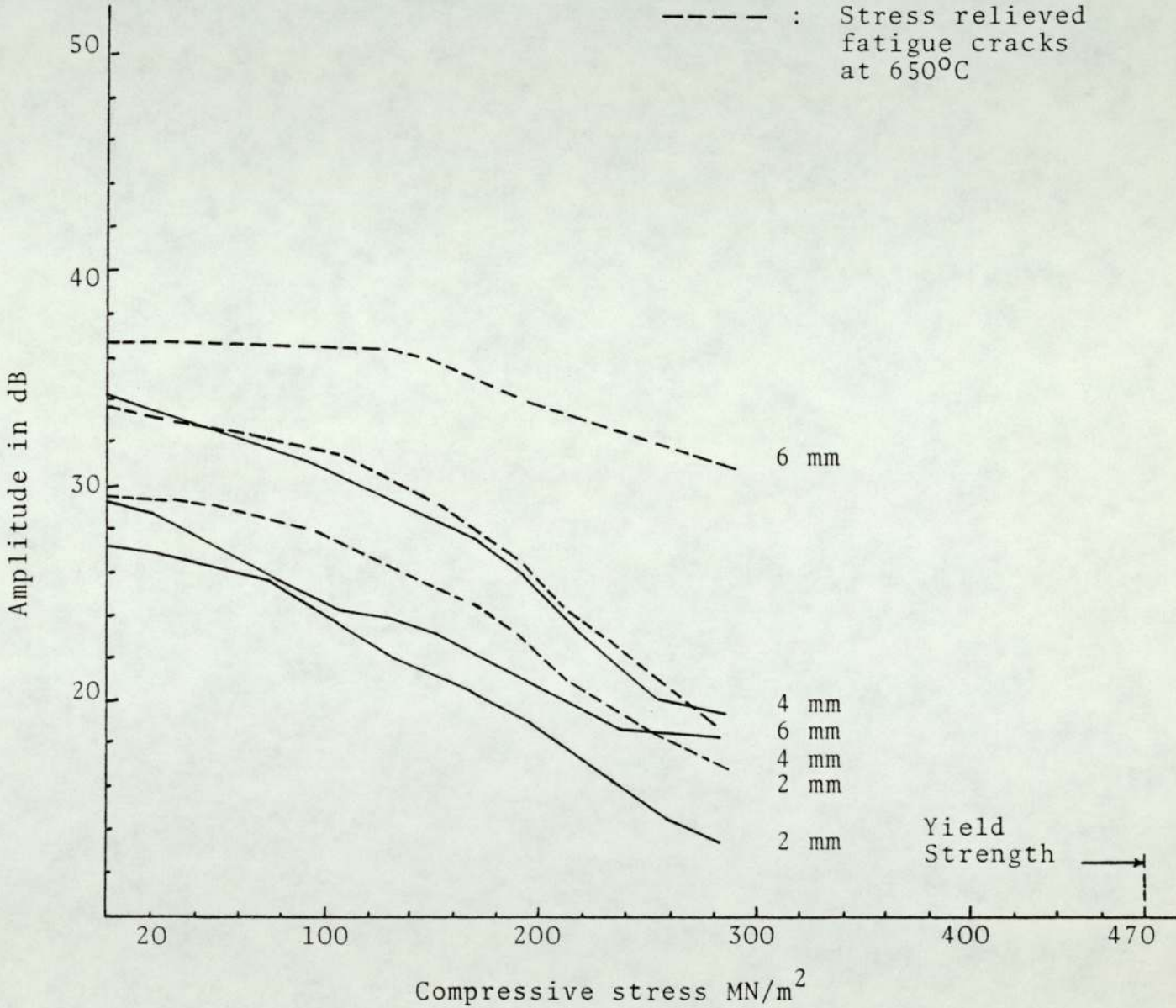
Probe : 45°, 5MHz

Scanning : ½ skip

Condition :

———— : Before stress relieving

----- : Stress relieved fatigue cracks at 650°C



The effect of stress relieving process on the detection of fatigue cracks under compressive stresses

APPENDIX 9

The first paper published in the British
Journal of Non-destructive Testing in
November 1980

The Influence of Compressive stresses and other factors on the detection of fatigue cracks using ultrasonics—

by S. I. Ibrahim[†] and V. N. Whittaker*

Under favourable conditions fatigue cracks can be readily detected by a variety of ultrasonic techniques. There are indications, however, that compressive stresses can render detection very difficult if not impossible. The factors which influence the detection of both stressed and unstressed cracks such as probe angle and frequency, crack size and type, material and scanning position have been investigated. Compressive bending stresses were found to have a considerable influence on the ease of crack detection in steel and an aluminium alloy. 'Complete closure' of certain crack configurations was found to occur under elastic compressive stresses when using certain ultrasonic techniques.

Literature Review

Fatigue is one of the most serious practical problems in metal construction. The fatigue strength of a material is affected by a vast number of factors. Therefore the prediction of the actual fatigue life of a real component or the detection of fatigue damage before a catastrophic failure is a very important but difficult task.¹ When inspecting structural members for fatigue cracks using ultrasonic techniques, one is faced with the problem of selecting suitable standard reference specimens for adjusting the ultrasonic test equipment and for interpreting defect signals. One difficulty is that fatigue cracks are poorer reflectors of acoustic energy than machined flaws of corresponding size and shape.² Fatigue crack detection is also affected by many variables such as crack orientation, crack location, crack type, surface finish, stress state and service history of the structure.³ Using artificial flaws for calibration, the shear wave technique badly underestimates the crack depth and overestimates the crack length.⁴ Another area which needs mentioning here, is the mismatch between the ultrasonic set and the probe. This has been stressed by Jackson.⁵ He claimed that many difficulties stem from mismatching. Selecting probes which have been designed to match the ultrasonic set can overcome these problems.

Size estimates of a defect depend upon the proportion of the ultrasonic beam reflected back to the probe. Thus 'reflectivity' is a decisive factor in estimating the size of a defect. Larger flaws produce greater directionality in the reflected signal than small flaws. Accordingly, to reduce the uncertainty of detecting planar defects oriented at an adverse angle to the ultrasonic beam, it has been found to be advantageous to use several angles from several directions. Examination from top and bottom surfaces of the plate is another valuable technique.⁶ Looking at a defect (crack) from two different directions at various angles increases the probability of coping with poor reflectivity due to crack orientation, tightness and smoothness.^{7,8} Center et al⁹ and Jackson⁵ claim that sizing of defects should be carried out using the shortest possible distance between probe and defect. When using full skip, the sound path may be extremely long causing too much attenuation. In which case, it may be more convenient to use $\frac{1}{2}$ skip testing.

Meyer¹⁰ and Gericke¹¹ claimed that an improvement in the detection of defects and in size evaluation can also be achieved by reducing the test frequency which gives increased beam spread. A determination of the frequency dependence of the defect echo amplitude will therefore yield information on the defect geometry, since the reflection of ultrasonic energy from a defect depends on the ratio of the defect size to the ultrasonic wave length.¹⁰

The angle probe choice is very important since it is desirable to have the sound beam strike as perpendicular as possible to get the greatest response. Upon reflection acoustic energy can be converted from one wave form to another. In particular, a significant amount of energy can be converted from the 60° shear mode to the longitudinal when the waves undergo double reflection at the intersection of a flaw and the surface of the specimen, since the reflection angle is different from the incidence angle. The energy converted to the longitudinal wave does not return to the probe.² This is also stressed by Doyle et al¹² who claimed that it was possible for the reflected pulse to disappear altogether at suitable angles and depths. This emphasises the caution needed in applying the pulse-echo technique. Thus thin flat cracks are difficult to detect and can become even more difficult when the crack is located in compressive stress fields. Conversely the application of tensile stress makes detection easier.^{3,13} Hence, any fatigue cracks present could pass undetected because of their reduced echo amplitude under compressive stress.¹⁴

Materials

See Tables I, II & III

Experimental Technique

Preparation of Fatigue Cracks

Three specimens from each alloy whose mechanical properties are given in Table III were machined to bars of dimensions 200 x 25 x 25mm for mild steel and 225 x 25 x 25mm for NP8. All specimens were finished by grinding a V-notch of 60° included angle and 2.0mm deep in all the bars as a crack starter. 2, 4 and 6mm fatigue cracks were propagated in both mild steel and NP8 bars using a 2-ton Amsler Vibrophore fatigue machine. The V-notches were then machined off and the surfaces finished by grinding. Table IV indicates the fatigue cracking conditions for both initiation and propagation stages for mild steel and aluminium alloy specimens.

[†]Formerly in the Department of Mechanical Engineering, Mosul University, Iraq, now in the Department of Metallurgy and Materials Engineering, University of Aston.

*University of Aston, Department of Metallurgy and Materials Engineering.

Ultrasonic Testing

A Baugh and Weedon ultrasonic flaw detector type PA1020 and probes were used throughout the whole study to avoid mismatching for optimum performance. Good coupling was necessary, hence the use of silicone grease and consistent binding was required using plastic insulation tape for strapping the probe carefully in position. Reference defects were not required as fatigue cracks of known depths are involved. Calibration was done using either the V1 or V2 block for mild steel and a minimum of two echo signals. In the case of the aluminium alloy specimens a machined block from the same alloy was prepared which corresponds to the international V2 block dimensions.

Compression Tests

The specimens containing fatigue cracks of known depths were placed in the Amsler 3-point bending jig. This was done after the probe had been securely bound for maximum echo signal height with the specified sensitivity. Static compression was applied by having the crack downwards. The resultant compressive stresses were kept below the yield strength of the material under test for two reasons (1) bending theory only applies up to the yield stress of the material and (2) to avoid permanent bending of the specimens, as bending will affect the echo signal from the crack. The elastic bending loads were introduced in small increments and the amplitude of the echo signal was recorded in dB, keeping the signal height at 80% FSH for each load increment. This procedure was continued until the pre-determined load was reached. This was treated as the loading cycle. The applied load was then reduced in small increments of the same magnitude as in the loading cycle and the echo amplitude was recorded for each load increment until zero load was reached, which indicates the end of the unloading cycle. However, the results reported here were all taken from the loading part of the cycle.

Results and Discussion

Defect size estimation by pulse echo techniques depends on the amplitude of the ultrasonic beam reflected back to the probe which is indicated as an echo height on the screen. This height is proportional to the reflected energy received from the defect. This is influenced by factors, such as defect orientation, shape and surface roughness. It is also influenced by the ultrasonic technique employed.¹² These facts were borne in mind throughout these experiments.

The first preliminary test carried out was on fatigue cracks in mild steel using 45° and 60° probes, 5MHz at 1/2 skip and full skip positions as shown in Fig. 1. The results shown in Figs. 2 and 3 indicate that the echo signal amplitude depends

on fatigue crack size (depth), compressive stress, and probe angle, for both 1/2 skip and full skip scanning. The 60° probe appeared to be strongly influenced by compressive stresses but at the same time gave a weaker response to fatigue cracks at zero load.

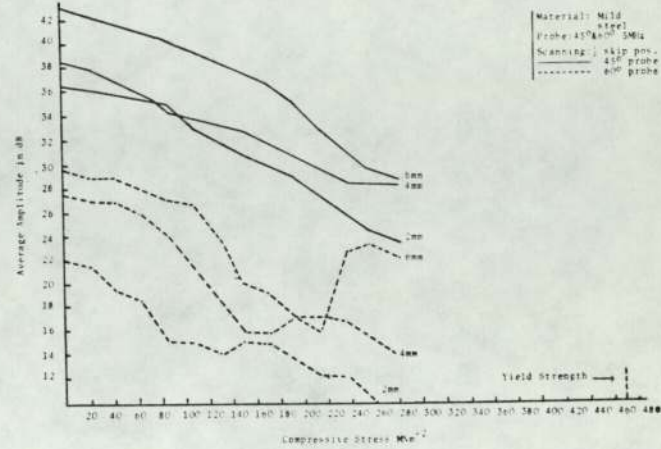


Fig. 2
Comparison between the response of fatigue cracks to compressive bending stress using 45° and 60° probes at 1/2 skip distance

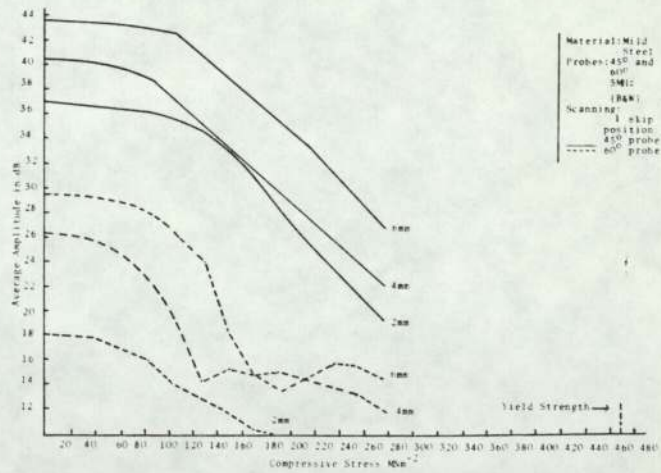


Fig. 3
Comparison between the response of fatigue cracks to compressive bending stress using 45° and 60° probes at 1 skip position

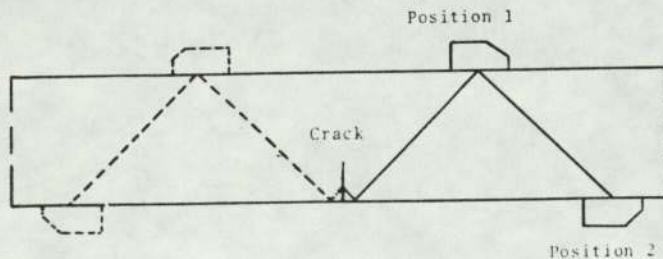


Fig. 1

Angle probe scanning at both 1/2 skip (position 1) and full skip (position 2) for maximum echo height from fatigue cracks scanned from both sides on each surface of the test bar

Further work using fatigue cracks of various depths in the NP8 test bars confirmed the low ultrasonic response from the 60° probe although again this appeared to be the most sensitive to compressive stresses as shown in Figs. 4, 5 and 6. This weak response from the 60° probe appeared to be in agreement with a number of investigators. Birchak and Gardner² related this low response to mode conversions. Significant amounts of energy can be converted from the 60° shear mode to the longitudinal, when the waves undergo double reflection at the intersection of the crack and the

surface of the specimen, since with a 60° probe the reflected angle is different from the incidence angle. The energy converted to the longitudinal waves does not return to the probe. Digiacoimo¹⁵ also observed that the ultrasonic reflection from a crack is a function of the probe angle. With a 60° probe he found that cracks less than 1/2 in. (~12.5mm) deep were not detected.

From the results obtained in this study, the 45° probe at 5MHz frequency gave the highest sensitivity (echo-signal amplitude). This applied when cracks were at zero load as shown in Fig. 7 and when under compressive loads as shown in Figs. 2, 3, 4, 5 and 6. The possible explanation for the high echo amplitude achieved with the 45° probe could be related to the fatigue crack facet orientation. This could be normal

or nearly normal to the incident beam direction when using the 45° probe. Some evidence for this could be seen from the fatigue crack fracture surface profile. There is an indication that relatively large portions of the fracture facets are oriented so that reflection from a 45° probe is favoured. Results from unstressed fatigue cracks in the aluminium alloy using 35°, 45°, 60°, 70° and 80° probes of 2MHz and 5MHz are shown in Fig. 7. This illustrates the high response of the 45° probe to fatigue cracks at both 2MHz and 5MHz and also shows the better response achieved with the 2MHz probes. Meyer's work¹⁰ also indicated that better response was achieved by using low frequency probes. Low frequency results in an increasing angle (beam spread) not only for the transmitter but also for the reflector on reflecting the beam, i.e. a wider

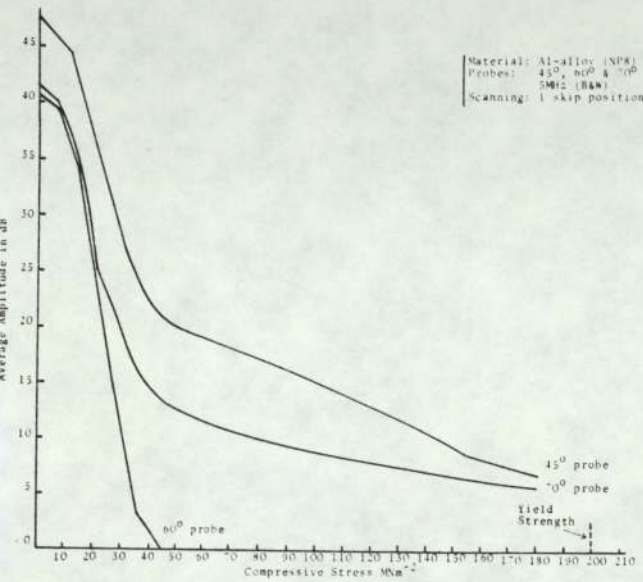


Fig. 4

Effect of probe angle on the response of a 2mm fatigue crack to compressive bending stress

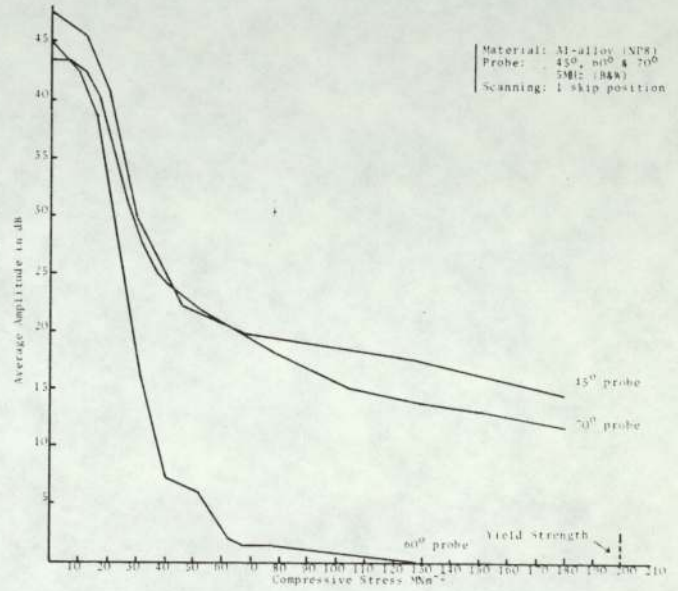


Fig. 5

Effect of probe angle on the response of a 4mm fatigue crack to compressive bending stress

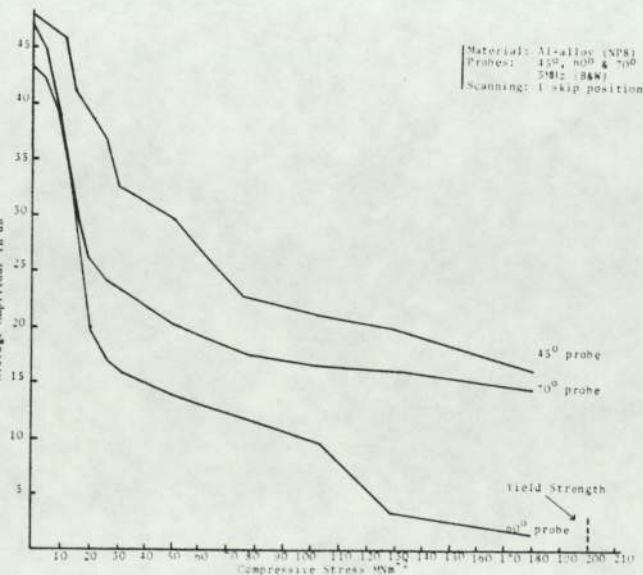


Fig. 6

Effect of probe angle on the response of a 6mm fatigue crack to compressive bending stress

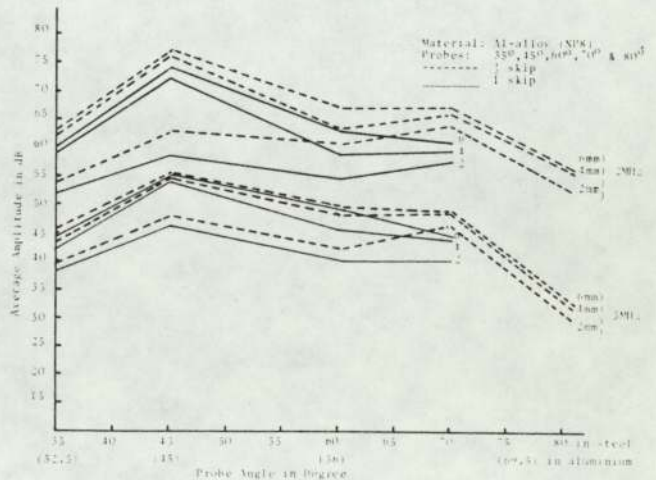


Fig. 7

Ultrasonic response of fatigue cracks of different depths under zero load to different angle probes.

area of the defect is covered by the beam. Gericke¹¹ also indicated that since the reflection of ultrasonic energy from a defect depends on the ratio of the defect size to ultrasonic wavelength, the defect echo amplitude is influenced by changes of ultrasonic wavelength. Hence a determination of the frequency dependence of the defect echo amplitude will therefore yield information on the defect geometry.

Three angle probes were used, 45°, 60° and 70° at 5MHz, to study the influence of compressive stresses on the fatigue cracks in NP8. The 45° probe, 5MHz, gave highest overall response but the lowest sensitivity to compressive stresses (Figs. 4, 5 and 6). This is in agreement with the results

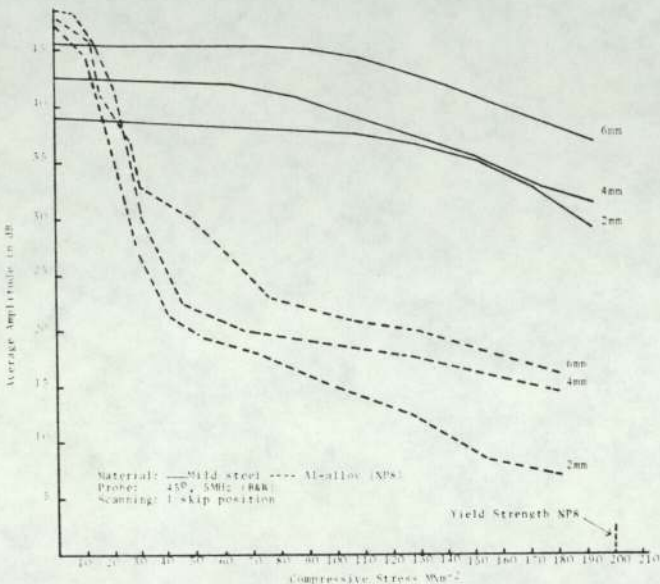


Fig. 8
Comparison between the response of fatigue cracks in mild steel and in NP8 to compressive bending stress (45° probe)

obtained from fatigue cracks in mild steel as shown in Figs. 2 and 3. Thus the 45° probe, 5MHz, gives the best response to fatigue cracks in both mild steel and the NP8.

Figures 8 and 9 illustrate the different responses from fatigue cracks of the same sizes in mild steel and NP8. It is clear that fatigue cracks in NP8 are more sensitive to compressive stresses than are cracks in mild steel. This sensitivity to compressive stress is clearly shown using the 60° probe in Fig. 9 where the fatigue cracks are seen to close rapidly. This higher closure rate may be related to the type of fatigue crack fracture surface, as smoother and tighter cracks were seen in NP8 than in mild steel. All the results obtained were averaged after scanning from both sides of each crack. Nearly all the cracks showed differing responses when scanned from opposite sides both under zero load and under compressive stresses. Figure 10 demonstrates one series of results from fatigue cracks in mild steel using a 45° probe, 5MHz, scanned at full skip position. This is possibly due to the individual crack facets giving strong reflections on one side but not on the other. This is in agreement with the work of Digiacom¹⁵ which indicated that the reflected energy distribution depends on geometry and reflectivity of the crack surface.

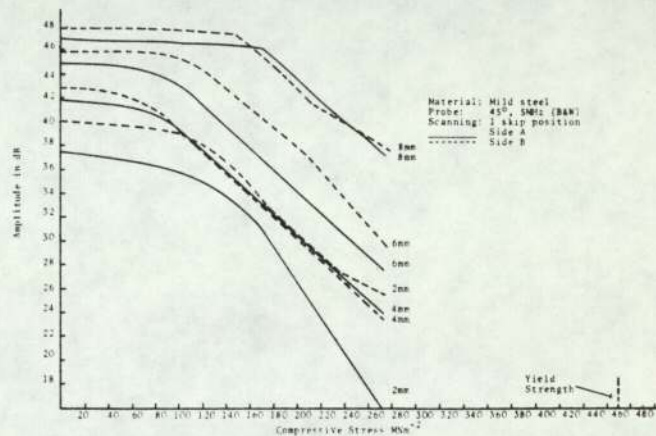


Fig. 10
The effect of compressive bending stresses on the response of fatigue cracks when examined from both sides

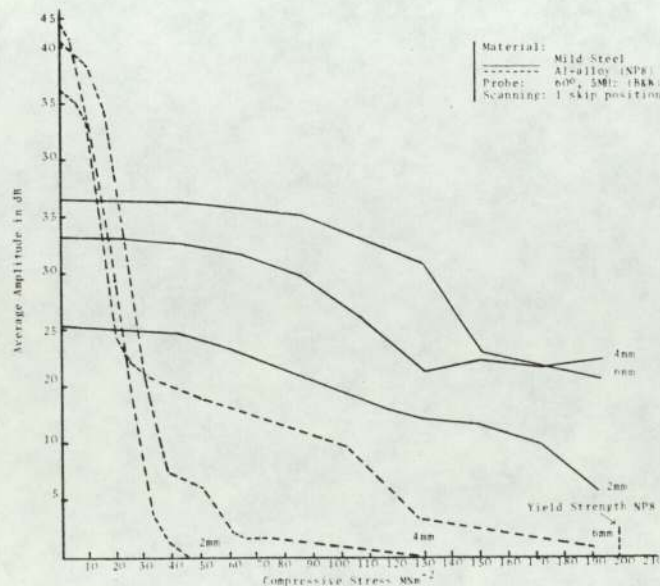


Fig. 9
Comparison between the response of fatigue cracks in mild steel and aluminium alloy to compressive bending stress (60° probe)

Conclusions

The results obtained in this study are considered to justify the following conclusions:

1. The reflection of the ultrasound from fatigue cracks is a function of the probe angle. In these experiments the 45° probe, 5MHz, gave the best response of all stress levels but the 60° probe, 5MHz, was the most sensitive to the influence of compressive stresses.
2. Apparent crack closure was found possible in the aluminium alloy (NP8) using a 60° probe, 5MHz, when cracks were under compressive stresses which were below the yield strength of the alloy.
3. The 2MHz probes showed higher crack echo amplitudes from unstressed fatigue cracks than the 5MHz probes.
4. Fatigue cracks in mild steel are less sensitive to the influence of compressive stresses than are those in NP8.
5. Examination from both sides of fatigue cracks, showed variations in ultrasonic response at all stress levels.
6. These results illustrate the dangers of using the returning echo amplitude as a measure of fatigue crack size.

TABLE I
Composition

Alloy	Analysed Composition Weight Percent					
	Fe	C	Si	Mn	P	S
Free cutting Mild steel	bal	0.10	Trace	0.88	0.021	0.23

TABLE II

Alloy	Specified Composition Weight Percent								
	Al	Mg	Cu	Si	Fe	Mn	Zn	Cr	Ti
Al-alloy NP8	bal	4.5-5.5	0.10	0.50	0.4	0.05-0.2	0.1	0.03-0.2	0.06-2.0

TABLE III
Mechanical Properties

Alloy	Tensile strength MNm ⁻²	Yield strength MNm ⁻²	%Elong ^a	%Red ^a in area	Hardness HV
Mild steel	510	471	36	57	203
NP8	326	199	29	24	87

TABLE IV

Stages	Mild Steel Specimens				Al Alloy Specimens			
	Main Load		Resonating Load		Main Load		Resonating Load	
	Ton	N	Ton	N	Ton	N	Ton	N
Initiation	0.6	5980	±0.4	±3990	0.2	1990	±0.18	±1790
Propagation	0.4	3990	±0.25	±2490	0.15	1490	±0.14	±1400

References

- Karjorlainen, L. P. and Moilanen, M., 'Detection of Plastic Deformation During Fatigue of Mild Steel by the Measurement of Barkhausen Noise', *NDT International*, April 1979, pp. 51-55.
- Birchak, J. R. and Gardner, C. G., 'Comparative Ultrasonic Response of Machined Slots and Fatigue Cracks in 7075 Aluminium', *Materials Evaluation*, Dec. 1976, pp. 275-280.
- Rummel Ward, D., Todd, Paul H. Jr, Rathke, Richard, A. and Castner, W. L., 'The Detection of Fatigue Cracks by Non-Destructive Test Methods', *Materials Evaluation*, Oct. 1974, pp. 205-212.
- Corbly, D. M., Packman, P. E. and Pearson, H. S., 'The Accuracy and Precision of Ultrasonic Shear Flaw Measurements as a Function of Stress on the Flaw', *Materials Evaluation*, May 1970, pp. 103-110.
- Jackson, B., 'The Use of Edge of Beam Methods for the Assessment of Defect Size', *British Journal of NDT*, July 1974, pp. 114-116.
- Abrahams, C. J., 'Practical Industrial Ultrasonic Examination', *Ultrasonics*, Jan.-March 1965, pp. 30-35.
- Bobbin, John E., 'Ultrasonic Weld Inspection', a Status Report, *NDT*, May-June 1960, Vol. 18, pp. 200-202.
- Whittle, M. J., 'Advances in Ultrasonic Flaw Detection', *CEGB Research*, Nov. 1979.
- Center, David E. and Roehrs, Robert J., 'Ultrasonic/Radiographic Examination of Heavy-Wall Pressure Vessel Weldments', *Materials Evaluation*, May 1969, pp. 107-117.
- Meyer, Hans-Jurgen, 'Probability of Detecting Planar Defects in Heavy Wall Welds by Ultrasonic Techniques According to Existing Codes', *International Institute of Welding—Annual Assembly, 1977, Copenhagen*.
- Gericke, O. R., 'Determination of the Geometry of Hidden Defects by Ultrasonic Pulse Analysis Testing', *The Journal of the Acoustic Society of America*, March 1963, Vol. 35 No. 3, pp. 364-368.
- Doyle, P. A. and Scala, C. M., 'Crack Depth Measurement by Ultrasonics', a review, *Ultrasonics*, July 1978, pp. 164-169.
- Seasler, John G., 'The Effect of Stress Fields on Ultrasonic Energy Reflected from Discontinuities in Solids', *International Advance in NDT*, 1977, Vol. 5, pp. 117-131.
- Coffey, J. M., 'Quantitative Assessment of the Reliability of Ultrasonics for Detection and Measuring Defects in Thick-Section Welds', *Proc. Con. on 'Tolerance of Flaw in Pressurised Components'*, Inst. Mech. Eng., 16-18, 1978, London.
- Digiacomo, G., Crisci, J. R. and Goldspiel, S., 'An Ultrasonic Method for Measuring Crack Depth in Structural Weldments', *Materials Evaluation*, Sept. 1970, pp. 189-204.

Your ref:

Our ref: PAW/003

1ST CLASS POST

S I Ibrahim Esq
University of Aston
The Department of Metallurgy
and Materials Engineering
Gosta Green
Birmingham
B4 7ET

2 June 1981

Dear Mr Ibrahim

I am delighted to inform you that you have been awarded the John Grimwade Medal for your paper "The Influence of compressive stresses and other factors on the detection of fatigue cracks using ultrasonics" judged to be the best submission by a member/members to appear in the Journal in 1980.

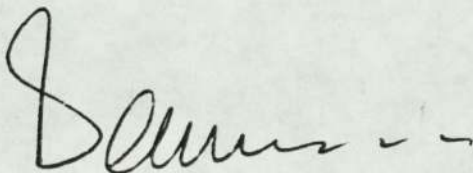
On behalf of the President and Council I congratulate you on this award. The presentation is planned to take place at the Conference dinner in Cambridge on 15 September 1981 and I do hope that you will be able to attend.

Early notice of the award will appear in the July Journal but in the meantime I would appreciate it if you would let me have some biographical notes of yourself together with a glossy unmounted head and shoulders print to arrive by 1 July. We will then make a comprehensive reference to the award and the first winners in the September Journal.

I have written in similar vein to your co-author.

Once again many congratulations.

Yours sincerely,



THE JOHN GRIMWADE MEDAL

By SCHÖNBERG

GENESIS

On 5 June, 1980, the idea to commemorate the services to NDT of the late Mr. E. J. Grimwade MC Hon FInstNDT was first mooted when the now President of the Institute Mr. J. G. Young proposed to Council that a medal be established for his purpose.

FINANCING THE PROJECT

Swift progress followed Council's acceptance of this idea. An appeal for funds was launched in the July 1980 Journal to which the members responded with alacrity and generosity. By year's end a fund of some £1486 had been established and an investment policy was drawn up by the F & GP Committee.

STRIKING THE MEDAL

The Council appointed a small sub-committee: Mr Young, Mr Wells and The Secretary, to superintend the procurement of medals the design of which was suggested in the original proposal to Council. Making the dies and striking the first batch of medals in sterling silver was undertaken by Messrs Toye Kenning & Spencer Ltd. who hold a warrant to supply insignia to HM The Queen and had earlier been entrusted with the manufacture of the President's Badge of Office, presented to the Institute by Mr. Wells last year.



Mr. V. N. Whittaker, BSc, MSc,
CEng, MIM, MInstNDT

BASIS OF THE AWARD

The original proposal was to award the medal to the author (or authors) of the best paper to be published in this Journal in each calendar year. Council modified this to restrict the award to members only and asked the P & T Committee to put in hand arrangements to determine the first winner.

JUDGING THE WINNING PAPER

Cognisant of the need for impartiality and confidentiality, Dr. Halmshaw and the P & T Committee devised a scheme by which each Committee member (except those in contention by reason of having had a paper published) was asked to judge the papers on a points basis and send an anonymous judgement to the Institute Accountants, Messrs Dove Naish and Partners. On an agreed closing date, the Accountants summarised the scores and notified the result.

THE WINNING PAPER

A majority of votes was cast in favour of a paper which appeared in Volume 22 Number 6 in November last: "The Influence of compressive stresses and other factors on the detection of fatigue cracks using ultrasonics" by Mr. S. I. Ibrahim and Mr. V. N. Whittaker.

THE AUTHORS

Mr. Whittaker has been a member of the Society/Institute since 1962. A Chartered Engineer and Member of the Institute of Metallurgists, in 1960 he became responsible for the NDT Laboratories at what is now the University of Aston, having earlier worked at Armstrong Siddeley Motors, Coventry as Development Metallurgist on gas turbines. Since then Mr. Whittaker has maintained close contact with industry as a consultant metallurgist dealing largely with problems of metal fatigue/failure; he has appeared as an expert witness in this field in the High Court. He has also published a number of papers on fatigue, creep and NDT and currently supervises three research students who are involved in various NDT topics.

Mr. Ibrahim, born in 1940 in Iraq, graduated from Flintshire College of Technology in 1966 with a BSc in Metallurgy. At Aston in 1975 he was awarded the MSc in Welding Technology and Management and then became Assistant Lecturer in Metallurgy in the Department of Mechanical Engineering at Mosul University where he has been responsible for the NDT laboratories since 1976. In 1979 he was granted leave to study for a PhD degree at Aston. Mr. Ibrahim, who expects to return to Mosul University in 1982 after completing his

thesis entitled "The influence of stress on the detection of flaws in welded joints using ultrasonics", joined the Institute last year.

AN IMPORTANT ADVANCE

The founding of the John Grimwade Medal award represents an important advance for the British Institute of Non-Destructive Testing. The late Mr. Grimwade was an outstanding personality and it is fitting that his name should be perpetuated by association with this medal, the Institute's first and which will be the senior of its kind.

Professor I. L. Dillamore, Head of the Department of Metallurgy and Materials Engineering at Aston University, commenting on the award said "... As to the importance of NDT, who could doubt it? On two fronts; the monitoring of quality for and performance of methods of mass production and in monitoring structural integrity in design critical components and assemblies there is simply no other way. There is a clear need for, and the challenge to, the field of endeavour that is of concern to your Institute. May your Institute long continue and may the John Grimwade Memorial Medal be the ultimate accolade for contributions to improvements in the methods, the applications and the understanding of non-destructive testing".



Mr. S. I. Ibrahim, BSc, MSc

APPENDIX 10

The second paper published in the British Journal
of Non-destructive Testing in September 1981

The Influence of Crack Topography and Compressive Stresses on the Ultrasonic Detection of Fatigue Cracks in Submerged Arc Welds—

S. I. Ibrahim* and V. N. Whittaker†

It is generally accepted that there is still insufficient knowledge concerning the interaction of ultrasound with real defects in materials. This study reports work which has been carried out to examine the interaction of ultrasound with fatigue cracks in the weld metal of QT-35 steel and also reports on the effects of compressive stresses. The results indicate that fatigue cracks can best be located using 45° probes. Heat-treatment prior to fatigue cracking allows fatigue cracks to be grown which are more readily detected and which are less prone to crack closure under compressive stresses. These results and others are interpreted in terms of the topography of the fatigue cracks.

Literature Review

In pulse/echo techniques it is customary to regard the presence of a signal as indicative of the existence of a flaw and the amplitude of the signal as related to flaw size⁽¹⁾.

The ultrasonic amplitude technique as currently used is however limited by its non-quantitative capabilities. In this sense, non-quantitative implies that current technology is capable only of producing a signal that indicates the presence of a flaw, but it can say very little about the characteristics of the flaw e.g., its size, shape, orientation and the material of which it is composed (void or inclusion). This limitation has been brought into sharp focus in recent years with the advent of fracture mechanics as a major structural design and maintenance philosophy⁽²⁾. When ultrasonic inspection is used in the pulse-echo mode (amplitude-technique), there are many features of a defect that can have a significant influence on its interrogation response and there are also many features of the material itself that influence the propagation of the ultrasound into and out of the material. Much recent work has been concerned with the effect of defect orientation, defect roughness and the effects of liquid ingress into flaws.

One of the most severe limitations of current amplitude techniques is that they are not capable of giving the size, shape and orientation of a flaw which lies in a stress field. A fully satisfactory answer will require a thorough study of the morphology of the metallurgical defects and of the reflection of elastic sound waves from them^(2,3,4).

In manual inspection, probes are used singly in the pulse-echo mode and several beam angles are necessary to increase the probability of detecting the specular reflection from smooth cracks, or the weak, diffuse scatter from rough or jagged cracks. The signal's strength depends on the amount of sound transmitted into the component and, more fundamentally, on the reflecting properties of the defects. Research is therefore required to indicate the smallest number of probes which provides the required level of confidence in the test⁽⁴⁾.

Recent work⁽⁵⁾ in both mild steel and Al-alloy has shown

*Formerly in the Department of Mechanical Engineering, Mosul University, Iraq, now in the Department of Metallurgy and Materials Engineering, University of Aston.

†University of Aston, Department of Metallurgy and Materials Engineering.

that the echo signal amplitude depends on fatigue crack size (depth), probe angle, frequency, scanning position, crack type and level of compressive stress. Using 45°, 60° and 70° probes, it was found that the 60° probe appeared to give a weaker response to fatigue cracks at zero load, but at the same time was more strongly influenced by compressive stresses. This weak response from the 60° probe appears to be in agreement with the work of a number of investigators and is related to mode conversions^(6,7,8,9). There is, therefore some risk of underestimating the size of flaw or even missing it altogether. The high response achieved with the 45° probe was thought to be related to the fatigue crack facet orientation. These facets were found to be normal or nearly normal to the incident beam direction when using 45° probes⁽⁵⁾. Center and Roehrs⁽¹⁰⁾ also suggested the importance of jagged irregular surfaces in crack detection. Though the entire face of a crack may not be in a plane perpendicular to the sound beam, many small facets of this surface are, and these facets reflect the sound back to the transducer.

This reflection behaviour of a defect, 'reflectivity', is thus a decisive factor in estimating the size of a defect⁽¹¹⁾.

Fatigue crack size estimation has been shown to be dependant upon the applied stress and hence, if compressive stresses are present the crack size is underestimated^(12,5).

Crack closure under compressive stresses is imperfect, as the area of contact depends on the compression of surface roughness peaks. The size of the surface irregularities relative to the acoustic wave length is an important parameter and in some instances complete 'ultrasonic transparency' has been reported at a stress level of only 20 Nmm⁻² (6,13).

Mechanical crack closure can be caused by plastic deformation left in the wake of a growing fatigue crack. It should be expected that material with a lower ductility will form a small plastic zone and thus show less crack closure. However, an 'acoustically' open crack is not the same as a mechanically open crack⁽¹⁴⁾. It should be noted that the difference between an 'acoustically' open and closed crack is only of the order of micrometers⁽⁷⁾. In crack closure the ultrasonic signal does not necessarily disappear completely, but if a large change in amplitude is observed, this is a very strong indication of crack closure⁽¹³⁾.

The present work investigates some of these problems by producing fatigue cracks of different surface topographies and studying their ultrasonic response when subjected to compressive stresses.

Experimental Techniques

Preparation of Welded Plate

The 1 inch (25 mm) thick QT35 steel plate of composition shown in Table I was first cut to the required welded plate dimensions of 275 × 375 mm. For uniformity this plate was then cut so that the rolling direction would be parallel to the welding direction. A double Vee-butt joint with 6 mm root face and 60 degree included angle was then prepared for welding. The welding procedure consisted of tacking the positioned plate at both ends and using run-on and run-off plates. The welding process employed was the submerged arc using the following welding conditions:

Current	600 amps
Voltage	30 volts
Welding speed	20 in./min. (500 mm/min.)
Filler wire diameter	4 mm
Flux	Lincoln No. 1

A multirun weld was made and after each run, the weld was wire brushed. After the second run, the plate was turned over to be welded from the other side to avoid bending due to distortion. Radiography indicated that the weld was 'defect free'. It was decided to investigate the response of fatigue cracks to compressive stresses in welds in three conditions.

1. as welded
2. stress relieved and
3. normalised.

Hence, the welded plate was cut into three equal plates, two of which were heat treated as follows:

- Stress relieving—600°C for 1 hour.
- Normalising—950°C for 1 hour.

Preparation of Fatigue Cracks

The welded plates representing the three conditions, having mechanical properties listed in Table II were machined to bars of dimensions 250 × 25 × 25 mm. All specimens were finished by grinding. A V-notch of 60° included angle and 2 mm deep was cut along the weld centre line as a crack starter. 2, 4 and 6 mm deep fatigue cracks were propagated using a 2-ton Amsler Vibraphore fatigue machine. The V-notches were then machined off and the surfaces were finished by grinding. Table III indicates the fatigue cracking conditions for both initiation and propagation stages.

Ultrasonic Testing

Both the ultrasonic flaw detector (type PA1020) and probes used throughout this study were manufactured by Baugh and Weedon to avoid mismatching for optimum performance. All the probes were set to obtain the maximum echo height possible from the fatigue crack surfaces by moving the probe forwards and backwards and by rotation. Screen calibration was found to be advantageous, as the exact echo signal position can be estimated from the geometrical sound path distance (range) of the probe used. This assists in disregarding, if present, any other spurious signals especially in the case of very small cracks. After obtaining the maximum echo signal, the ultrasonic sensitivity level is adjusted by bringing down the signal to a reasonable height on the screen.

The sensitivity level used throughout the tests was set to bring the maximum echo signal down to 80% full screen height. This was found to be adequate for all the range of crack depths and the testing conditions used. Good coupling was achieved, by using silicone grease and binding the probe to the sample with insulating tape.

The most significant probe parameters, e.g. frequency, beam angle and scanning position were varied to find out their optimum values. 2 and 5 MHz 45°, 60° and 70° angle probes were used at both $\frac{1}{2}$ -skip and full-skip scanning positions.

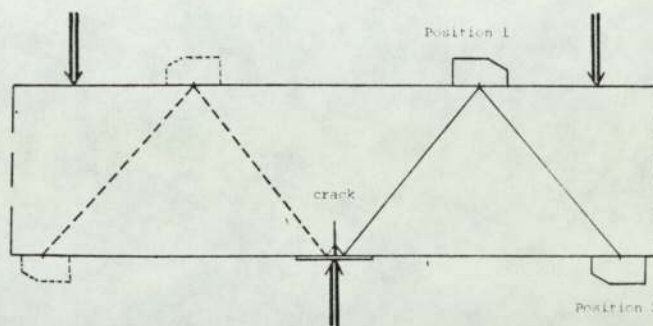


Fig. 1
Angle probe scanning of fatigue cracks using the maximum echo amplitude technique at both $\frac{1}{2}$ -skip (position 1) and full-skip (position 2)

Fatigue cracks of different depths in the submerged arc weld in the as welded condition were examined with the probes. Elastic compressive bending stresses were applied to these cracks and their corresponding echo amplitudes were observed. It was found that the 5 MHz probes at $\frac{1}{2}$ -skip positions were able to differentiate best between cracks of various sizes in the as welded condition as shown in Fig. 6. Accordingly this technique was used to study the other conditions.

Compression Test

For details of this test see reference (5). The probes were bound to the bend test pieces at $\frac{1}{2}$ - and full-skip positions as previously indicated so that the cracks could be suitably interrogated. These test pieces were then mounted onto the Amsler 3-point bending rig as shown in Fig. 1.

Static compressive stresses were applied by having the crack facing downwards. Stress levels were kept below the yield strength of the material. The compressive stresses were increased in small increments and at each level of stress the amplitude of the echo signal was recorded in dB, keeping the signal height at 80% FSH. This was continued until the predetermined load was reached.

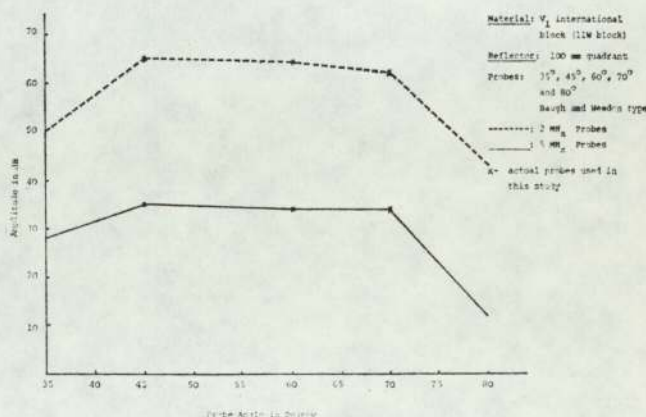


Fig. 2
Ultrasonic echo amplitude response of different angle probes from the 100 mm quadrant of the IIW block

Results and Discussion

The ultrasonic reflection intensities shown in Fig. 2 were obtained using the 100 mm quadrant in the IIW calibration block V_1 as the reflecting surface, hence giving the same sound path distance for all the probes. These results clearly show, that these probes (45° , 60° and 70°) have the same ultrasound reflection intensities. This is true at both 2 MHz and 5 MHz. Figure 3 represents the beam spread charts for these probes at 2 MHz and 5 MHz frequencies, which indicate that the 2 MHz probes, have greater beam spread and nearly twice the beam width of the 5 MHz probes.

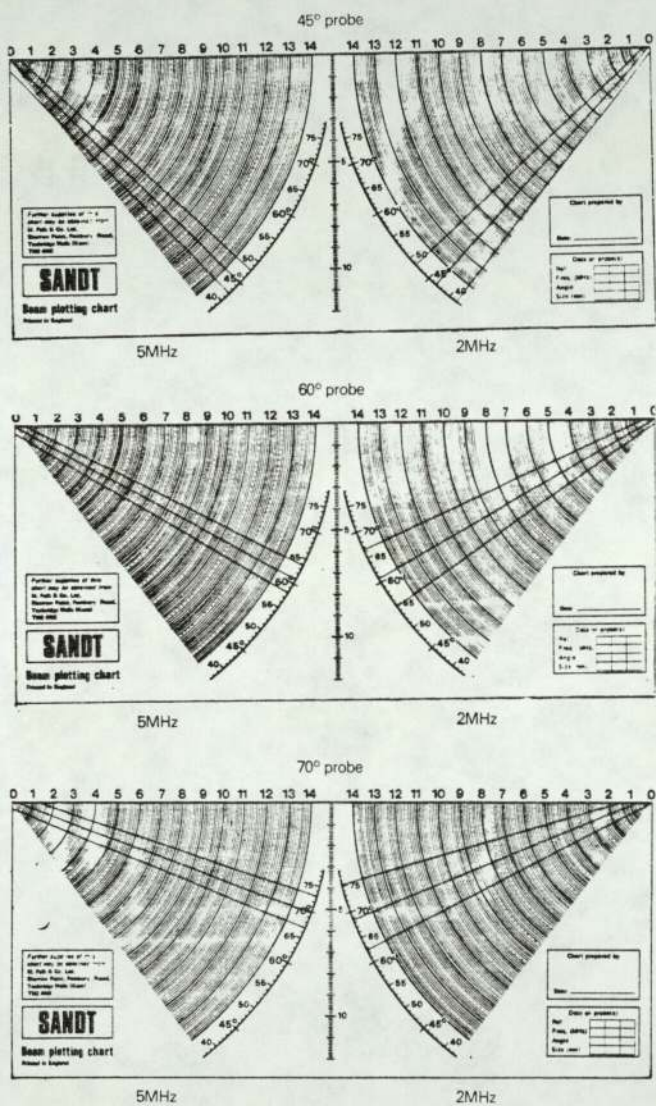


Fig. 3
Vertical beam spread chart of the 45° , 60° and 70° probes at both 2 MHz and 5 MHz frequencies

By varying the probe parameters and scanning position, it was possible to obtain the results shown in Figs. 4 and 5 for fatigue cracks of different depths, i.e. 2, 4 and 6 mm under various levels of compressive stresses. These results are somewhat inconsistent when the 2 MHz probes are used both at $\frac{1}{2}$ -skip and full-skip scanning, especially with the 60° and 70° probes. The 2 MHz probes also, give no clear indication of crack closure under compressive stresses, except with the 2 mm crack when using the 45° probe, full-skip scanning.

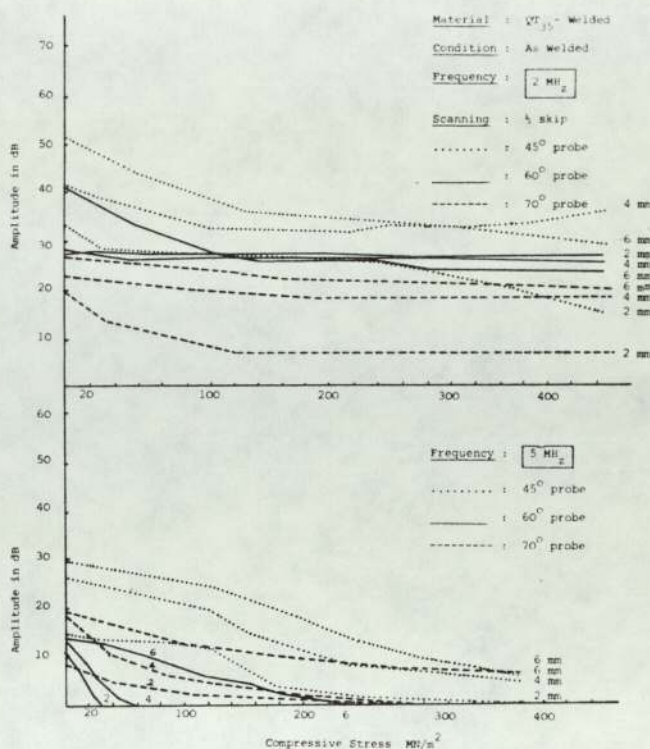


Fig. 4
Signal amplitude responses from fatigue cracks under compression using the 2 and 5 MHz probes at the $\frac{1}{2}$ -skip position

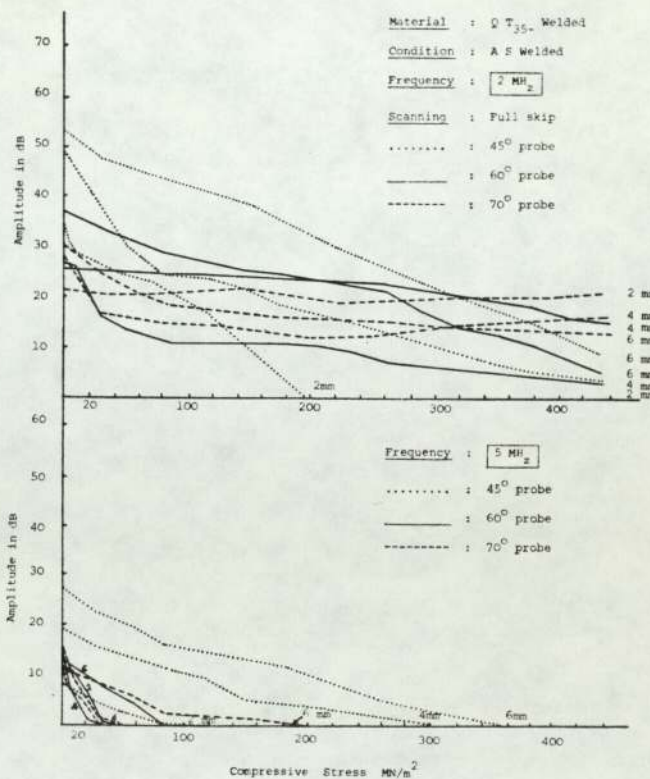


Fig. 5
Signal amplitude responses from fatigue cracks under compression using the 2 and 5 MHz probes at the full-skip position

This is because of the high echo-amplitude characteristics of the 2 MHz probes compared with the 5 MHz probes.

For the 5 MHz probes, the results show much better response to compressive stresses at both 1/2-skip and full-skip positions. Crack closure seems to be a common phenomenon when using all the 5 MHz probes at full-skip scanning, although they vary in their crack closure tendency as shown in Fig. 5.

The 5 MHz probes at the 1/2-skip scanning position were best able to differentiate between cracks of different depths and this remained true both at zero load and under compressive stresses (Fig. 4).

The experiments clearly demonstrate that the 5 MHz 45° probe, operating at the 1/2-skip position offers the best chance of distinguishing between vertical fatigue cracks of different sizes which are under the influence of compressive stresses.

The 60° probe shows a rather weak amplitude response but at the same time proved to be the most sensitive probe to compressive stresses giving apparent crack closure at low stress levels (Fig. 6). The weak response of the 60° probe has been confirmed by a number of investigators who all attributed this to mode conversion when the waves undergo double reflection at the intersection of the crack and the specimen surface.^(5,6,7,8,9) Digiacomo et al⁽⁷⁾ also observed that the ultrasonic reflection from a crack is a function of the probe angle and with a 60° probe found that cracks less than 1/2 in. (~12.5 mm) deep were not detected.

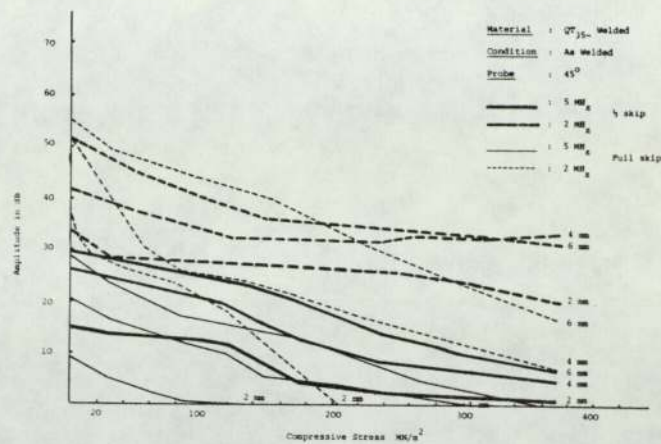


Fig. 7
Ultrasonic response to fatigue cracks under compression using 45° probes at different frequencies and scanning positions

at 1/2-skip scanning position. It also shows clearly why the 45° probe can be considered to represent the best probe compared with the performance of 60° and 70° probes.

There are certain situations in practice where limited access may allow only the full-skip technique to be used. In this case faster apparent crack closure is to be expected (Fig. 7). Figure 7 also covers other less favourable conditions for the 45° probe, and even under these conditions if compared with the performance of either the 60° or 70° probes the 45° probe can still be considered the most reliable.

It has been shown earlier from the results obtained in Fig. 2, that the signal strength measured in terms of the maximum echo-amplitude is of the same intensity for all the probes 45°, 60° and 70° when the curved 100 mm quadrant is used as the reflecting surface. When fatigue cracks are considered however, the ultrasonic reflection proved to be strongly influenced by the probe beam angle, Fig. 6. The 45° probe, 5 MHz gave the highest overall response over the whole range of compressive stresses, whilst at the same time this probe proved to be the least sensitive to compressive stresses. Therefore it is possible to conclude that the strength of the signal is related to the reflecting properties of the fatigue cracks. The fatigue cracks here are in a plane which is not perpendicular to the sound beam, and they tend to have jagged irregular surfaces with many small facets, as shown in Fig. 12.

Center and Roehrs⁽¹⁰⁾ have confirmed the presence of these small facets, and suggest that they reflect the sound back to the probe. Thus a possible explanation for the overall high echo-amplitude response of the 45° probe could be related to the favourable orientation of crack facets. Some evidence for this could be seen from the fatigue crack fracture surface profile in the as welded condition in Fig. 12. There is an indication that relatively large portions of the fracture facets are oriented so that reflection from a 45° probe is favoured. Hence ultrasonic detection of fatigue cracks is influenced by the surface topography of the crack.

Figure 8 shows the results obtained from fatigue cracks grown in stress relieved and in normalised welds. These fatigue cracks are of the same depths (2, 4 and 6 mm) as previously, and were propagated using exactly the same initiation and propagation condition as used for the as welded samples (Table III). The results have been compared with those obtained from the original as welded samples, and show similar trends, i.e. the high echo-amplitude response from the 45° probe and the low response from the 60° probe. This is found to be true for all the cracks in the different weld conditions.

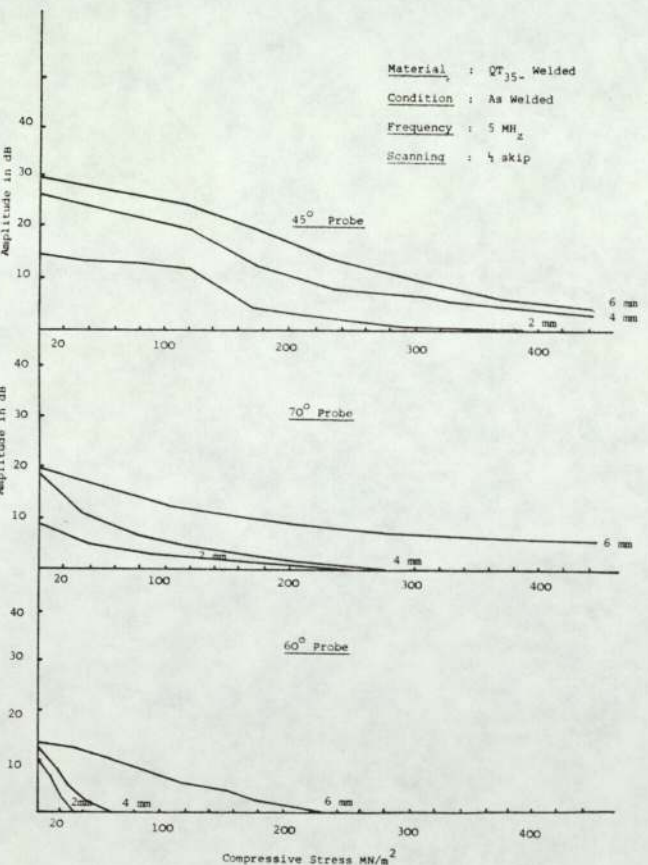


Fig. 6
Optimum ultrasonic techniques for detecting fatigue cracks under both zero load and compressive stresses when using 45°, 60° and 70° probes (5 MHz at 1/2-skip scanning)

Figure 6 represents the optimum condition for the echo-amplitude technique when the three most common probes, the 45°, 60° and 70° are to be considered, i.e. 5 MHz frequency

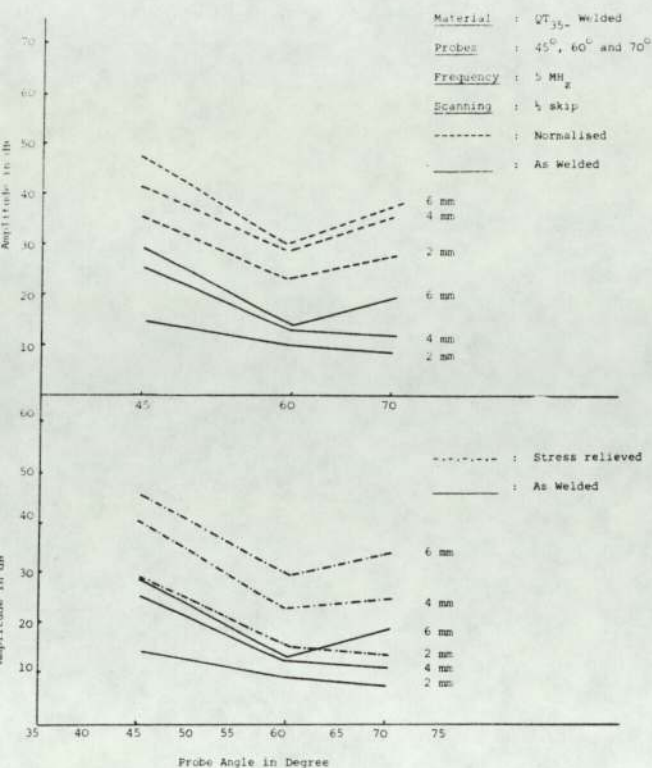


Fig. 8

Response to fatigue cracks under zero load in submerged arc welds in the as welded, stress-relieved and normalised conditions using 45° , 60° and 70° probes, 5 MHz at $\frac{1}{2}$ -skip scanning

The results also demonstrate the overall low response in echo-amplitude from fatigue cracks in the as welded condition, compared with those cracks in the stress relieved or normalised conditions. This applied to all three probes used.

The high echo-amplitudes obtained from cracks of the stress relieved and normalised welds can be mainly related to the different crack topography as shown in Fig. 12. This shows the as welded condition to have a relatively smooth surface with fine crack facets compared with coarser well defined facets covering a large portion of the cracks in both stress relieved and normalised welds.

These individual crack facets are oriented so that reflection from a 45° probe is favoured, especially those cracks in the normalised welds. The other factor which must be considered in addition to the crack topography, is the attenuation losses due to the possible changes in the metallurgical structure. This was found to have little, or no effect, as the difference in attenuation losses between the as welded and normalised welds, for example, is only 0.08 dB/mm. In addition, the material thickness involved was less than 25 mm, and only a small portion of the weld is covered by the ultrasonic beam, especially when using 45° , 5 MHz probe at $\frac{1}{2}$ -skip scanning position which represents the optimum technique in this study.

It has been shown earlier that 2 MHz probes produced unreliable results, compared with the 5 MHz probes. Figure 10 shows the effect of probe frequency on the oscilloscope trace produced by 2 mm and 6 mm fatigue cracks in the as welded condition using 70° probes, at 5 MHz and 2 MHz and $\frac{1}{2}$ -skip scanning. The signals from the 2 MHz probes are characterised by poor signal/noise ratios which could make small crack detection difficult if not impossible.

This is possibly due to the wide beam spread (see Fig. 3), which allows other reflectors to be picked up; e.g. crack corners, crack tips, far edge of specimen, surface reflection,

grain boundaries and others. This effect becomes even worse when full skip scanning is applied, since although the beam angle remains the same, the beam spread increases with distance.

In the case of 5 MHz, the signals are sharper and clearer with very much less noise interference, because of the narrower beam (Fig. 3) and a switch to 5 MHz probes might therefore prove beneficial. Figure 11 shows a comparison between the response of 2 mm cracks in the as welded and normalised welds using 2 MHz, 45° , 60° and 70° probes, at the $\frac{1}{2}$ -skip scanning position. This figure clearly shows the weak echo-amplitude signals from the 2 mm crack in the as welded condition compared with those from normalised weld. There is more than 20 dB difference in the amplitude response of these cracks in different weld conditions. Because of the high amplification that is needed to enhance the weak signal in the as welded samples the oscilloscope trace becomes noisy with signals from variety of sources such as inclusions micro-cracks or grain boundaries in the crack region. These photographs confirm the results shown in Fig. 8 which again indicate the higher response from the normalised condition.

Figure 9 shows that post-weld treatments substantially reduce the effect of compressive stresses on crack closure. This is due to the relatively high echo-amplitude response over the whole stress range. The best results obtained in this series of tests appeared to be those from cracks in the stress relieved weld, since in this case there is a clear distinction between the responses from the cracks of different depths. Hence, both post-weld treatments assist in crack detection when compressive stresses are present. The variation in the ultrasonic echo-amplitude from fatigue cracks under zero load in the as welded, stress relieved and normalised welds has earlier been related to the corresponding variation in their crack surface topography.

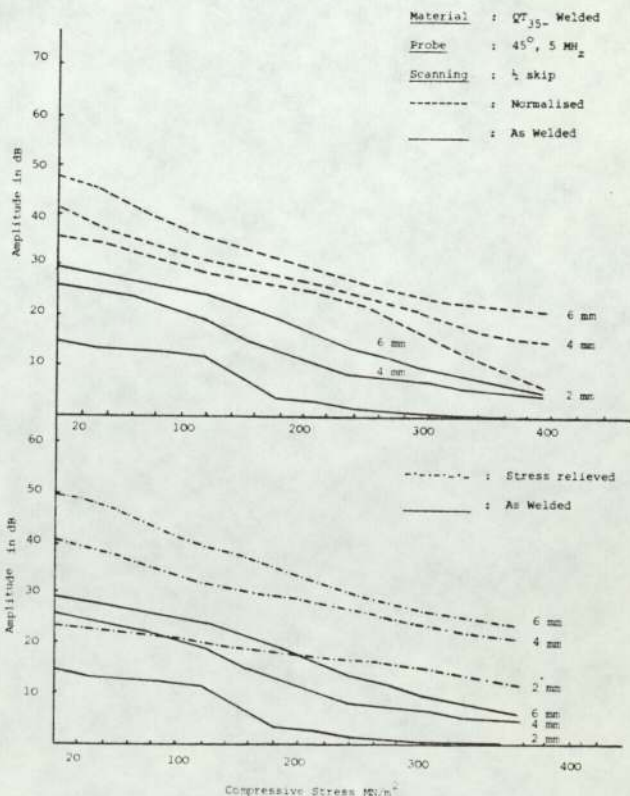


Fig. 9

Signal amplitude responses from fatigue cracks under compression in the as welded, stress-relieved and normalised welds using a 45° probe, 5 MHz at $\frac{1}{2}$ -skip scanning

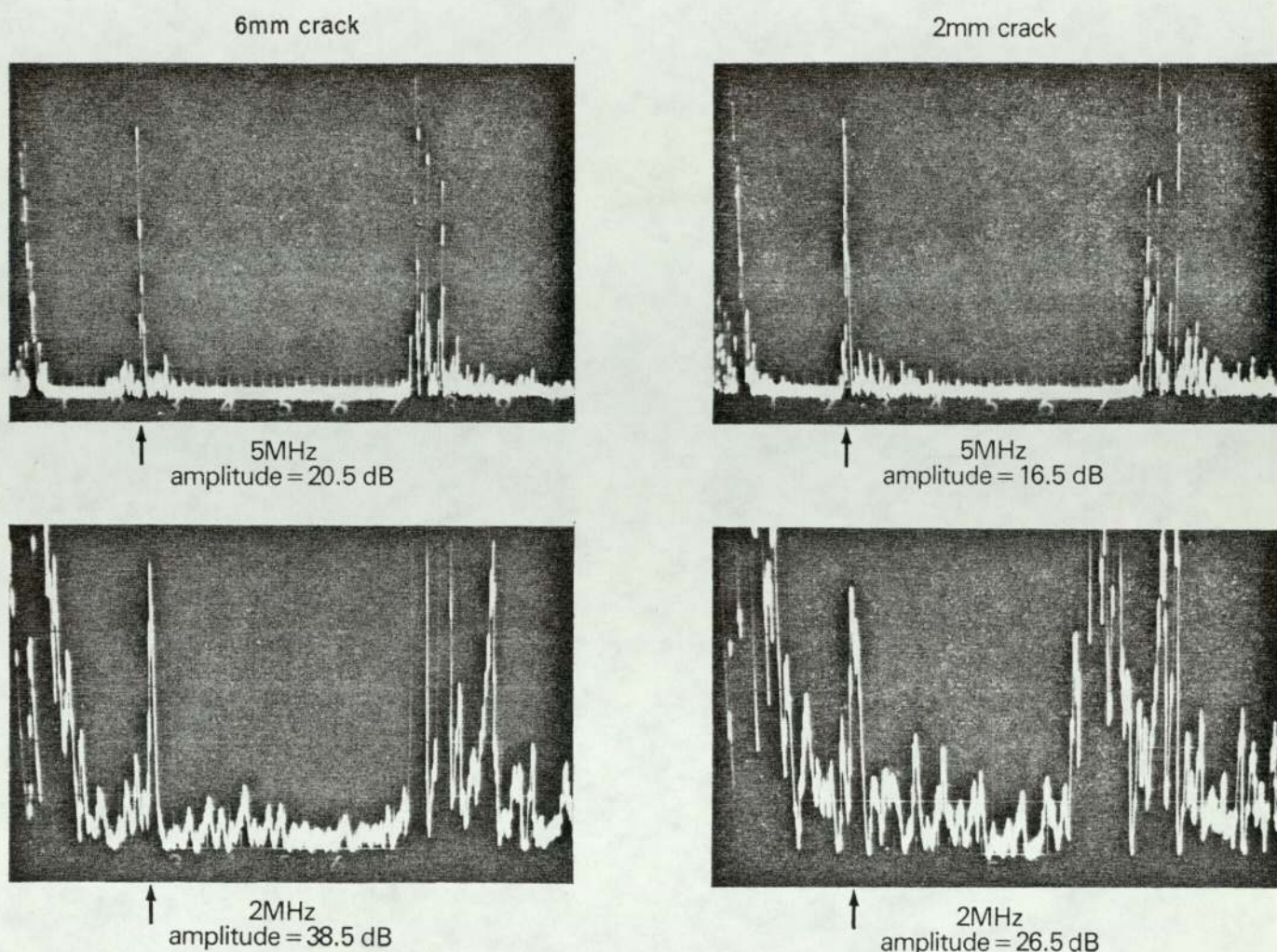


Fig. 10
 Ultrasonic screen traces of the signals from 2 mm and 6 mm fatigue cracks using 2 MHz and 5 MHz 70° probes at the $\frac{1}{2}$ -skip position

Variations in crack surface topography can also explain the changes in ultrasonic response under compressive stress, which occurs in the different structures. Birchak and Gardner⁽⁶⁾ claimed that fatigue crack closure is imperfect as the area of contact depends on the compression of surface roughness peaks. The effective displacement, therefore depends on the size of surface irregularities.

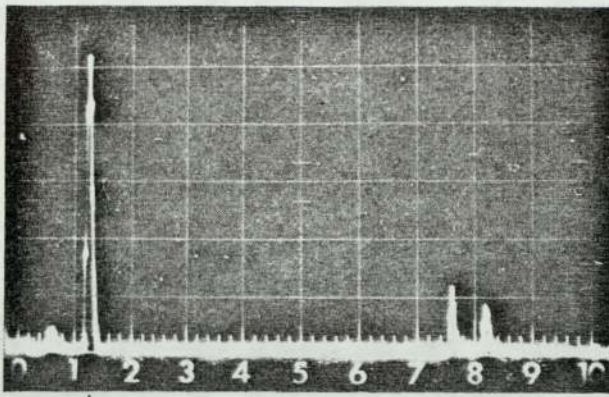
It is therefore possible to conclude that crack surface topography plays an important role in acoustic crack closure which results from compressive stresses. Accordingly the relative ease of crack closure associated with the cracks in the as welded condition can be related to the smooth and fine crack facets and the relatively weak overall echo-amplitude response. The gradual and slow closure rate which is associated with the cracks in the stress relieved and normalised welds can be related to the coarser but well-defined facets, which because of their favourable orientation give a strong overall response. Presumably their well-defined facets make mechanical closure difficult.

Conclusions

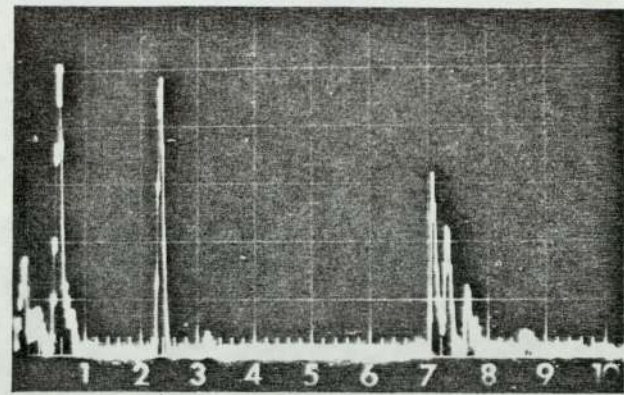
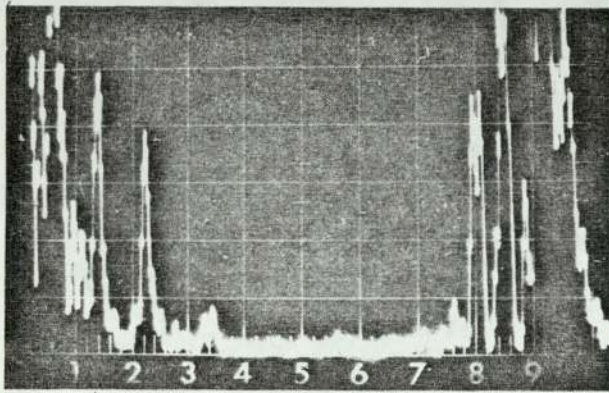
In detecting fatigue cracks in the weld metal of QT35 the following conclusions can be drawn:

1. The 45°, 5 MHz probe at $\frac{1}{2}$ -skip positions gave the best results in detecting all three crack sizes in the three weld conditions.
2. Elastic compressive stresses produced complete crack closure when the 60°, 5 MHz probe was used at the $\frac{1}{2}$ -skip position in the as welded condition.
3. Using the 45° probes crack reflectivity was considerably increased when the fatigue cracks were grown in heat treated weld metal.
4. This is attributed to the nature of the crack surface facets and their effect on reflection of the ultrasound in these conditions.

45° probe

normalised
amplitude = 64.5 dB

70° probe

normalised
amplitude = 43.5 dBas welded
amplitude = 42 dB

60° probe

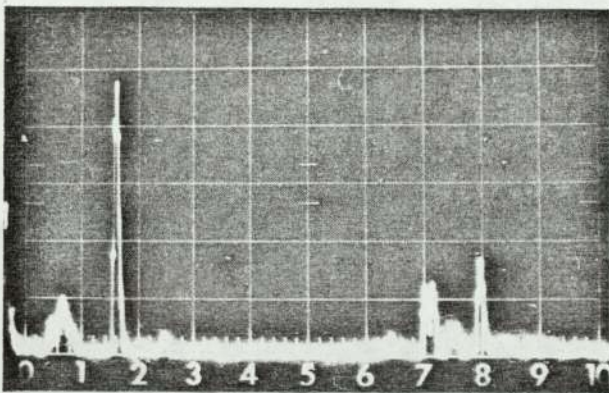
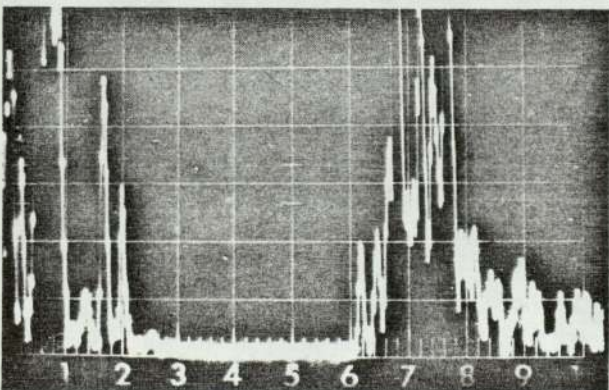
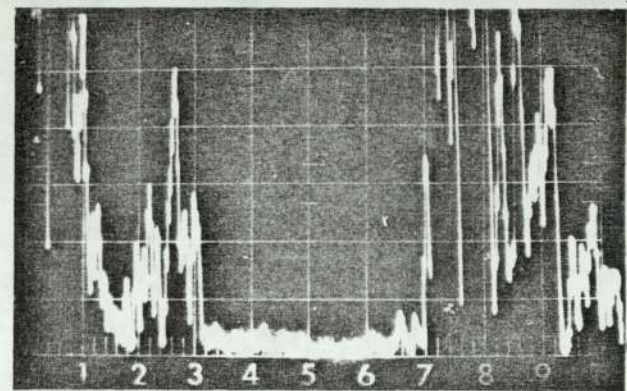
normalised
amplitude = 47.5 dBas welded
amplitude = 28 dBas welded
amplitude = 20 dB

Fig. 11

Comparison between the ultrasonic screen traces of 2 mm fatigue cracks in the as-welded and normalised welds using 45°, 60° and 70° probes, 2 MHz at $\frac{1}{2}$ -skip scanning

References

1. Carson, J. M. and Rose, J. L. An Ultrasonic Non-destructive Test Procedure for the Early Detection of Fatigue Damage and the Prediction of Remaining Life. *Materials Evaluation*, April 1980, Vol. 38, No. 4, pp 27-39.
2. Thompson, D. O. and Thompson, R. B. Quantitative Ultrasonics. *Phil. Trans. R. Soc. London, A*, 292, pp. 233-250 (1979).
3. Sharpe, R. S. Current Limitations of Nondestructive Testing in Engineering. *Phil. Trans. R. Soc. London, A*, 292, pp. 163-174 (1979).
4. Coffey, J. M., Oates, G. and Whittle, M. J. The Future of Ultrasonic Examination in Engineering. *Phil. Trans. R. Soc. London, A*, 292, pp. 285-298 (1979).
5. Ibrahim, S. I. and Whittaker, V. N. The Influence of Compressive Stresses and Other Factors on the Detection of Fatigue Cracks Using Ultrasonics. *British Journal of NDT*, Nov. 1980, Vol. 22, No. 6, pp. 286-290.
6. Birchak, J. R. and Gardner, C. G. Comparative Ultrasonic Response of Machined Slots and Fatigue Cracks in 7075 Aluminium. *Materials-Evaluation*, Dec. 1976, pp. 275-280.
7. Digiaco, G., Crisci, J. R. and Goldspiel, S. An Ultrasonic Method for Measuring Crack Depth in Structural Weldments. *Materials Evaluation*, Sept. 1970, pp. 189-204.

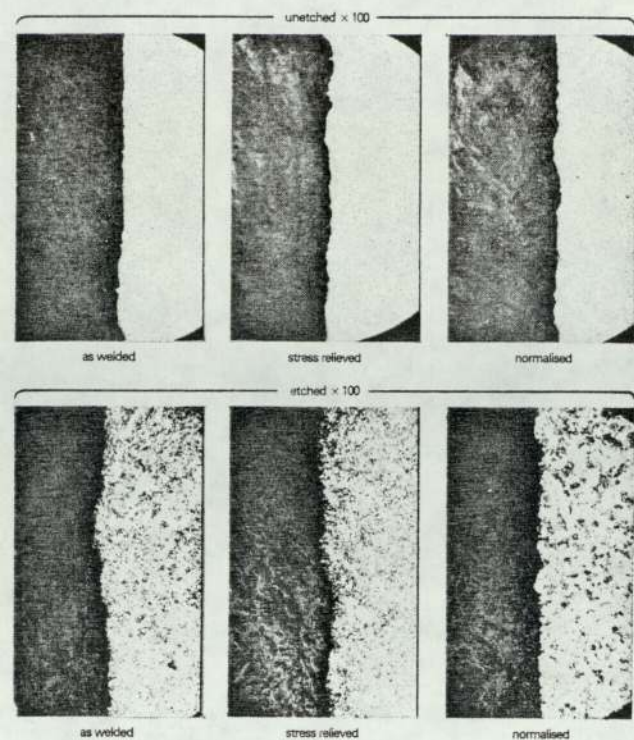


Fig. 12

The surface topography of fatigue cracks grown in submerged arc welds in the as welded, stress-relieved and normalised conditions

8. Procedures and Recommendations for the Ultrasonic Testing of Butt Welds, The Welding Institute, Cambridge, 1971, pp. 10-11.
9. Juva, A. and Lieto, J. The Ultrasonic Examination of Thin Austenitic Stainless Steel Butt-Welds, British Journal of NDT, Vol. 22, July 1980, pp. 191-195.
10. Center, D. E. and Roehrs, R. J. Ultrasonic/Radiographic Examination of Heavy Pressure Vessel Weldments, Materials Evaluation, May 1969, pp. 107-117.
11. Abrahams, C. J. Practical Industrial Ultrasonic Examination, Ultrasonics, Jan.-March 1965, pp. 30-35.
12. Corbly, M. D., Packman, P. E. and Pearson, H. S. The Accuracy and Precision of Ultrasonic Shear Wave Flaw Measurements as a Function of Stress on the Flaw, Materials Evaluation, May 1970, pp. 103-110.
13. Golan, S., Adler, L., Cook, K. V., Nanstad, R. K. and Bolland, T. K. Ultrasonic Diffraction Technique for Characterisation of Fatigue Cracks, Journal of Non-destructive Evaluation, March 1980, Vol. 1, No. 1, pp. 11-19.
14. Schijve, J. Fatigue Cracks, Plasticity Effects and Crack Closure, Engineering Fracture Mechanics, 1979, Vol. 11, pp. 167-221.

Acknowledgements

The authors wish to thank Professor I. L. Dillamore of the Department of Metallurgy and Materials Engineering and Professor R. H. Thornley of the Department of Production Technology and Management for the provision of laboratory facilities. Thanks are also due to Mr. J. Foden and Mr. S. Witherington for assistance in the laboratories and to Dr. D. R. Andrews for helpful advice.

TABLE I
Composition

Alloy	Specified Composition Weight Percent										
	Fe	C	Mn	Si	S	P	Ni	Cr	Mo	V	Al
Welded plate (QT35)	bal	0.10	0.93	0.16	0.023	0.014	1.05	0.81	0.34	0.11	0.005
Filler wire (S ₃ Mo)	bal	0.14	1.52	0.23	—	—	—	—	0.46	—	—

TABLE II
Mechanical Properties

Alloy	Yield strength MN/m ²	Tensile strength MN/m ²	Elongation %	Reduction in area %	Hardness HV
Parent metal (QT35)	556	669	28	70	250
<i>Welds</i>					
As welded	568	766	23	50	260
Stress relieved	408	531	25	60	230
Normalised	309	488	29	55	225

TABLE III
Fatigue Cracks Initiation and Propagation Conditions

Stages	QT-35 steel-welded			
	Main load		Resonating load	
	Tons	N	Tons	N
Initiation	0.76	7600	±0.70	±7000
Propagation	0.60	6000	±0.50	±5000

APPENDIX 11

The third paper to be published in the British
Journal of Non-destructive Testing early in 1982

Your ref: MET/NWT/GD

Our ref: PAW/003

V N Whittaker Esq
The Department of Metallurgy
and Materials Engineering
The University of Aston
Gosta Green
Birmingham
B4 7ET

14 July 1981

Dear Mr Whittaker

Dr Halmshaw has passed me a copy of the paper Ultrasonic Inspection of Fatigue Cracks in the Haz of Austenitic Weldments using Shear Wave Probes and I write to advise that this has been accepted for publication. It will appear in the British Journal of NDT early in 1982.

I have corrected the errors you mentioned in your letter of 23 June 1981 to Dr Halmshaw and that paper should be published before the end of this year.

I thank you and your associates for your continuing support.

Yours sincerely,


Frank W Beaumont
General Editor
British Journal of NDT

ULTRASONIC INSPECTION OF FATIGUE CRACKS IN THE HAZ OF AUSTENITIC
WELDMENTS, USING SHEAR WAVE PROBES.

by

S.I.IBRAHIM, P.A.KAPRANOS &

V.N.WHITTAKER

Abstract

Ultrasonic inspection of austenitic weldments has always been considered difficult when using conventional methods. However, there is now some experimental evidence to suggest that, shear wave inspection techniques can be applied to inspect these weldments in certain circumstances.

This work investigates the effectiveness of shear wave inspection of fatigue cracks in the HAZ of these austenitic weldments. The limitations of these techniques are demonstrated, and possible solutions are proposed.

Introduction

The need to establish NDT techniques for the examination of welds in austenitic materials has become of great importance due to the extensive use of these materials in the construction of power stations, and particularly nuclear power plants.

In the assessment of internal weld quality for in-service work required on nuclear reactor pressure vessels, ultrasonic examination is an indispensable tool.

However, the methods of examination as practised on ordinary carbon steel welds are not directly applicable to welds in austenitic stainless steel, for in these welds, the microstructure dominates the wave propagation response (1,2).

When producing stainless steel welds, the initial austenitic phase is preserved in grains which grow along the heat dissipation lines, up to an appreciable size. Even in multipass welds, the grain can be very large due to epitaxial growth between passes and usually no refinement is possible.

The solidification process during welding initially produces a columnar grain structure in each weld bead. Grains grow along the maximum thermal gradients in the bead along a $[100]$ crystallographic axis(2). Growth in this direction is faster than in others and this leads to the rapid disappearance of unfavourably oriented grains. Deposition of subsequent weld metal reheats the bead and, although in the case of a ferritic weld the columnar grain structure is destroyed by the austenite-ferrite phase transformation that occurs as the solid cools, no such transition occurs in the austenitic alloys, and consequently the columnar grain structure survives.

Furthermore, each new weld bead remelts the surface of the preceding beads and the new beads grow epitaxially on the existing ones. Consequently large columnar grains are produced as shown in Figure 1. This shows a macrosection of a 25mm double-U-weld, made by the manual metal arc (MMA) process, using 316 Stainitrode 63.30 electrodes.

This coarse and anisotropic structure of the austenitic weld metal, presents a number of difficulties to ultrasonic examination, the two most serious of these being the high level of spurious signals and the severe attenuation.

A great deal of research has been going on in the last decade on this topic and numerous papers on the testing of austenitic welds have been published, but different opinions have been expressed on the usefulness of ultrasonic examination of these welds.

It has been established however, and is generally accepted that attenuation is a function of the actual orientation of the ultrasonic beam with respect to the austenitic grain direction(1,4) and that attenuation is a minimum at approximately 45° to the grain axis, whilst maxima occur at 0° and 90° .

It was also established that ultrasonic velocity is strongly dependent on the angle made by the direction of wave propagation and the axes of the columnar grains existing in these weldments (1,3,4,5). A maximum occurs at approx. 50° , and two distinct minima occur when the direction of the waves is parallel to the grain axes (0°), and when perpendicular to them(90°) , the former being the lower in value.

Sound waves propagated in these weldments, are skewed during their passage through the weld material, due to the angular variation of the velocity, and tend to be refracted towards the direction of maximum velocity. An ultrasonic beam propagating along this direction of maximum velocity will be focused by this effect, and one propagating in the direction of minimum velocity will be defocused (6).

These effects of velocity and attenuation variations and the consequent beam skewing, present serious difficulties in the inspection of these weldments by conventional shear wave probes. However, P.A.Kapranos (2), A.Juva & J Lieto (7), B.S.Gray, et al (8), E.R.Reinhardt (9) and C.J.Abrahams (10), all have found that pulse-echo shear wave ultrasonics is a viable volumetric inspection technique when certain conditions such as plate thickness, weld geometry, size of grain structure (of parent metal and weld metal) are met.

There is usually a demand to use at least two beam angles to cover the volume of a weld under ultrasonic inspection, and when choosing a suitable probe for austenitic weld inspection, the use of shear wave angle probes should always be considered first.

In this paper, the performance of shear wave angle probes in inspecting fatigue cracks in 316 austenitic weldments is experimentally investigated, and a comparison of different probe angles (45° , 60° , 70°) and different frequencies (2 & 5 MHz) is made, in order to establish the most effective combination of angle and frequency for inspecting these cracks.

Experimental Procedure

Materials

Table 1 shows details of the plate material. The weld was made by the manual metal arc(MMA) process, and the root area was ground out to sound metal from one side and then filled up in accordance with Table 2.

Preparation of Fatigue cracks

The welded plate, having mechanical properties listed in Table 3, was machined to a bar of dimensions 22.5 x 31 x 300 mm, and finished by grinding. Using a V-notch of 60° included angle and 2 mm depth, a fatigue crack was propagated using a 2 Ton Amsler Vibraphore fatigue machine (12).

Table 4 indicates the fatigue cracking conditions for both initiation and propagation stages.

Ultrasonic Testing

An ultrasonic flaw detector (type PA 1020) and a set of shear wave angle probes manufactured by Baugh & Weedon were used throughout the investigation. Signals coming from the fatigue crack surfaces were maximised by moving the probe forwards and backwards and by rotation. Ultrasonic sensitivity level was adjusted by bringing the maximum echo signal from the cracks to 80% full screen height (FSH). Accurate calibration was found to be essential in the detection of the fatigue cracks, especially when propagating the sound through the weld metal, and continuous checks of screen calibration were maintained throughout testing.

Frequency, beam angle and scanning position (through parent metal and through weld metal) were varied, in order to establish optimum values. Conventional shear wave angle probes of 45° , 60° , 70° and 2 & 5 MHz frequencies were used at $\frac{1}{2}$ skip scanning positions.

Compression Test

Full details of this test can be obtained in reference 11. Figure 2 shows the test piece under investigation. The probes were bound to the test piece at $\frac{1}{2}$ skip scanning position and then the assembly was mounted onto the bending rig. Static compressive stresses were applied, and then increased in small increments in order to record the echo signal at each increment. The signal height at each stage was kept at 80% FSH, and stress levels were kept below the yield strength of the material.

Results & Discussion

Recent work on surface opening fatigue cracks in ferritic steel submerged arc welds, has shown that the optimum ultrasonic technique for detection of these cracks utilizes a 45° 5 MHz probe at the $\frac{1}{2}$ skip scanning position. (12) The same work also shows that the 60° probe has a rather weak amplitude response but proves to be the most sensitive probe to compressive stresses, giving an apparent crack closure at low stress levels.

Comparing the above results with this present work, it is clear that the performance of the angle probes has been drastically reversed in that the 2 MHz probes gave much higher response than the 5 MHz, probes, However, the 5 MHz probes showed much higher sensitivity to crack closure at low stress levels. In addition unacceptable signal/noise ratios were achieved when the waves were propagated through the bulk of the weld metal.

The 2 MHz 45° probe, when used at $\frac{1}{2}$ skip scanning position, proved to be the most efficient in detecting fatigue cracks of different sizes in the HAZ of the 316 austenitic weldment. This was true whether the inspection was carried out from the parent metal side or the weld metal side.

Figures 7 and 8, show CRT screen traces of 8 mm fatigue cracks, when using 45° , 60° and 70° shear angle probes, with 2 and 5 MHz frequencies, at $\frac{1}{2}$ skip scanning positions.

It can be deduced from the traces and the respective echo amplitudes that the 2 MHz, 45° angle probe appears to offer the best response from the 8mm fatigue crack inspected from either side of the weld.

The traces also demonstrate the difficulty of deciding which of the signals is coming from the crack in the case of the 5 MHz probes when the beam is passing through the weld metal.

The poor performance of the 5 MHz probes is not unexpected, since grain boundary scattering is strongly dependent on the D/λ ratio (13).

Papadakis (13) has given equations for the attenuation (a) caused by grain boundary scattering:

Rayleigh scattering	when $\lambda \gg D$	$a = k_1 f^4 D^3$
Stochastic "	when $\lambda \sim D$	$a = k_2 f^2 D$
Diffusive "	when $\lambda < D$	$a = k_3 D^{-1}$

where f is the frequency of the ultrasound and k_1 , k_2 and k_3 are dependant on the elastic anisotropy of the crystals.

If Rayleigh or Stochastic Scattering are operative, the use of lower frequencies is clearly advantageous.

Work carried out by one of the authors (2), using the same weld configuration and materials, and with horizontal holes as reflectors (see Fig. 9), agrees with the results of this present work, in showing that the 2 MHz 45° probe offers the best combination for inspecting these artificial flaws in the parent metal/ weld metal interface. It is also clear that the 2 MHz probes in general are far more efficient when interrogating flaws where the sound beam passes through the weld metal.

During the present and previous investigations when the sound beam was propagated through the weld metal, differences in the values of screen and geometrical ranges were observed, with an overall increase in attenuation levels. The differences in the range values are a result of beam bending taking place when the sound beam reaches the parent metal/weld metal interface. This bending is dependent on the angle of approach of the sound beam, since the velocity of ultrasound inside the weld metal itself depends strongly on the angle between the weld grain axes and the sound beam direction.

Table 5, gives values for the geometrical/screen ranges, for $\frac{1}{2}$ skip scanning positions, through parent metal and through weld metal. When the beam passes through weld metal it can be seen that the 45° probes produce the biggest differences in geometrical and screen ranges. This could be explained by the fact that when the 60° or 70° probes are used, the velocities in the parent metal and weld metal are similar, thus reducing the bending effect.

Beam deviation, mode conversion at grain boundaries and grain boundary scattering, were the main factors for the increase in attenuation levels. The $\frac{1}{2}$ skip scanning position is considered to be the most suitable because it minimises the additional attenuation that a sound beam would suffer when travelling longer distances.

The results were very encouraging in that, fatigue cracks situated in the HAZ of these austenitic weldments, were readily inspectable with high signal amplitudes and at acceptable signal/noise ratios, using both 2 and 5 MHz shear angle probes. The 2 MHz, 45° probe which is considered to give the best results for inspecting these cracks, could detect a 2mm fatigue crack in the HAZ when scanning at $\frac{1}{2}$ skip from the parent metal side, and a 4mm crack when scanning from the weld metal side.

With same conditions the 5 MHz, 45° probe could detect the 2mm crack from the parent metal side, but from the weld metal side the performance was reduced to unacceptable levels of sensitivity and signal/noise ratios, with the addition of many spurious signals, due to mode conversion and beam skewing.

From the weld side it was only under the application of elastic compressive stresses that the signals returning from the cracks, using 45° , 60° and 70° probes, were identified with a degree of certainty, and even then the 4mm and 6mm cracks exhibited closure when interrogated with the 70° probe at low stress levels. The 4mm crack also exhibited similar behaviour with the 45° , 5 MHz probe.

The identification of signals coming from the fatigue cracks under static compression, illustrated the unreliability of the 5 MHz probes for use when the ultrasound is propagated through the austenitic weld structure. It also emphasized the need for accurate screen calibration and beam plotting if the 2MHz probes were to be used to propagate ultrasound through the weld metal.

The superiority of the 2 MHz probes over the 5 MHz, was demonstrated during the tests and at the same time the advantages of using 45° angle probes instead of 60° and 70° were seen.

It is now felt necessary to establish performance data for 2 MHz shear angle probes in detecting fatigue cracks situated in the austenitic weld metal itself. Accordingly a series of samples are under preparation by the authors to continue this work. It is expected that difficulties will be met, but it is hoped that the results of this present study will provide the necessary guidance for the inspection procedures to be used.

Ultimately, similar performance data are to be obtained by using longitudinal wave probes for inspecting fatigue cracks in austenitic weldments, resulting no doubt in a very useful comparison between the two techniques.

Conclusions

1. Fatigue cracks in the HAZ of austenitic weldments were readily detected using shear waves of both 2 and 5 MHz frequencies, and 45° , 60° and 70° probe angles, provided the soundwaves travelled through parent metal only.
2. When the soundbeam was propagated through the austenitic weld metal, the 2 MHz probes were superior to 5 MHz.
3. The 45° , 2 MHz probe used at $\frac{1}{2}$ skip scanning positions offers the best possibilities of detecting fatigue cracks, when the soundwaves travel through parent metal and/or weld metal .
4. 60° angle probes appear to be sensitive to crack closure at low levels of elastic compressive stresses.

Acknowledgements

The authors would like to thank Mr B J Lack of NEI John Thompson Ltd., for providing the welds. Thanks are also due to Mr. E. Watson for his help in preparing the test pieces, and Mr. P. Cox for the photographic material in this work.

References

1. BAIKIE B.L., et al, 1976. Ultrasonic inspection of austenitic welds. Journal of Brit. Nuclear Energy Soc. (3) 257-261.
2. KAPRANOS P.A. 1980. Ultrasonic inspection of austenitic weldments. 1st year Research Report. Dept. of Metallurgy and Materials Engineering University of Aston in Birmingham.
3. KAPRANOS P.A., AL-HEIALY MMH. & WHITTAKER V.N. 1981. Ultrasonic velocity measurements in 316 austenitic weldments. Accepted for publication by The British Journal of NDT March 81.
4. Tomlinson J.R., et al, 1980. Ultrasonic inspection of austenitic welds. Brit. J. NDT (22) (3) 119-127.
5. GILLAN M.T. 1980. Ultrasonic wave propagation in austenitic stainless steel weld metal. Theoretical Physics Division, AERE Harwell, Oxfordshire. Report HL80 / 1528, May 1980.
6. SILK M.G. Inspecting austenitic welds. Research techniques in Nondestructive testing, Vol.4. Academic Press 1980 p. 393-449
7. JUVA A. & LIETO J. 1980. The ultrasonic examination of thin austenitic stainless steel butt welds. Brit. J. NDT (22) (4) 191-195.
8. GRAY B.S. 1980. Longitudinal wave ultrasonic inspection of austenitic weldments. OECD CSNI Specialists Meeting on Reliability of Ultrasonic inspection of austenitic stainless steel components. Brussels, Belgium, 29-30 May 1980.

9. REINHARDT E.R. 1978. EPRI Program to improve Nuclear Code inspection methods. Materials Evaluation. May 1978 (36) (6) 36-42.
10. ABRAHAMS C.J. 1972. Tube-to-tube butt welds in austenitic steel (thin wall), their ultrasonic examination using assisted hand-scanning methods. Brit. J. NDT (14) (3) 66-72.
11. IBRAHIM S.I. & WHITTAKER V.N. 1980. The influence of compressive stresses and other factors on the detection of fatigue cracks using ultrasonics. Brit. J. NDT (22) (6) 286-290
12. IBRAHIM S.I. & WHITTAKER V.N. 1981. The influence of crack topography and compressive stresses on the ultrasonic detection of fatigue cracks in submerged arc welds. Accepted for publication by Brit. J. NDT March 1981.
13. PAPADAKIS E.P. 1965. Revised grain-scattering formulas and tables. J. Acoust. Soc. Am. 37 , p. 703-710.

List of Figures

1. Macrograph of the 316 austenitic weld, etched in Ferric Chloride.
2. Test piece mounted on bending rig.
3. Geometrical and Screen ranges, graphical representation.
4. Response to fatigue cracks under zero load, using 45° , 60° and 70° , 2 & 5 MHz probes, at $\frac{1}{2}$ skip scanning position.
5. Signal amplitude responses from fatigue cracks in HAZ under compression, using 45° , 60° and 70° , 2 MHz probes at $\frac{1}{2}$ skip scanning position.
6. Signal amplitude responses from fatigue cracks in HAZ under compression, using 45° , 60° and 70° , 5 MHz probes at $\frac{1}{2}$ skip scanning position.
7. Comparison between the ultrasonic screen traces of the 8mm fatigue crack in the HAZ of the austenitic weld, with the soundwaves travelling through parent metal and/or through weld metal, using 45° , 60° and 70° 2 MHz probes at $\frac{1}{2}$ skip scanning position.
8. Comparison between the ultrasonic screen traces of the 8mm fatigue crack in the HAZ of the austenitic weld, with the soundwaves travelling through parent metal and/or through weld metal, using 45° , 60° and 70° 5 MHz probes at $\frac{1}{2}$ skip scanning position.

9. 316 austenitic weldment, containing artificial defects.

Material	Thickness	C	Cr	Ni	Mo	Ti	Method of Manufacture
316 s.s	25mm	0.029	16.8	11.39	2.28	0.033	Rolled plate

Table 1. Details of parent plate material.

Material & Thickness	Weld Preparation ⁿ	Electrode size & current		Electrode Type	Heat Input
		Root runs	Fill-up		
25mm	Double-U	10 swg 100/110 amps	10 swg 100/110 amps	316 Staintrode 63.30	Minimum

Table 2. Welding details

Alloy	Yield strength (MN/m ²)	Tensile strength (MN/m ²)	%Elongation	%Reduction in area	Hardness Hv
Weld metal	333	655	76	66	317
Parent metal	309	605	67	58	282

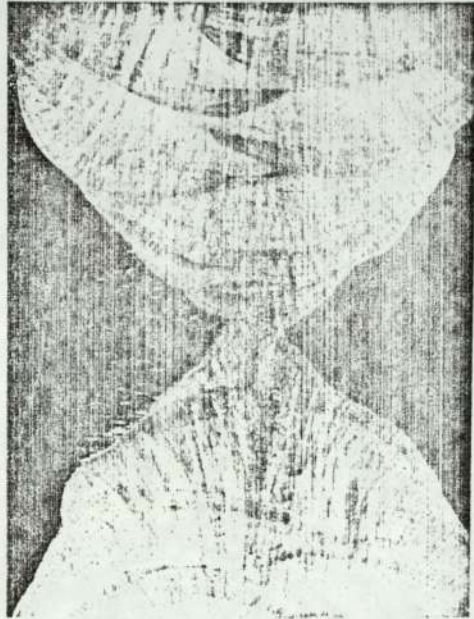
Table 3. Mechanical properties

Stages	Austenitic stainless steel weldment			
	Main load		Resonating load	
	Tons	Newtons	Tons	Newtons
Initiation	0.76	7600	+ 0.70	+ 7000
Propagation	0.60	6000	+ 0.50	+ 5000

Table 4. Fatigue crack initiation and propagation conditions

Probe angle (Deg) Measured		Frequency (MHz)	Max.echo amplitude (dB)	Geometrical Range (mm)	Screen Range (mm)	
In mild st.		In st.st.				
Parent metal	43	41	2	73.5	30.5	31
	61	59	2	58	39	40
	69	66	2	56	56	58
	45	42	5	47	31	33.5
	61	56	5	36	36	37.5
	70	67	5	30	55	57
Weld metal	43	41	2	46	37	41
	61	59	2	40	44	47
	69	66	2	42	48.5	52
	45	42	5	7	36.5	38.5
	61	56	5	6	44	46
	70	67	5	4	52	52

Table 5. Screen range/geometrical range values obtained from an 8 mm fatigue crack in the HAZ of a 316 austenitic stainless steel weldment (double-U).



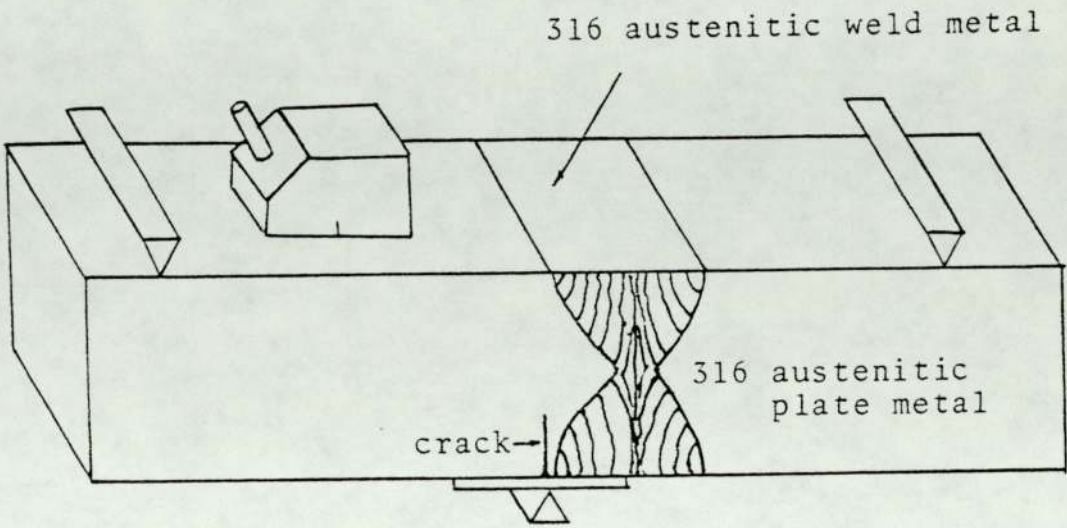


FIGURE. 2.

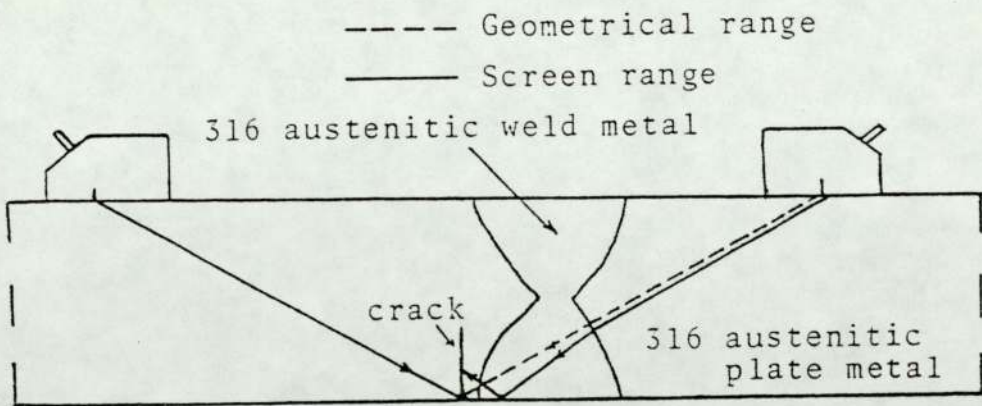


FIGURE. 3.

FIGURE 4.

HAZ Fatigue Cracks under
zero load

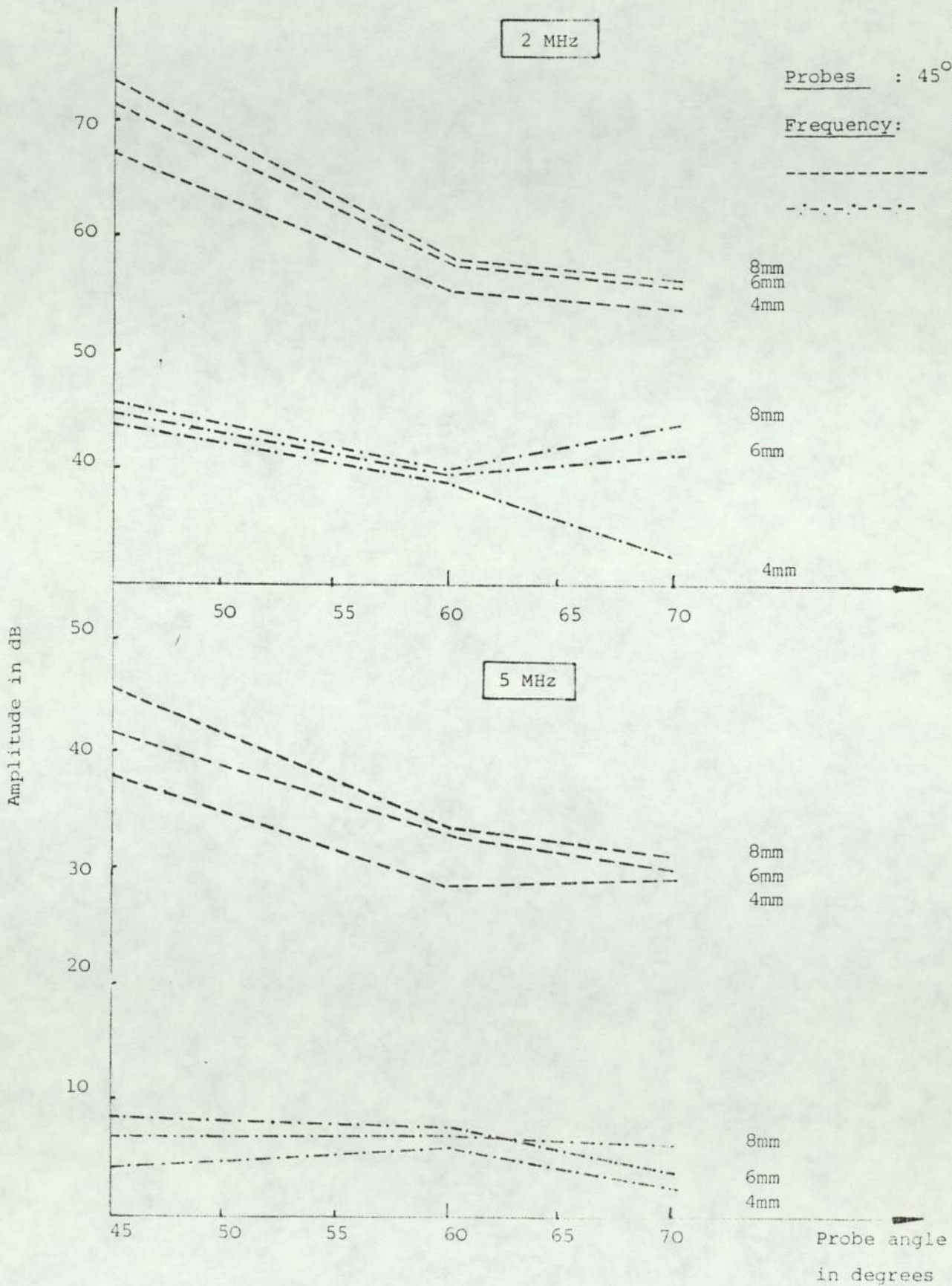
Material : 316 aust.
plate
welded.

Probes : 45°, 60°, 70°.

Frequency: 2 & 5 MHz

----- Parent me

-.-.-.-.- Weld meta



HAZ Fatigue Cracks

Material: 316 aust

plate

welded

Probes: 45°, 60°, 70°

Frequency 2 MHz

Scanning: 1/2 skip

----- Through par metal

----- Through we metal

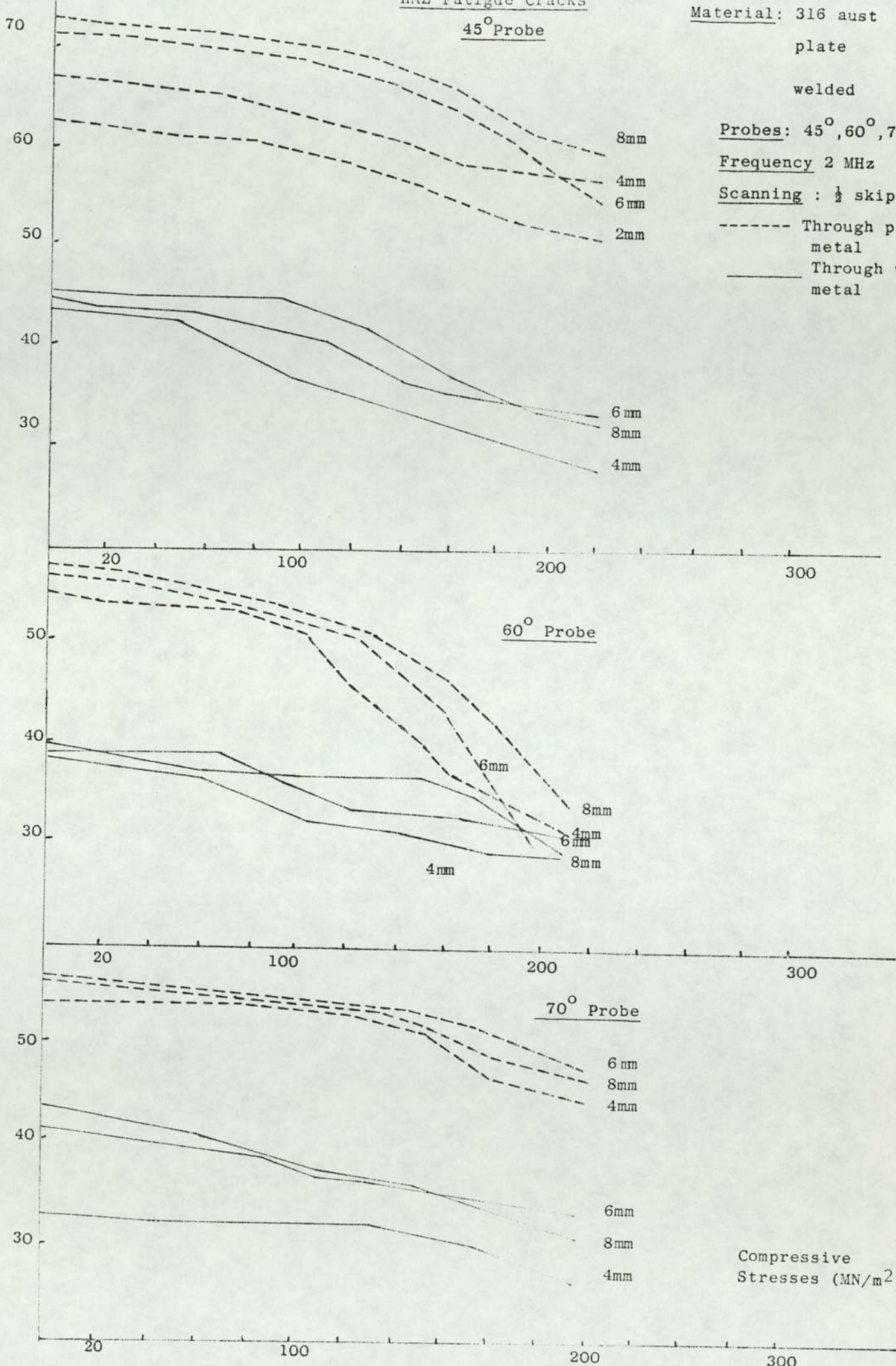


FIGURE 5. 170

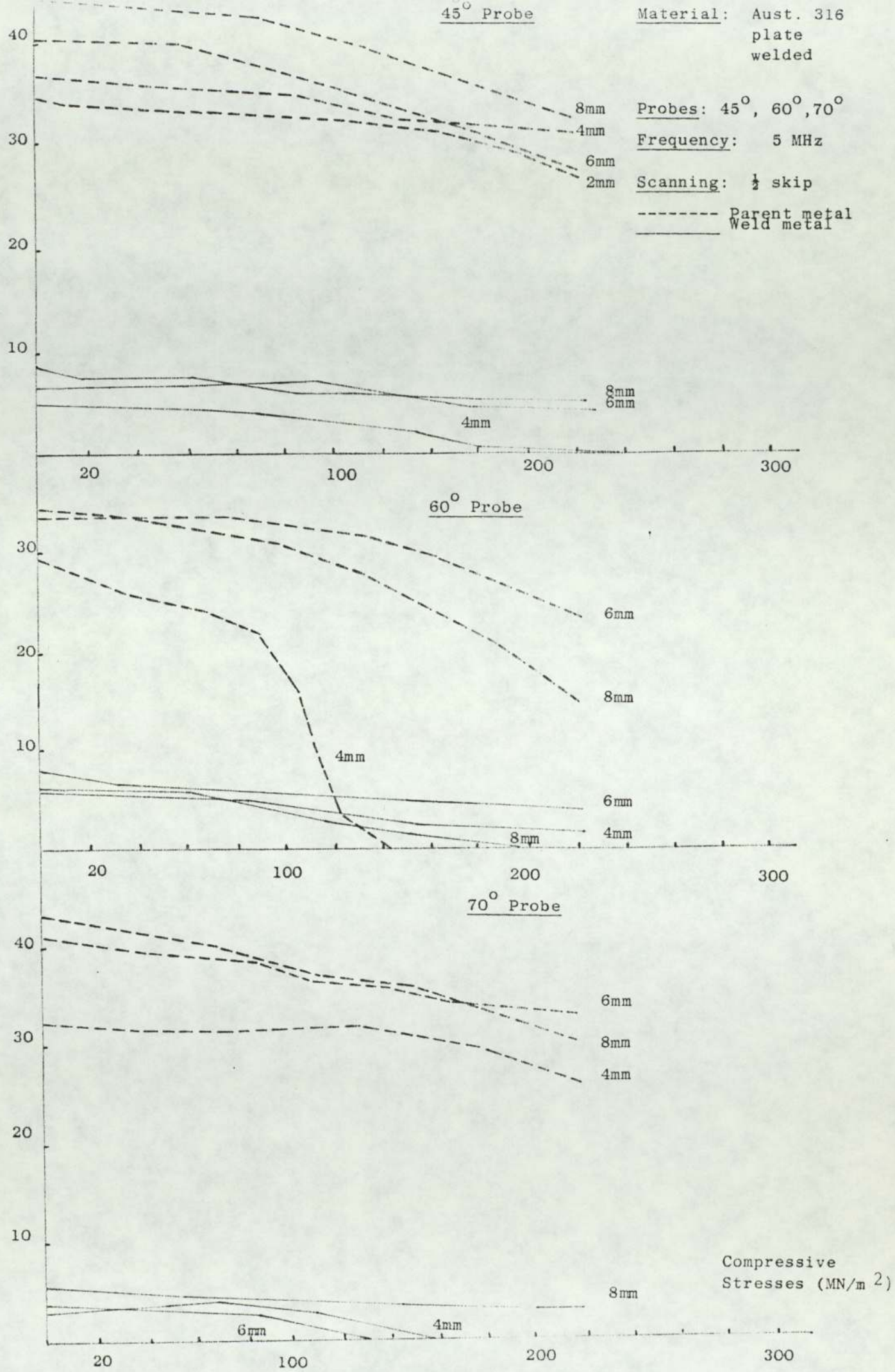


FIGURE 6.

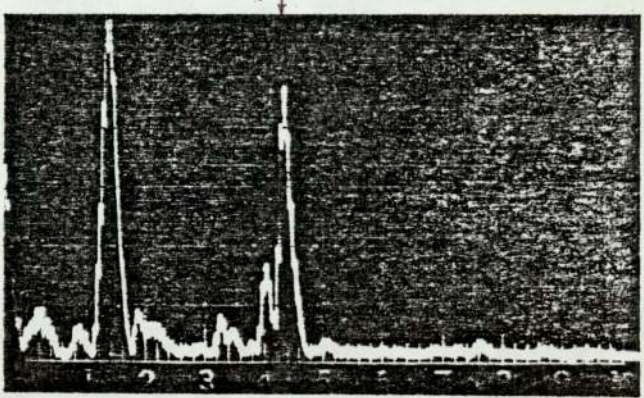
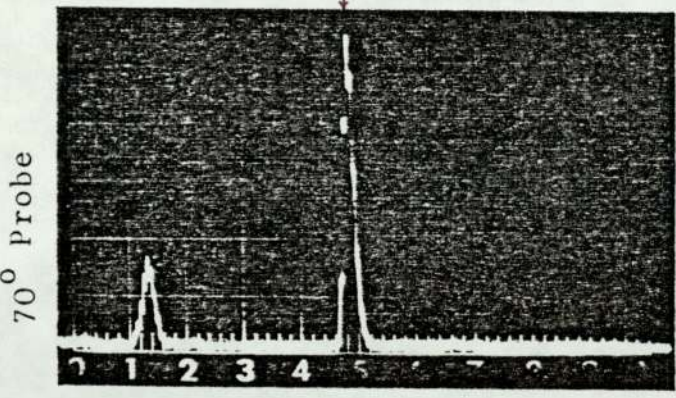
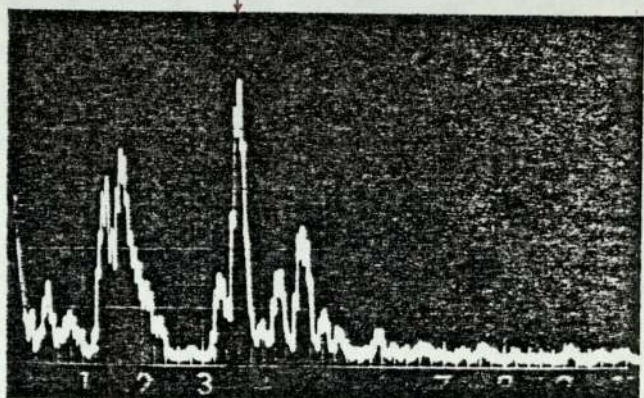
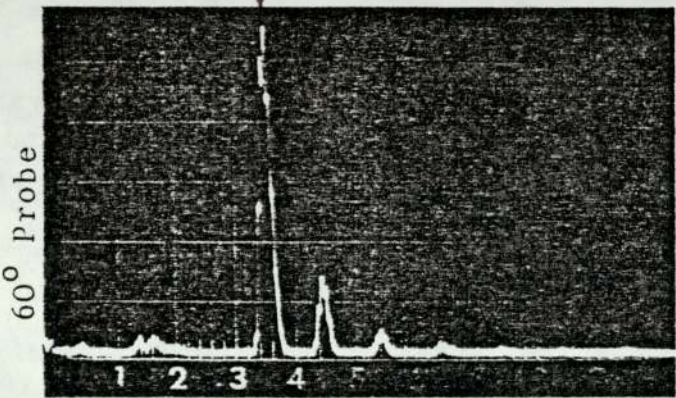
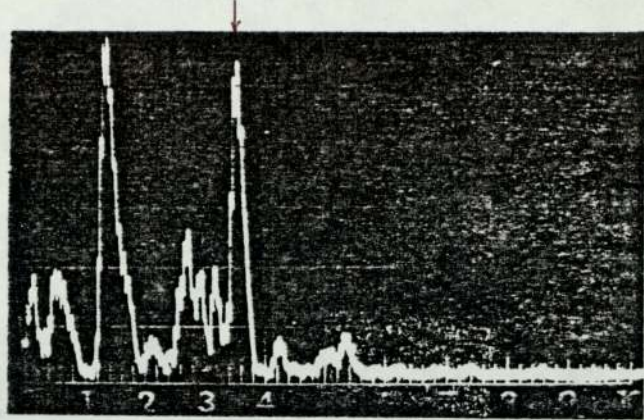
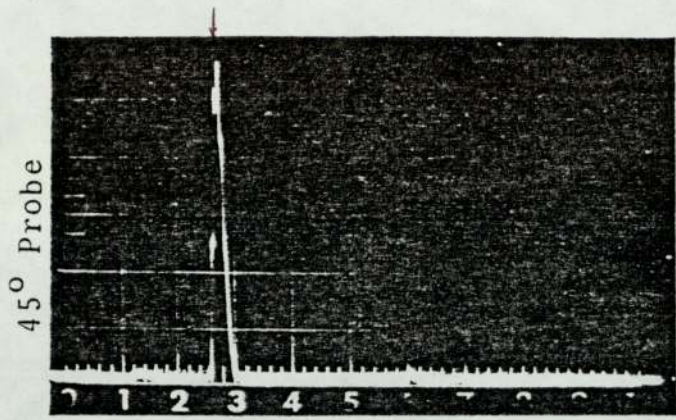
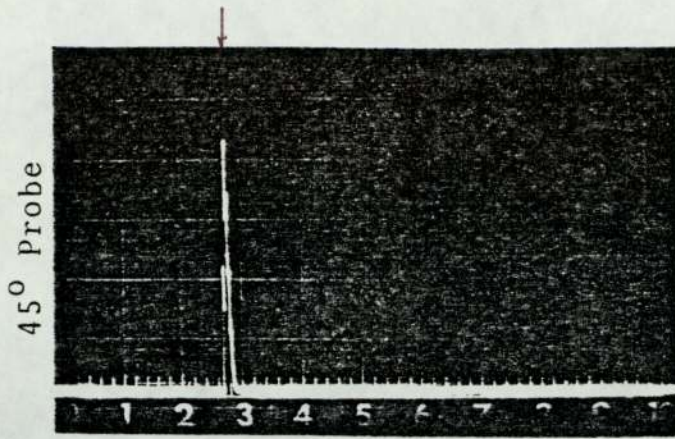
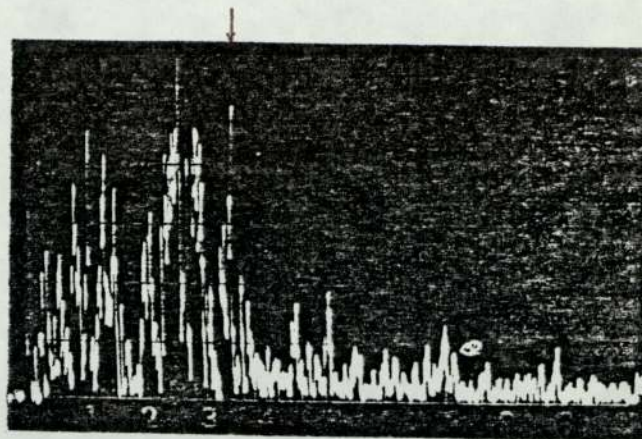


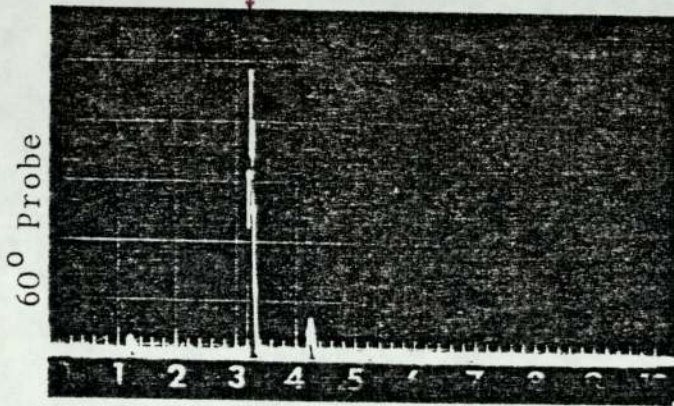
FIGURE 7.



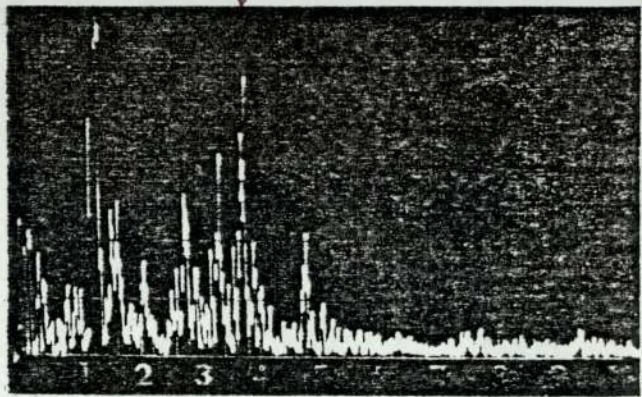
Parent metal
amplitude = 47 dB



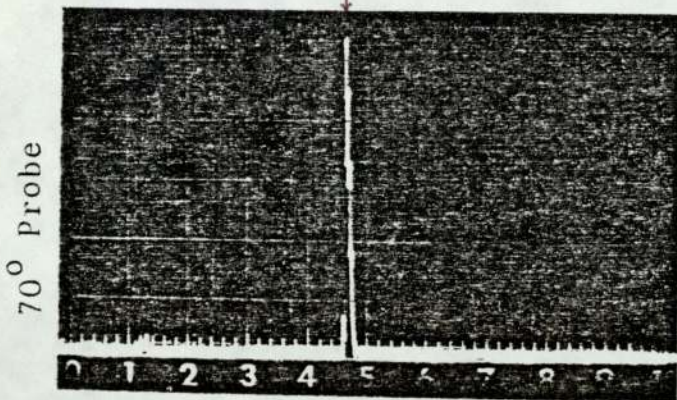
Weld metal
amplitude = 7 dB



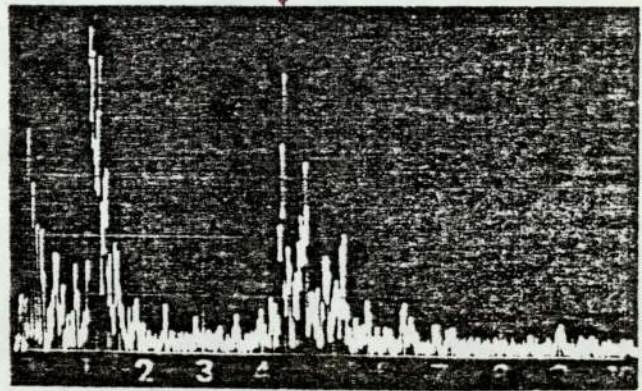
Parent metal
amplitude = 36 dB



Weld metal
amplitude = 6 dB



Parent metal
amplitude = 30 dB



Weld metal
amplitude = 4 dB

FIGURE 8.

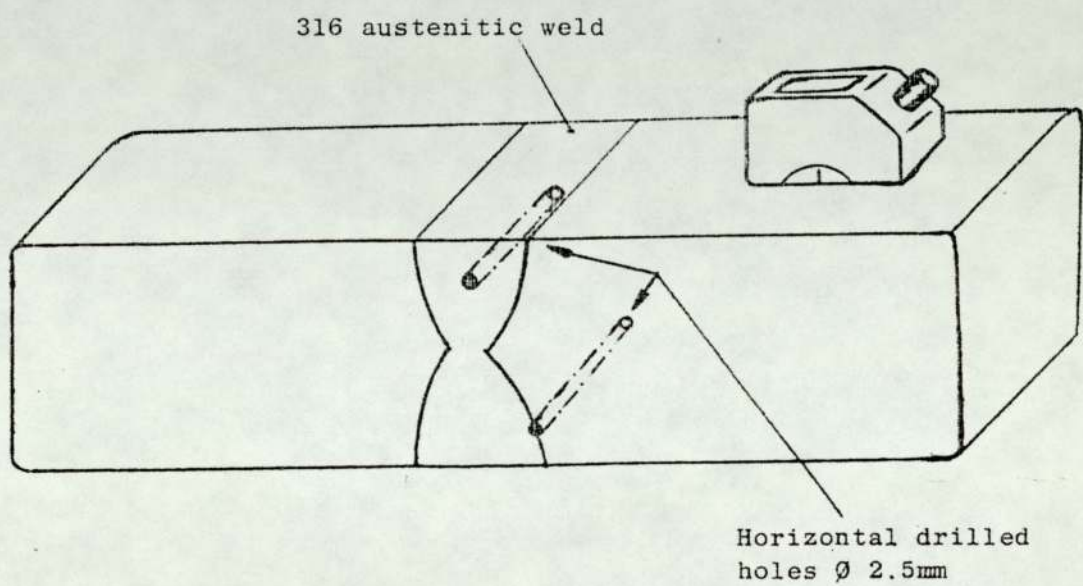


Figure 9